Ocean circulation variability in the western South Atlantic during the Holocene

Dissertation zur Erlangung des
akademischen Grades eines Doktors
der Naturwissenschaften

Dr. rer. nat.

im Fachbereich 5 (Geowissenschaften)
der Universität Bremen

vorgelegt von:

Ines Voigt

Bremen, Januar 2013

- E r k l ä r u n g -

Name: Ines Voigt

Anschrift: Graudenzer Str. 30-34, 28201 Bremen

Hiermit versichere ich, dass ich

1. die Arbeit ohne unerlaubte fremde Hilfe angefertigt habe,

2. keine anderen als die von mir angegebenen Quellen und Hilfsmittel benutzt habe und

3. die den benutzten Werken wörtlich oder inhaltlich entnommenen Stellen als solche kenntlich gemacht habe.

Bremen, den 10. Januar 2013

- G u t a c h t e r -

Prof. Dr. Rüdiger Henrich

Prof. Dr. Gerold Wefer

- A c k n o w l e d g e m e n t s -

The study was funded through DFG Research Center / Cluster of Excellence „The Ocean in the Earth System“ and was supported by the Bremen International Graduate School for Marine Sciences (GLOMAR) that is funded by the German Foundation (DFG) within the frame of the Excellence Initiative by the German federal and state governments to promote science and research at German universities.

First of all I would like to thank Prof. Dr. Rüdiger Henrich for his continuous support of my Ph.D. study, for his motivation, enthusiasm and patience. Thanks for allowing me to work with such independence and giving me the opportunity to develop my own self-sufficiency.

I also wish to thank Prof. Dr. Gerold Wefer who has agreed to evaluate this dissertation.

I would like to express my gratitude to my co-authors, Dr. Cristiano Chiessi, Dr. Jeroen Groeneveld, Dr. Benedict Preu, Prof. Dr. Alberto Piola, Dr. Till Hanebuth, Dr. Tillmann Schwenk, Dr. Stefan Mulitza and Dr. Matthias Prange, for discussions and revisions that greatly improved the quality of the manuscripts in this dissertation. Thanks for the close collaboration from which I greatly benefitted, and which ultimately made me a better scientist over the past three years.

I'm particularly obliged to Dr. Cristiano Chiessi from University of Sao Paulo for supporting, inspiring, and encouraging me over the past three years. Thank you for the trust and the whole lot of new thinking approaches!

Bremen International Graduate School for Marine Sciences (GLOMAR) gave me further the opportunity to educate myself by attending courses with various topics. GLOMAR supported me financially giving me the chance to present my work during international conferences, and further to stay for two months in South America in March/April 2012 from which I and my research work highly benefited. Talking about GLOMAR: I wish to thank the other members of my GLOMAR thesis committee, Prof. Dr. Dorrik Stow, Dr. Sabine Kasten and Dr. Torsten Bickert, for their encouragement, insightful comments, and hard questions.

I thank all members of the Paleoceanography – Sedimentology Group at the University of Bremen for the comprehensive help.

Special thanks also go to my South American colleagues: Thank you, Dr. Roberto Violante and Dr. Graziella Bozzano not only for the scientific discussions, but also for welcoming me so warmly during my research stay.

During my PhD time, I was fortunate enough to be surrounded by a great group of people who really supported me - Katja, Janna, Benedict, Claudi, Maria, Anna, Yann, Jeroen, Linda, Jan, Hendrik, Tim, Sebastian and many others. Life and work in Bremen would have been less beneficial.

Without my beloved family, I would certainly not be where I am today. Thank you for all your love, support and assistance.

Finally I would like to thank Moritz. Your support, encouragement, patience and unwavering love were undoubtedly the bedrock upon which the past ten years of my life have been built. Thank you so much!

- S u m m a r y -

The western South Atlantic forms a key location in the global ocean conveyor belt. Different water masses formed in remote areas of the world extend into that area and generate a highly complex vertical stratification structure. In the upper ocean, this structure is dominated by the encounter of southward-flowing Brazil Current and northward-flowing Malvinas-(Falkland) Current generating one of the most energetic regions of the world ocean; the Brazil-Malvinas Confluence (BMC). In the deep ocean, the vertical stratification structure is dominated by contributions from intermediate- and deep water masses, including the Antarctic Intermediate Water (AAIW) which represents an active player in the Atlantic meridional overturning circulation (AMOC). The western South Atlantic is thus critical in understanding global ocean-climate changes. However, a detailed insight into the past remains a significant challenge in climate research due to the lack of high temporal resolution climate archives.

The presented research of this thesis focuses on the surface- and intermediate water circulation in the western South Atlantic during the Holocene with special emphasize on sedimentation processes in the Mar del Plata Canyon. Results of this research highlight the extraordinary potential of a submarine canyon for reconstructing paleoceanographic and paleoclimatic changes with high temporal resolution, and clearly demonstrate that a good knowledge of sediment transport phenomena is an indispensable precondition for understanding paleoceanographic/paleoclimatic changes, particularly in such highly energetic current regimes as the western South Atlantic.

The first step was to validate such a combined sediment transport and high-resolution climate archive in the western South Atlantic (**Chapter 2**). Here, we focused on the Mar del Plata Canyon at the continental margin off northern Argentina (GeoB13832-2, GeoB13833-2, GeoB13862-1 and GeoB13861-1). The canyon is incorporated into a Contourite Depositional System which is formed by northward-flowing Antarctic water masses (e.g., AAIW). A broad variety of methods including grain-size analysis, bulk sediment geochemistry and CTD casts were used to obtain a new conceptual model for sedimentation processes taking place in submarine canyons that are located at current-controlled continental margins. The results highlight that due to the interaction with an intermediate nepheloid layer (INL) generated by the AAIW, the Mar del Plata Canyon acts as a (temporary) sink for enhanced accumulation of modern sediments, and therefore holds a great potential as a Holocene climate archive. Sediment core Geo13862-1

retrieved from the Mar del Plata Canyon at 3600 m depth reveals a 750 cm long Holocene sequence and thus provides the basis for this study.

As a second step, changes in the AAIW circulation were addressed (**Chapter 3**). The formation of AAIW is linked to the strength of the AMOC and therefore is an important component of our climate system. The high potential of AAIW to contribute to changes of the AMOC makes it important to understand its natural variability and the underlying mechanisms involved in its formation. Due to the interaction of the AAIW nepheloid layer with the Mar del Plata Canyon, the sedimentation rates and particle sizes in the canyon are primarily current-controlled and thus linked directly to changes in current strength of AAIW. The "sortable silt" paleocurrent record of GeoB13862-1 reveals millennial-scale perturbations in the AAIW overturning circulation during the Holocene. During times of Southern Hemisphere cold events and poleward intensified Southern Westerly Winds (SWW), the AAIW circulation strengthened in response to higher ice/freshwater fluxes toward regions of AAIW renewal. The strengthening of AAIW circulation occurred during periods of reduced North Atlantic Deep Water (NADW) circulation and vice versa, and thus provides strong evidence for a Holocene NADW-AAIW seesaw. Incursion of cold and fresh AAIW into the North Atlantic may have been involved in the freshening of the North Atlantic and thereby contributed to the reduction of NADW. These results demonstrate the sensitivity of AAIW formation to enhanced atmospheric forcing and enable a detailed assessment of Southern Hemisphere water mass conversion during the Holocene, and its linking with climate variability in both hemispheres.

Finally, the third paper focused on past migration shifts of the Brazil-Malvinas Confluence (**Chapter 4**). Three high- resolution $\delta^{18}O$ records of planktonic foraminifer G. inflata (GeoB6211, GeoB13862-1 and GeoB6308) situated along a north–south transect in the western South Atlantic document millennial-scale shifts of the BMC during the Holocene. The variability of the SWW and their control on the sub(surface) circulation in the western South Atlantic appears to be the dominant forcing mechanism for past shifts of the BMC. The latitudinal shifts of the SWW were part of large-scale reorganizations of the global atmospheric circulation including synchronous southward shifts of the mid-latitudes westerlies over both hemispheres during Holocene cold events. This provides strong evidence for an atmospheric see-saw mechanism operating during the Holocene that is conceptually different to the mechanism proposed to control modern and future changes in the westerlies.

-Zusammenfassung-

Der Südwest Atlantik stellt eine Schlüsselregion im globalen ozeanischen Strömungssystem dar und ist somit entscheidend für das Verständnis des globalen Ozean-Klima-Systems. Die Oberflächenzirkulation wird geprägt durch die Brazil-Malvinas Confluence (BMC) - einem Zusammenfluss des warmen, südwärts fließenden Brasil-Stroms mit dem kühlen, nordwärts fließenden Malvinas (Falkland)-Strom. Die Tiefenzirkulation im Südwest Atlantik wird insbesondere durch das Antarktische Zwischenwasser (AAIW) bestimmt, das eine entscheidende Rolle in der Atlantischen Meridionalen Umwälzbewegung (AMOC, Atlantic meridional overturning circulation) darstellt. Aufgrund des komplexen Strömungsregimes und fehlender hochauflösender Klimaarchive, ist bislang nur wenig bekannt über die Paläozeanographie des Südwest Atlantiks.

Das Ziel der vorliegenden Dissertation ist daher eine detaillierte Rekonstruktion der Oberflächen- und Zwischenwasserzirkulation während des Holozäns basierend auf dem Verständnis sedimentdynamischer Prozesse im Mar del Plata Canyon.

In solch komplexen Strömungsregimen, ist eine gute Kenntnis der Sedimenttransportprozesse eine unabdingbare Voraussetzung für das Verständnis paläozeanographischer und paläoklimatischer Veränderungen. Der erste Teil der Dissertation zielt daher auf die sedimentdynamischen Prozesse im Mar del Plata Canyon (**Chapter 2**). Der argentinische Kontinentalhang wird primär durch hangparallele Bodenwasserströmungen geprägt. Im Speziellen, die partikelbeladene Strömung des AAIW bedingt großräumige Ablagerungs- und auch Erosionsformen. Hochauflösende sedimentologische und geochemische Untersuchungen der Sedimente aus dem Mar del Plata Canyon (GeoB13832-2, GeoB13833-2, GeoB13862-1 und GeoB13861-1) zeigen, dass der Canyon das lokale Strömungsmuster der partikelbeladenen Bodenwasserströmung so verändert, dass die mitgeführten Sedimente im Canyon zur Ablagerung kommen. Die Sedimentationsraten im Mar del Plata Canyon sind mit bis zu 150 cm pro 1000 Jahre während des gesamten Holozäns ungewöhnlich hoch. Dieser Umstand erlaubt eine hochauflösende Rekonstruktion der Oberflächen- und Zwischenwasserzirkulation des Südwest Atlantiks während des Holozäns.

Der zweite Teil der Dissertation befasst sich mit Änderungen der AAIW Zirkulation während des Holozäns (**Chapter 3**). Aufgrund der Interaktion mit dem AAIW stellen die Sedimente im Mar del Plata Canyon ein hochauflösendes Klimaarchiv für paläozeanographische Veränderungen der AAIW

Zirkulation dar. Die Bildung von AAIW ist mit der AMOC gekoppelt und ist damit wesentlicher Bestandteil des globalen Klimasystems. Dennoch ist bisher wenig bekannt über die zugrunde liegenden Mechanismen bei der Bildung von AAIW und die damit verbundene natürliche Variabilität der Zwischenwasserzirkulation. Paläoströmungsanalysen mittels "sortable silt" des Sedimentkerns GeoB13862-1 zeigen kurzfristige Veränderungen der AAIW Zirkulation während des Holozäns. Eine Zunahme der AAIW Bildung ist auf die verstärkte Zufuhr von (Meereis)-Süßwasser während Phasen kurzfristiger Abkühlung und südwärts verlagerter Westwinde in der Südhemisphäre zurückzuführen. Die Ergebnisse der Studie zeigen, dass die Bildung von AAIW sensitiv gegenüber atmosphärischen Veränderungen und darüber hinaus eng gekoppelt mit globalen Veränderungen des Ozean-Klimasystems ist. Die verstärkte Zufuhr des kalten und salzarmen AAIW in den Nord Atlantik hat vermutlich zu einer Abnahme der NADW (North Atlantic Deep Water) Bildung beigetragen. So geht die Zunahme der AAIW Bildung einher mit einer Abnahme der Tiefenwasserbildung im Nord Atlantik, und deutet demnach auf einen AAIW-NADW Kopplungsprozess während des Holozäns hin.

Der dritte Teil der Dissertation befasst sich mit Veränderungen der Oberflächenzirkulation, im Speziellen mit Verlagerungen der BMC während des Holozäns (**Chapter 4**). Entlang eines N-S Transektes verschiedener Sedimentkerne (GeoB6211, GeoB13862-1 und GeoB6308) zeigen paläoklimatische Isotopenuntersuchungen ($\delta^{18}O$) planktischer Foraminiferen abrupte Verschiebungen des BMC, die vermutlich in einem direkten Zusammenhang zu Verschiebungen der südlichen Westwindzone stehen. Die Ergebnisse verdeutlichen, dass sich die südliche Westwinde und demnach auch die BMC während abrupter Kältephasen im Holozän nach Süden verlagerten. Wie bereits die Ergebnisse der zweiten Studie (**Chapter 3**) nahe legen, haben die südwärts verlagerten Westwinde enormen Einfluss auf die AAIW Zirkulation. Darüber hinaus, deutet die gleichzeitige Südwärtsverlagerung der nördlichen Westwindzone auf einen atmosphärischen Kopplungsprozess zwischen der Nord- und Südhemisphäre hin und verdeutlicht daher große Umstrukturierungen der globalen atmosphärischen Zirkulation während holozäner Kältephasen.

-Table of Content-

Chapter 1: Introduction

Global climate has fluctuated throughout the entire Earth history. Glacial-interglacial cycles have waxed and waned throughout the Quaternary Period (the past 1.8 million years). The present interglacial, the Holocene, is of particular interest because it has sustained the growth and development of modern human society. The Holocene spans the period of the last 11.700 years. Although the climate of the Holocene is considered as relatively stable compared to the last glacial, it has also been shown that it was interrupted by a series of millennial-scale cold events (e.g. *Bond et al., 2001; Wanner et al., 2011*). However, the global complexity of the millennial-scale mode of Holocene climate instability remains poorly understood. Although the western South Atlantic is critical in understanding large-scale changes in the global ocean-climate system during the Holocene – a detailed insight into the past has long been hampered by a lack of high temporal resolution sediment records, and thus remains a significant challenge in Holocene climate research.

1.1. Ocean circulation

"The western South Atlantic has been referred to as the 'cross-roads of the world ocean circulation', because it hosts water formed in remote areas of the world, and brought into this region by the large-scale ocean circulation" (*Piola and Matano, 2001*). Among other important characteristics, the western South Atlantic is characterized by **(1)** the Brazil-Malvinas Confluence (BMC), a prominent feature in the upper-level circulation that emerges from the encounter of southward-flowing Brazil Current and northward-flowing Malvinas (Falkland) Current (e.g., *Peterson and Stramma, 1991*), **(2)** the Antarctic Intermediate Water (AAIW) circulation (e.g., *Stramma and England, 1999*) which has profound effects on sedimentation processes along the continental margin off northern Argentina (e.g., *Hernández-Molina et* al., *2009*), and **(3)** the significant freshwater discharge of the La Plata River that drains the second largest basin in South America (*Mechoso et al., 2001*).

1.1.1. Brazil-Malvinas Confluence

The upper-level circulation in the western South Atlantic is characterized by the Brazil- and Malvinas western boundary currents and their confluence, the Brazil-Malvinas Confluence (BMC) (**Fig. 1**) (*Peterson and Stramma, 1991*).

The warm-water Brazil Current (BC) represents the western portion of the subtropical gyre in the South Atlantic and originates near 10 °S, where the South Equatorial Current bifurcates. The BC carries warm, saline and nutrient-depleted subtropical waters southward along the continental slope of South America (**Fig. 1**). It is one of the weakest western boundary currents in the world (*Peterson and Stramma, 1991*). Although the flow strengthens at more southern latitudes under the influence of a recirculation cell, the maximum poleward transport is not exceeding 20 Sv (1 Sv = 106 m^3/s). Near 38 °S the BC collides with the Malvinas-(Falkland) Current (MC) that transports cold, fresh and nutrient-rich subantarctic waters northward along the continental slope of South America. The MC represents a northward branch of the Antarctic Circumpolar Current (ACC) **(Fig. 1**) and is assumed to be a strong current with maximum equatorward transport of 41.5 Sv (*Vivier and Provost, 1999*).

The subantarctic waters of the MC and the subtropical water masses of the BC collide in the upper 800 m of the water column, and thereby

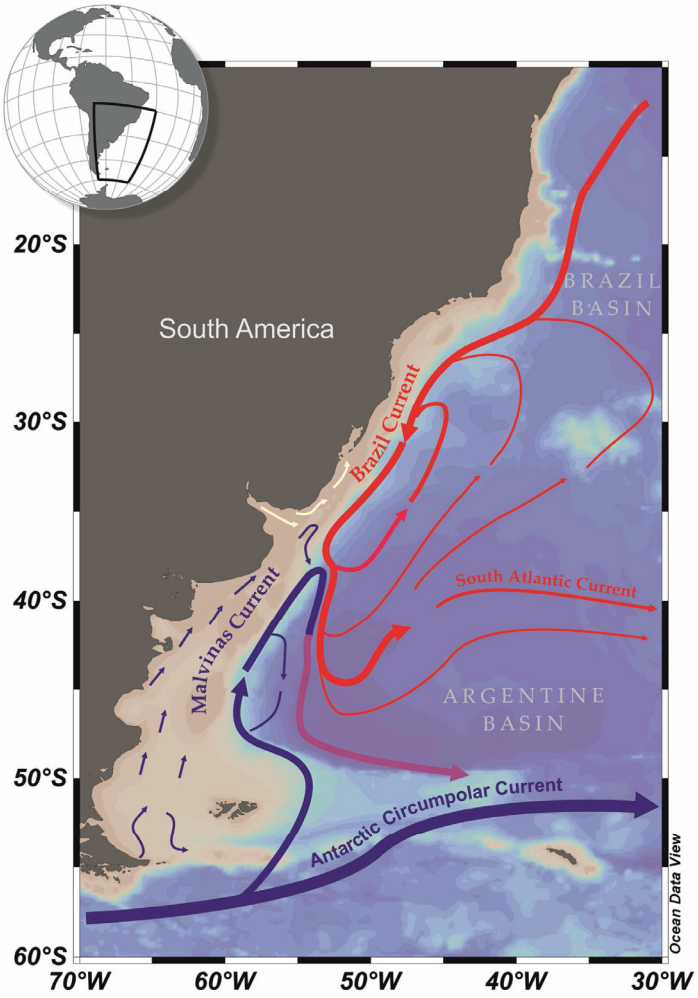

Figure 1 Schematic representation of upper-level circulation of the South Atlantic western boundary currents (*Piola and Matano 2001*). Blue lines represent the (sub)Antarctic water flows, associated with the Antarctic Circumpolar Current (ACC) and the Malvinas-(Falkland) Current. Red lines represent the flow of the subtropical waters associated with the Brazil Current.

generate one of the most energetic regions of the world, the Brazil-Malvinas Confluence (*Gordon, 1989*). In the confluence zone, strong thermal gradients in the (sub)surface waters are observed, often reaching 1 °C/km (*Olson et al., 1988*). After the confluence, both currents turn eastward and flow offshore in a series of large-scale meanders and eddies.

The upper portion of the water mass carried poleward by the Brazil Current is referred to as the South Atlantic Surface Water (SW). The mixed layer of the SW is characterized by high potential temperature (θ > 20 °C) and salinity (S > 37 psu) down to ~100 m water (*Piola and Matano, 2001*) (**Fig. 2A**). Below the SW, but still within the Brazil Current, there is a sharp thermocline and halocline that is referred to as the South Atlantic Central Water (SACW). The SACW is well characterized down to ~600 m water depth and shows rather uniform properties throughout its range and a very stable θ – S pattern (*Stramma and England, 1999*) (**Fig. 2A**).

The upper portion of the water mass carried equatorward by the MC is referred to as Subantarctic Surface Water (SASW) (**Fig. 2B**). The SASW is substantially colder (θ < 15 °C) and fresher (S < 34.2 psu) than the corresponding layer of the Brazil Current (*Piola and Matano, 2001*). Although the SASW of the Malvinas Current and the SACW of the Brazil Current occupy the same density range (σ_θ ~ 25.5 – 27.0 kgm^{-3}), they have very different thermohaline characteristics, which leads to the formation of alternate layers of sub-Antarctic and subtropical water in the BMC (*Piola and Matano, 2001*). The water mass structure of the MC and the BC at intermediate depths (500 -

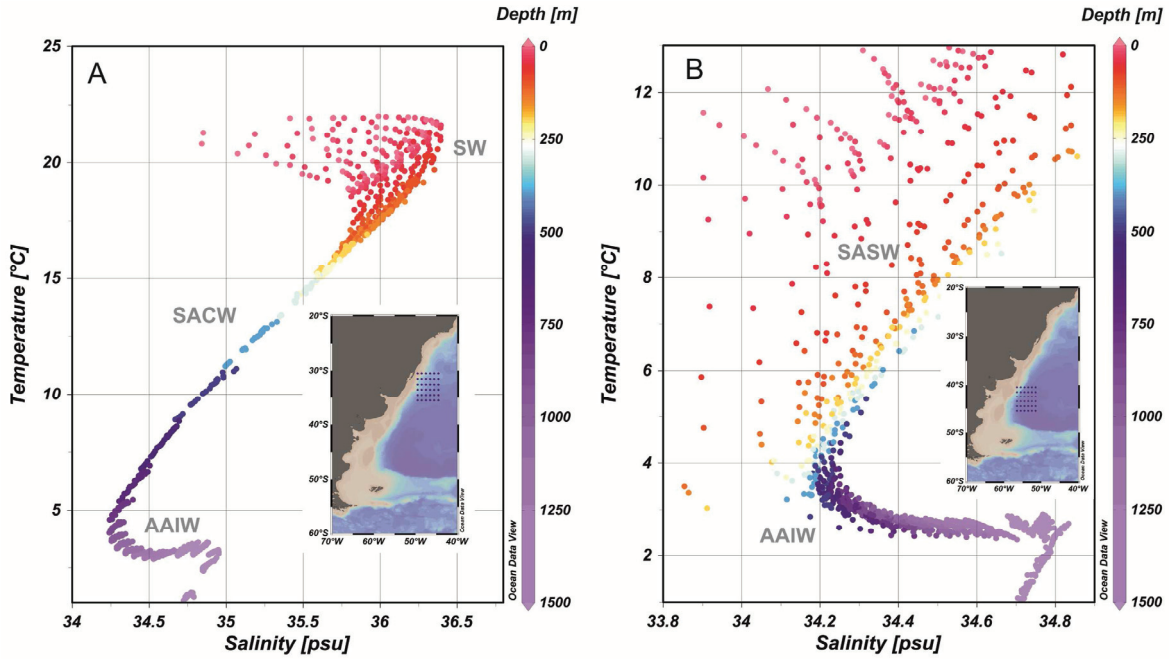

Figure 2 Temperature-salinity diagrams for selected stations in the western South Atlantic (World Ocean Atlas 2009; *Locarnini et al., 2010*). **A:** Temperature-salinity diagram for stations located between 30.5°S and 35.5°S, and 40.5°W and 45.5°W (north of the Brazil-Malvinas Confluence). **B:** Temperature-salinity diagram for selective stations located between 40.5°S and 45.5°S, and 51.5°W and 56.5°W (south of the Brazil-Malvinas Confluence). AAIW - Antarctic Intermediate Water, SACW - South Atlantic Central Water, SASW - Subantarctic Surface Water, SW - South Atlantic Surface Water.

1000 m) is dominated by the presence of the Antarctic Intermediate Water (AAIW) (**Fig. 2A/B**).

A marked seasonal variability in the location of the confluence, up to 900 km along the continental shelf break, has been described by several studies (*Garzoli and Bianchi, 1987; Olson et al., 1988; Garzoli and Garraffo, 1989; Goni and Wainer, 2001*). During austral summer (DJF) the confluence reaches its southernmost extent; while during austral winter (JJA) it reaches its northernmost extent. Seasonal shifts of the BMC can be explained by out-of-phase changes in the mass transport of both the MC and the BC, coupled with a latitudinal displacement of the local wind stress patterns.

1.1.2. Antarctic Intermediate Water Circulation

The circulation of the Antarctic Intermediate Water (AAIW) is thought to make an important contribution to the global ocean–climate system. The mid-depth oxygen maximum and salinity minimum (S ~ 34. psu) layer characterizing AAIW in the South Atlantic is formed around the tip of South America (*e.g., Piola and Gordon, 1989*) (**Fig. 3**). The underlying mechanisms for the formation of AAIW have long been an area of research resulting in a variety of processes that are still under debate (*McCartney, 1977; Georgi, 1979; Molinelli, 1981; Piola and Georgi, 1982; Piola and Gordon, 1989*). It appears to be consensus that AAIW is formed by isopycnal exchange of cold, fresh Antarctic surface water

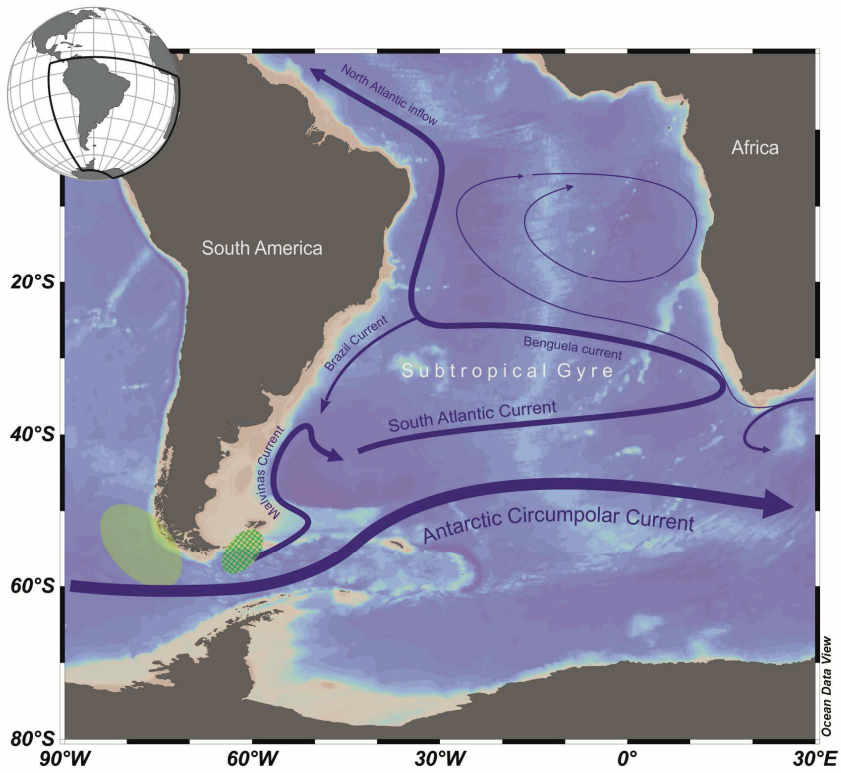

Figure 3 Schematic representation of Antarctic Intermediate Water (AAIW) circulation in the South Atlantic (*Stramma and England 1999*). Main AAIW source region is indicated by the yellow ellipse, and the region of strong mixing by the green ellipse.

across the Antarctic Polar Front (APF), and by contributions of Sub-Antarctic Mode Water (SAMW) that originates from deep winter convection along the Subantarctic Zone (SAZ) (e.g., *Piola and Gordon, 1989*). AAIW is advected through the Drake Passage with the Antarctic Circumpolar Current (ACC) and northward along the South American continent into the adjacent South Atlantic subtropical gyre (**Fig. 3**).

The injection of cool, fresh AAIW into the South Atlantic subtropical gyre is thought to have important implications for the Atlantic heat and salinity budget and possibly the rate of North Atlantic Deep Water (NADW) formation (*Graham et al., 2011*). In the present-day climate, the formation of NADW in the North Atlantic is fed by upper-thermocline water, and in part, by modified less dense AAIW (e.g., *Rintoul, 1991*). AAIW thus supplies a large fraction of the northward flow required to balance the export of NADW, and therefore represents an active player in the Atlantic meridional overturning circulation (AMOC).

In the South Atlantic the AAIW circulate in the wind-driven gyres (**Fig. 3**). The northward injection of AAIW along the base of the wind-driven gyres occurs mainly through lateral advection and along-isopycnal diffusion (*England et al., 1993*). Consequently, vertical and lateral mixing processes modify the properties of AAIW entering the North Atlantic through increasing its salinity and decreasing its dissolved oxygen concentration. A spreading of the AAIW from the South Atlantic to the North Atlantic is identified by a salinity minimum near the equator (*Wüst, 1935*), and can be traced up to 24 °N (*Reid, 1994*). At around 60 °N in the North Atlantic, far from the Antarctic source, and beyond the boundary of the recognizable salinity minimum, AAIW can be traced by a silica maximum (*Tsuchiya, 1989*). The density increase of AAIW, as a consequence from substantial alteration of properties in the water column, is important for a considerable sinking of the AAIW to the NADW depth level in the North Atlantic.

1.1.3. La Plata River

The La Plata is the second largest drainage basin in South America (**Fig. 4**). It drains nearly 20 % of the surface area of South America and discharges about 23,000 m^3/s of freshwater on the western South Atlantic shelf (*Mechoso et al.,*

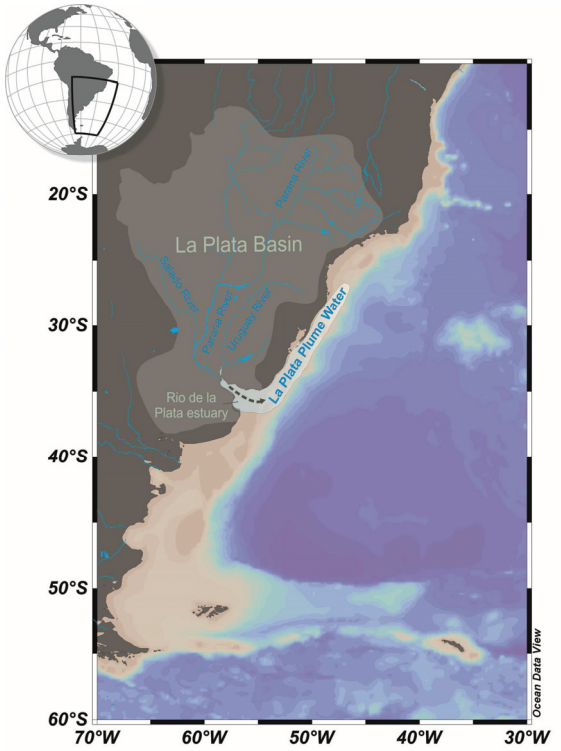

Figure 4 Schematic outflow pattern of the La Plata River plume. Present-day plume extension is directed northward along the Uruguayan and Brazilian shelf (*Piola et al., 2000*).

2001). This freshwater source over the continental shelf influences the pelagic ecosystem by injecting nutrients, and thereby favoring the increase in phytoplankton biomass (*Hubold, 1980a, 1980b ; Carreto et al., 1995*). The present-day extension of the La Plata plume is governed by the seasonal wind regime; the plume extends to the north in winter beyond 30 °S (more than 1000 km), but is limited to 32 °S in summer (*Piola et al., 2005; Piola et al., 2008*). The annual mean plume extension is directed northward (*Piola et al., 2000*) which is also recognized in the sediment distribution off the La Plata estuary, where fluviomarine sediments have been traced on the Uruguayan middle shelf (e.g., along the northern river margin) (*Urien and Ewing, 1974*) (**Fig. 4**). Surface sediments collected to the northeast of the La Plata estuary are thus characterized by high organic carbon concentrations up to three times higher with values exceeding 2.5 % compared to the adjacent areas (*Frenz et al., 2003*).

1.2. Atmospheric circulation

1.2.1. The Southern Westerly Winds

The Southern Westerly Winds (SSW) are the prevailing winds in the Southern Hemisphere mid-latitudes blowing from west to east between the high-pressure areas of the subtropics and the low-pressure area over Antarctica. At the present-day, the SWW influence the region between ~30 °S and ~70 °S, with the strongest wind centred at around ~50 °S. The westerly wind belt is largely symmetric over the Southern Hemisphere, due to the absence of significant land masses to the south of 35 °S. During austral summer (DJF), the northern margin of the westerly wind belt shows a more southward confined pattern, while during austral winter (JJA), it extends further to the north. The SWW are an important component of the global climate system, through the wind-driven upwelling of deep water in the Southern Ocean and the potentially resulting atmospheric CO_2 variations (*Anderson et al., 2009; Toggweiler, 2009*). Changes in the position and strength of SWW may have significant implications for ocean circulation and global climate changes. However, understanding SWW variability along with forcings and feedbacks remains a significant area of investigation.

1.3. Area of Investigation

The Mar del Plata Canyon is a relatively straight, deeply incised feature at the continental margin off northern Argentina at ~38 °S (**Fig. 5**). The canyon is incorporated into a significant Contourite Depositional System (CDS), whose sedimentation processes are primarily controlled by northward-flowing Antarctic water masses, in particular by the Antarctic Intermediate Water (AAIW) (*Hernández-Molina et al., 2009; Preu et al., 2012*). As most of the world's canyons (*Harris and Whiteway, 2011*), the Mar del Plata Canyon does not have an obvious connection to the shelf or an onshore river system (e.g., La Plata River) from where sediment material might be delivered directly to the canyon (*Krastel et al., 2011*). The canyon

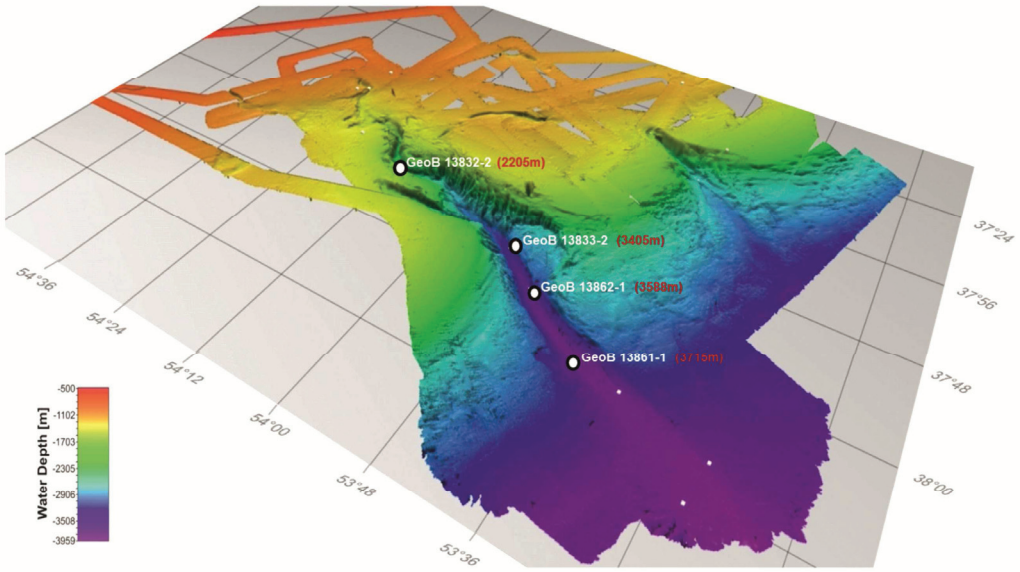

Figure 5 Bathymetric map of the Argentinean continental slope in the vicinity of the Mar del Plata Canyon (see Table 1 for core locations) (*Krastel and Wefer, 2012*).

head is located at a water depth of ~1000 m and extends from there on ~110 km downslope to a water depth of 3900 m. Several gravity cores were recovered from the thalweg of the Mar del Plata Canyon **(Fig. 5, Table. 1**). The cores were collected during research cruise M78/3 a,b with the German RV METEOR (*Krastel and Wefer, 2012*).

Table 1| Sediment cores Mar del Plata

Cruise	Core ID	Latitude	Longitude	Water depth (m)	Recovery (cm)
M78/3a	GeoB13832-2	37°90.23' S	54°14.12' S	2205	556
M78/3a	GeoB13833-2	37°95.20' S	53°83.68' S	3405	796
M78/3b	GeoB13862-1	38°09.18' S	53°60.98' S	3588	1016
M78/3b	GeoB13861-1	38°01.85' S	53°74.50' S	3715	668

1.4. Motivation

The western South Atlantic forms a highly dynamic current region. Along the western boundary of the western South Atlantic strong deep-ocean currents (also referred as contour currents) shape the continental margin significantly by eroding, transporting and depositing sediments at the sea floor. In particular Antarctic water masses generate an association of various depositional (drifts) and erosive features along the continental margin off northern Argentina, which together are described as a Contourite Depositional System (CDS) *(Hernández-Molina et al., 2009*). Although drift deposits are well described from (sub)-recent deposits throughout the world's deep ocean environments (*Rebesco et al., 2008*), submarine canyons incorporated into CDSs have not long been perceived yet. The traditional approach of submarine canyon systems rather implies that sediment discharged by nearby river systems and/or by sediment movements across the continental shelf is carried down the canyon by gravitational mass-wasting processes (i.e.,

sediment gravity flows) associated with glacial/interglacial sea-level oscillations. However, recent studies suggest an infilling of submarine canyons by current activity (i.e., by drift progradation) (*Mulder et al., 2006*). Other studies propose that submarine canyons may significantly alter the hydrodynamics of contour currents (*Marchès et al., 2007*), whereas the details of this interaction are not fully understood. The impact of current activity on the sedimentation processes in the canyon, however, remains speculative. Strong deep-ocean currents such as the Antarctic Intermediate Water (AAIW) in the western South Atlantic may rework/resuspend unconsolidated sediments from the sea floor, and may transport considerable amounts of sediment in suspension, thereby forming a so-called bottom-nepheloid layer (NL). These considerations give rise to a major question: To what extent can a submarine canyon in the western South Atlantic acts as a (temporary) sinks for modern sediments by the interaction with a NL, and therefore can provide a great potential for a climate archive?

1.5. Scientific Objectives

1.5.1. Interaction of the Mar del Plata submarine canyon with the Antarctic Intermediate Water

As most of the world's canyons the Mar del Plata Canyon do not have any obvious connection to the shelf or an onshore river system (*Krastel et al., 2011*) and therefore is isolated from shelf-originated down-slope processes (*Harris and Whiteway, 2011*). The canyon intersects a Contourite Depositional System, whose sedimentation processes are primary influenced by Antarctic water masses (e.g., Antarctic Intermediate Water (AAIW)). That raises the possibility that sediment dynamics in the canyon may be primarily affected by the AAIW.

The first objective of this project therefore is to focus on the sediment deposits in the Mar del Plata Canyon in order to assess a possible interaction with the AAIW.

(1) To assess if the Mar del Plata Canyon interacts with the Antarctic Intermediate Water

A submarine canyon as a climate archive has been addressed only very recently (*Henrich et al., 2010*). If sedimentation processes in the Mar del Plata Canyon are indeed affected by the AAIW then sediment material transported with the AAIW should be traceable in the canyon. In that case the Mar del Plata Canyon may act as a climate archive for past changes in the current strength of AAIW, which in turn can be used to improve the basic understanding of past circulation changes of AAIW in western South Atlantic.

1.5.2. Reconstruction of Antarctic Intermediate Water strength

Grain-size analysis ("sortable silt" paleoflow proxy) (*McCave et al., 1995*) in the Mar del Plata

Canyon may provide a great potential to infer past changes in AAIW formation and ocean circulation strength in the western South Atlantic. The present interglacial, the Holocene, is of particular interest because the role of AAIW in the global ocean-climate system during the Holocene remains poorly understood. Recent progress in understanding natural variability of AAIW is mainly based on climate model simulations showing that increased westerly wind field drives ocean cooling and freshening via (respectively) air-sea and ice-ocean fluxes and thus contribute directly to AAIW formation (*Ribbe, 2001; Saenko and Weaver, 2001; Santoso and England, 2004*). The correlation to wind stress implies that natural variability of AAIW strongly depends upon wind forcing and indicates a high sensitivity to Southern Hemisphere climate changes. However, the influence of the SWW on the intermediate water circulation during the Holocene remains speculative. The following objective aims to test the hypothesis of a SWW-AAIW linkage during the Holocene.

(2) To determine the response in AAIW formation and circulation to changes in the strength/position of SWW during the Holocene.

The circulation of AAIW is thought to make an important contribution to the Atlantic meridional overturning circulation (AMOC). The potential role the AAIW plays in contributing changes in the AMOC makes it important to understand its natural variability and the underlying mechanisms involved in its formation. A possible change in AAIW formation and circulation may significantly impact the variability of the AMOC.

3) Determine the response in AMOC to changes in AAIW formation and circulation

1.5.3. Response of BMC to changes in the strength/position of SWW

However, there is surprisingly little systematic knowledge about past variations of the SWW during the Holocene. Proxy-based reconstructions of the paleo-SWW have been discussed controversially, in which contradicting results regarding the strength and/or the position of the SWW (*Fletcher and Moreno, 2012*). Hence, understanding Holocene variability of the SWW along with forcings and feedbacks remains a significant challenge in climate research. The tight coupling between the Brazil-Malvinas Confluence (BMC) and the local wind field (*Oke and England, 2004; Sijp and England, 2008; Lumpkin and Garzoli, 2011*) makes the BMC frontal system ideal for reconstruction of past variability of the SWW and thus provide a great potential to infer past changes in the SWW belt. A north–south transect of three marine $\delta^{18}O$ cores (GeoB6211, GeoB13862-1, GeoB6308) from the mid-latitudes of the western South Atlantic that covers the present extent of the BMC may enable to record past shifts of the BMC throughout the Holocene (*Chiessi et al., 2007*). The expected shifts of BMC are thought as a direct response to the local

wind field, and may provide a reconstruction of SWW variability during the Holocene.

4) Determine N-S shifts of Brazil- Malvinas Confluence in response to the local wind field

In particular the coupling processes between the SWW and the ocean are important in global climate and are critical in understanding the complexity of global climate changes. To valid ocean circulation changes in the western South Atlantic (e.g., AAIW, BMC) in the context of large-scale atmosphere circulation changes in the Southern Hemisphere may provide new insights into the Southern Hemisphere ocean-climate system during the Holocene

1.6. Paleoceanographic Proxies

1.6.1. Grain-size - Sortable Silt

The most useful sedimentological technique is grain-size analysis. The use of grain size, and its link to bottom-current strength was first suggested by *Ellwood and Ledbetter (1977)* showing a direct relationship between subtle changes in mean particle size in the silt fraction (2-63 μm) and bottom-current strength. *McCave et al., (1995)* took this technique a step further, identifying the "sortable silt" fraction (i.e., terrigenous 10-63 μm fraction); the fraction of the sediment whose size sorting varies in response to hydrodynamic processes (**Fig. 6**). The sortable silt was proposed as a more sensitive indicator of bottom-current strength than the total 2-63 μm "silt mean size" of *(Ellwood and Ledbetter, 1977)*, which included cohesive material (2-10 μm). The cohesive material is dominantly deposited as aggregates, and therefore is not a simple function of the processes responsible for their transport and deposition, and this limits their usefulness for paleocurrent reconstructions.

The relations between bottom-current strength and the "sortable silt" fraction includes some important concepts:

- Shear stress is a function of current velocity
- Settling velocity is a function of grain size
- As currents strengthen, shear stress increases along the seafloor and particles can become reworked/ resuspended. As currents weaken, particles settle out and redeposit on the seafloor

Strong currents can thus generate a turbulent boundary layer above the seafloor, the so-called bottom nepheloid layer (NL). Thereby, the particles can get sorted based on their settling velocity and can either transported within the NL or can settle out.

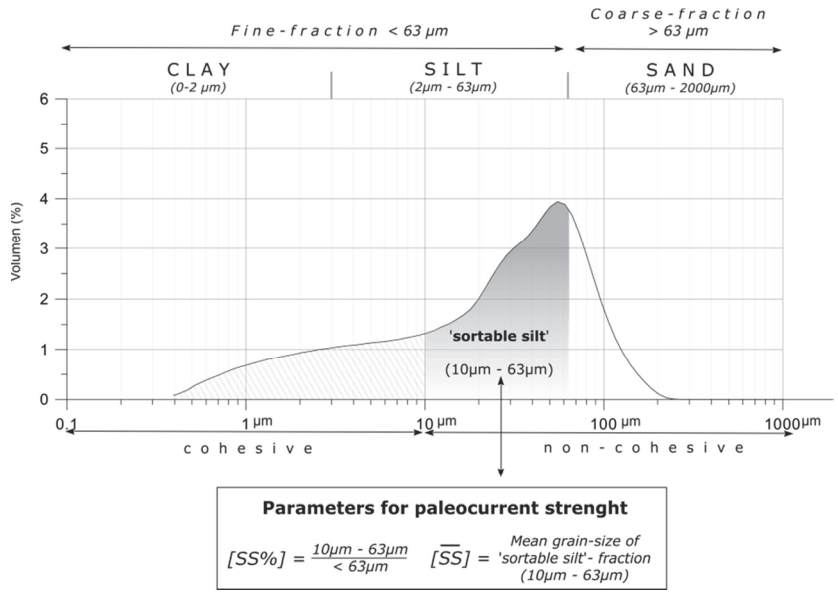

Figure 6 "Sortable silt" parameters that respond to changes in current strength.

The deposited sediment on the ocean floor can in turn be examined to determine properties of the ocean currents, whereas the sorting in the sediment reflects the relative bottom-current strength. Accordingly, the weight percentage (SS%) and mean size ($\overline{SS}$) of the 10–63 µm terrigenous silt fraction have been argued to be proxies for near-bottom paleocurrent intensity, where higher values reflect stronger near-bottom flow, and vice versa (*McCave et al., 1995*) (**Fig. 6**). The biogenic material (i.e., carbonate, opal, and organic matter) is not considered because it may be delivered by pelagic sedimentation from the overlying surface waters and therefore has to be removed.

Accordingly, a number of paleoceanographic studies have been undertaken by using the "sortable silt" in the North Atlantic (e.g., *Bianchi and McCave, 1999; Hall et al., 2004*), South Atlantic (e.g., *Kuhn and Diekmann, 2002*), Indian (e.g., *McCave et al., 2005*) and Pacific oceans (e.g., *Hall et al., 2001*).

1.6.2. Stable isotopes measurements

Urey (1947) and *Emiliani (1954, 1955)* pioneered the use of the stable oxygen isotope composition ($\delta^{18}O$) of planktonic foraminifera to reconstruct paleotemperatures. Today, $\delta^{18}O$ of the foraminiferal shells is one of the most powerful tools to reconstruct paleoenvironmental changes of the global surface ocean.

Oxygen bears three stable isotopes that appear in certain proportions compared to each other. The lightest isotope ^{16}O is the most abundant (99.76 %), whereas ^{17}O and ^{18}O account for only 0.04 % and 0.2 %, respectively. The various isotopes have slightly different chemical and physical properties because of their mass differences. However, for paleoclimate studies only ^{16}O and ^{18}O are used.

The oxygen isotope composition of a sample ($\delta^{18}O$) is given by ^{18}O:^{16}O ratio and is expressed as the deviation relative to a standard:

$$\delta^{18}O\ (‰) = \left[\frac{(^{18}O/^{16}O)_{sample} - (^{18}O/^{16}O)_{standard}}{(^{18}O/^{16}O)_{standard}} \right] * 1000$$

The resulting values are expressed in per mil (‰) units; negative values represent lower ratios in the sample (i.e., less ^{18}O than ^{16}O and, therefore, isotopically lighter) and positive values represent higher ratios in the sample (more ^{18}O than ^{16}O and, therefore, isotopically heavier).

The reconstruction of paleoenvironmental changes from the analysis of foraminiferal shells is thereby based on the assumption that the ^{18}O:^{16}O ratio stored in the carbonate shell reflects the ratio of the seawater, modified by the temperature of the sea water (through fractionation of the ^{18}O and ^{16}O isotopes). The $\delta^{18}O$ of planktonic foraminifera is thus primarily a function of ambient temperature and the isotopic composition of the seawater in which foraminiferal calcification takes place. The relationship is expressed by the paleotemperature equation of the following format (*Shackleton, 1974*):

$$T = 16.9 - 4.38\ (\delta^{18}O_{calcite} - \delta^{18}O_{seawater}) + 0.1\ (\delta^{18}O_{calcite} - \delta^{18}O_{seawater})^2$$

Where T is the in-situ temperature during calcification (°C), $\delta^{18}O_{calcite}$ represents the oxygen isotopic composition of the calcite (‰, VPDB) and $\delta^{18}O_{seawater}$ for the oxygen isotopic composition (‰, VPDB) of the seawater in which the calcification takes place (often assumed for the past) (*Urey, 1947; Epstein et al., 1953; Shackleton, 1974*).

Temperature effect

The $\delta^{18}O$ of planktonic foraminifera ($\delta^{18}O_{calcite}$) is determined by the temperature dependant fractionation between ^{16}O and ^{18}O that occurs during the production of solid $CaCO_3$ ("carbonate precipitation"). If carbonate precipitation takes place in the chemical equilibrium with the seawater, then ^{18}O is slightly concentrated in the foraminiferal shell relative to that in seawater. This process is temperature dependent, with the concentrating effect diminishing as the temperature of the seawater increases. Accordingly, high $\delta^{18}O_{calcite}$ values coincide with cold waters relative to low $\delta^{18}O_{calcite}$ values corresponding to warm waters.

Salinity effect

The $\delta^{18}O$ of planktonic foraminifera is also controlled by the isotopic composition of the seawater ($\delta^{18}O_{seawater}$) in which carbonate precipitation takes place. The $\delta^{18}O_{seawater}$ is in turn intimately linked with the hydrological cycle including evaporation and subsequent return of freshwater to the ocean (directly via precipitation and via runoff/iceberg melting). Thus, changes in $\delta^{18}O_{seawater}$ depend primarily on the evaporation-precipitation (E-P) balance. That is also described as the 'salinity effect' because both salinity variations and $\delta^{18}O_{seawater}$ respond to E – P patterns (*Craig and Gordon, 1965*). The relationship between $\delta^{18}O_{seawater}$ and salinity varies considerably throughout the ocean. Accordingly, high salinities and high $\delta^{18}O_{seawater}$ values generally occur at low

latitudes, and low salinities and low $\delta^{18}O_{seawater}$ values are found at high latitudes.

Global ice volume effect

Throughout the Quaternary large variations in the $\delta^{18}O_{seawater}$ were driven by fluctuations in the continental ice volume in response to glacial/interglacial climate variability. Under glacial conditions, a greater than normal proportion of the earth's water was locked up in isotopically very light glacial ice. This means that the remaining sea water was isotopically heavier than normal (i.e., $\delta^{18}O_{seawater}$ was higher than normal). This so called global "ice volume effect" was estimated to be about 1.3‰ for the last deglaciation (*Fairbanks, 1989*), and these changes have to be considered when SSTs are reconstructed from the $\delta^{18}O$ of planktonic foraminifera.

Secondary effects

However, the $\delta^{18}O$ of planktonic foraminifera is not only controlled by the physical/chemical properties of the water column (e.g., temperature, isotopic composition of the ambient water), but also by the impact of life processes, such as calcification, respiration and photosynthesis of the symbiotic algae (collectively known as "vital effects") (*Duplessy et al., 1970*). These vital effects cause deviations from the oxygen isotopic equilibrium with the ambient seawater, and differ from one species of foraminifera to another.

Dwelling Globorotalia inflata

Each planktonic foraminifer species favors certain environmental settings, with respect to temperature, salinity, nutrient and light conditions (*Hemleben et al., 1989*). Deep-dwelling planktonic foraminifera inhabit the top few hundred meters of the ocean (*Bé, 1977*) and constitute potential recorders of thermocline conditions (*Fairbanks et al., 1982; Cléroux et al., 2007*). Globorotalia inflata is one of the most abundant deep-dwelling transitional water species in the South Atlantic (*Bé and Hutson, 1977; Niebler and Gersonde, 1998*) and lives in waters with a temperature range between 8-18 °C (e.g., *Bé and Hamlin, 1967*). Its occurrence in the western South Atlantic amounts to >20 % of the total planktonic foraminiferal assemblage in surface sediments between 30-50 °S. During its ontogenetic cycle, G. inflata migrates through the upper few hundred meters of the water column (e.g., *Lončarić et al., 2006; Wilke et al., 2006; Cléroux et al., 2007*). Thereby, G. inflata adds a secondary calcite crust to its primary calcite test at greater depth (e.g., *Caron et al., 1990*) which can significantly affect the shell chemistry. Although maximum abundances of G. inflata often occur within the thermocline (e.g., *Fairbanks et al., 1982*), calcification of the tests takes place from the surface mixed layer to water depths possibly deeper than 500 m (e.g., *Wilke et al., 2006*). Evidences for shell chemistry changes by addition of secondary calcite during ontogeny make a careful selection of individual G. inflata specimens important when using them for geochemical proxy analyses. However, the apparent calcification depth of G. inflata in the western South Atlantic mid-latitudes is constant with a depth of 350-400 m within the permanent thermocline (*Groeneveld and Chiessi,*

2011). Thus, even under considerably different upper water column structures, G. inflata provides great potential of recording past thermocline conditions as well as variations of oceanic fronts (i.e., Brazil-Malvinas Confluence Zone) (*Chiessi et al., 2007*) which highlights its applicability in paleoceanographic research.

1.7. Outline

The main part of this dissertation is divided into three manuscripts which are under review or will soon be submitted to peer-reviewed international scientific journals.

The first manuscript (**Chapter 2**) - *A submarine canyon as a climate archive- Interaction of the Antarctic Intermediate Water with the Mar del Plata Canyon (Southwest Atlantic)* - highlights the interaction of the Mar del Plata Canyon with an intermediate nepheloid layer generated by the Antarctic Intermediate Water (AAIW) in the western South Atlantic. We present a new conceptual model for sedimentation processes taking place in submarine canyons located at current-influenced continental margins. Due to the interaction with the AAIW the Mar del Plata canyon act as a (temporary) sink for enhanced accumulation of modern sediments, and thus constitutes a great climate archive in the western South Atlantic, where high temporal-resolution sediment records are virtually absent.

In the second manuscript (**Chapter 3**) – *Holocene millennial-scale oscillations of Antarctic Intermediate Water strength* - a high temporal resolution reconstruction of Holocene changes in the AAIW circulation is presented. Due to the interaction of the AAIW with the Mar del Plata Canyon, sedimentation rates and particle sizes in the canyon are linked directly to changes in current strength of AAIW. The "sortable silt" paleoflow proxy of the sediment core GeoB13862-1 enables a detailed reconstruction of millennial- to orbital scale changes in the AAIW formation and circulation and provides insights into forcing- and feedback mechanisms during the Holocene. Studies of AAIW variability, especially for the Holocene, are of great interest as the formation and circulation of AAIW is thought to make an important contribution to the global ocean-climate system.

The third manuscript (**Chapter 4**) - *Holocene oscillations of Southern Westerly Winds in response to North Atlantic climate perturbations* - focusses on the time-space variability of the Brazil-Malvinas Confluence (BMC), a prominent feature in the upper-level circulation of the western South Atlantic. The reconstruction is based on three $\delta^{18}O$ records (GeoB6211, GeoB13862-1, GeoB6308) of planktonic foraminifer *G. inflata* situated along a north–south transect that covers the present extent of the BMC. The tight coupling between the confluence and the local wind field make the BMC a high sensitivity region for past shifts of the Southern Westerly Wind (SWW). In this context reconstructions of BMC frontal region allowing a reliable proxy for past variation of the SWW. The results enable a detailed discussion about the underlying forcing mechanisms of latitudinal shifts of the SWW and provide insights into the role of an interhemispheric climate link during the Holocene.

1.8. References

Anderson, R.F., Ali, S., Bradtmiller, L.I., Nielsen, S.H.H., Fleisher, M.Q., Anderson, B.E., Burckle, L.H., 2009. Wind-Driven Upwelling in the Southern Ocean and the Deglacial Rise in Atmospheric CO2. Science 323 (5920), 1443-1448.

Bé, A.W.H., 1977. An ecological, zoogeographic and taxonomic review of recent planktonic foraminifera In: Ramsay A.T.S. (Ed.) Oceanic Micropaleontology. Academic, San Diego, Calif.

Bé, A.W.H., Hamlin, W.H., 1967. Ecology of Recent Planktonic Foraminifera: Part 3: Distribution in the North Atlantic during the Summer of 1962. Micropaleontology 13 (1), 87-106.

Bé, A.W.H., Hutson, W.H., 1977. Ecology of Planktonic Foraminifera and Biogeographic Patterns of Life and Fossil Assemblages in the Indian Ocean. Micropaleontology 23 (4), 369-414.

Bianchi, G.G., McCave, I.N., 1999. Holocene periodicity in North Atlantic climate and deep-ocean flow south of Iceland. Nature 397 (6719), 515-517.

Bond, G., Kromer, B., Beer, J., Muscheler, R., Evans, M.N., Showers, W., Hoffmann, S., Lotti-Bond, R., Hajdas, I., Bonani, G., 2001. Persistent Solar Influence on North Atlantic Climate During the Holocene. Science 294 (5549), 2130-2136.

Caron, D.A., Roger Anderson, O., Lindsey, J.L., Faber Jr, W.W., Lin Lim, E.E., 1990. Effects of gametogenesis on test structure and dissolution of some spinose planktonic foraminifera and implications for test preservation. Marine Micropaleontology 16 (1–2), 93-116.

Carreto, J., A. Lutz, V., Carignan, M.O., Cucchi Colleoni, A.D., De Marco, S.G., 1995. Hydrography and chlorophyll a in a transect from the coast to the shelf-break in the Argentinian Sea. Continental Shelf Research 15 (2–3), 315-336.

Chiessi, C.M., Ulrich, S., Mulitza, S., Pätzold, J., Wefer, G., 2007. Signature of the Brazil-Malvinas Confluence (Argentine Basin) in the isotopic composition of planktonic foraminifera from surface sediments. Marine Micropaleontology 64 (1–2), 52-66.

Cléroux, C., Cortijo, E., Duplessy, J.-C., Zahn, R., 2007. Deep-dwelling foraminifera as thermocline temperature recorders. Geochem. Geophys. Geosyst. 8 (4), Q04N11.

Craig, H., Gordon, L.I., 1965. Deuterium and oxygen-18 variations in the ocean and the marine atmosphere. In: Tongiorgi, E. (Ed.) Stable isotope in oceanographic studies and paleotemperatures. Spoleto, Pisa (Consiglio Nazionale delle Ricerche, Laboratorio di Geologia Nucleare).

Duplessy, J.C., Lalou, C., Vinot, A.C., 1970. Differential Isotopic Fractionation in

Benthic Foraminifera and Paleotemperatures Reassessed. Science 168 (3928), 250-251.

Ellwood, B.B., Ledbetter, M.T., 1977. Antarctic bottom water fluctuations in the Vema Channel: Effects of velocity changes on particle alignment and size. Earth and Planetary Science Letters 35 (2), 189-198.

Emiliani, C., 1954. Depth habitats of some species of pelagic Foraminifera as indicated by oxygen isotope ratios. American Journal of Science 252 (3), 149-158.

Emiliani, C., 1955. Pleistocene Temperatures. The Journal of Geology 63 (6), 538-578.

England, M.H., Godfrey, J.S., Hirst, A.C., Tomczak, M., 1993. The Mechanism for Antarctic Intermediate Water Renewal in a World Ocean Model. Journal of Physical Oceanography 23 (7), 1553-1560.

Epstein, S., Buchsbaum, R., Lowenstam, H.A., Urey, H.C., 1953. Revised carbonate-water isotopic temperature scale Geological Society of America Bulletin 64 (11), 1315-1326.

Fairbanks, R.G., 1989. A 17,000-year glacio-eustatic sea level record: influence of glacial melting rates on Younger Dryas event and deep-ocean circulation. Nature 342, 637-642.

Fairbanks, R.G., Sverdlove, M., Free, R., Wiebe, P.H., Be, A.W.H., 1982. Vertical distribution and isotopic fractionation of living planktonic foraminifera from the Panama Basin. Nature 298 (5877), 841-844.

Fletcher, M.-S., Moreno, P.I., 2012. Have the Southern Westerlies changed in a zonally symmetric manner over the last 14,000 years? A hemisphere-wide take on a controversial problem. Quaternary International 253 (0), 32-46.

Frenz, M., Henrich, R., Höppner, R., Stuut, J.-B., Wagner, T., 2003. Surface sediment bulk geochemistry and grain-size composition related to oceanic circulation along the South American continental margin in the Southwest Atlantic. In: Wefer, G., Mulitza, S., Ratmeyer, V. (Eds.), The South Atlantic in the Late Quaternary: Reconstruction of Material Budget and Current Systems. Springer, Berlin.

Garzoli, S.L., Bianchi, A., 1987. Time-Space Variability of the Local Dynamics of the Malvinas-Brazil Confluence as Revealed by Inverted Echo Sounders. J. Geophys. Res. 92 (C2), 1914-1922.

Garzoli, S.L., Garraffo, Z., 1989. Transports, frontal motions and eddies at the Brazil-Malvinas currents confluence. Deep Sea Research Part A. Oceanographic Research Papers 36 (5), 681-703.

Georgi, D.T., 1979. Modal Properties of Antarctic Intermediate Water in the Southeast Pacific and the South Atlantic. Journal of Physical Oceanography 9 (3), 456-468.

Goni, G.J., Wainer, I., 2001. Investigation of the Brazil Current front variability from

altimeter data. J. Geophys. Res. 106 (C12), 31117-31128.

Gordon, A.L., 1989. Brazil-Malvinas Confluence–1984. Deep Sea Research Part A. Oceanographic Research Papers 36 (3), 359-384.

Graham, J., Stevens, D., Heywood, K., Wang, Z., 2011. North Atlantic climate responses to perturbations in Antarctic Intermediate Water. Climate Dynamics 37 (1-2), 297-311.

Groeneveld, J., Chiessi, C.M., 2011. Mg/Ca of Globorotalia inflata as a recorder of permanent thermocline temperatures in the South Atlantic. Paleoceanography 26 (2), PA2203.

Hall, I.R., Bianchi, G.G., Evans, J.R., 2004. Centennial to millennial scale Holocene climate-deep water linkage in the North Atlantic. Quaternary Science Reviews 23 (14–15), 1529-1536.

Hall, I.R., McCave, I.N., Shackleton, N.J., Weedon, G.P., Harris, S.E., 2001. Intensified deep Pacific inflow and ventilation in Pleistocene glacial times. Nature 412 (6849), 809-812.

Harris, P.T., Whiteway, T., 2011. Global distribution of large submarine canyons: Geomorphic differences between active and passive continental margins. Marine Geology 285 (1–4), 69-86.

Hemleben, C., Spindler, M., Anderson, O.R., 1989. Modern Planktonic Foraminifera. Springer, New York

Henrich, R., Cherubini, Y., Meggers, H., 2010. Climate and sea level induced turbidite activity in a canyon system offshore the hyperarid Western Sahara (Mauritania): The Timiris Canyon. Marine Geology 275 (1–4), 178-198.

Hernández-Molina, F.J., Paterlini, M., Violante, R., Marshall, P., de Isasi, M., Somoza, L., Rebesco, M., 2009. Contourite depositional system on the Argentine Slope: An exceptional record of the influence of Antarctic water masses. Geology 37 (6), 507-510.

Hubold, G., 1980a. Hydrography and plankton off southern Brazil and Rio de la Plata, spring cruise: August–November 1978. Atlântica 4, 1– 22.

Hubold, G., 1980b Second report on hydrography and plankton off southern Brazil and Rio de la Plata, autumn cruise: April– June 1978. Atlântica 4, 23–42.

Krastel, S., Wefer, G., 2012 Report and preliminary results of RV METEOR Cruise M78/3. Sediment transport off Uruguay and Argentina: from the shelf to the deep sea ; 19.05.2009 – 06.07.2009, Montevideo (Uruguay) – Montevideo (Uruguay) Berichte aus dem Fachbereich Geowissenschaften 285 (Fachbereich Geowissenschaften, Bremen).

Krastel, S., Wefer, G., Hanebuth, T., Antobreh, A., Freudenthal, T., Preu, B., Schwenk, T., Strasser, M., Violante, R., Winkelmann, D., party, M.s.s., 2011. Sediment dynamics and geohazards off Uruguay and the de la Plata River region (northern Argentina and Uruguay). Geo-Marine Letters 31 (4), 271-283.

Kuhn, G., Diekmann, B., 2002. Late Quaternary variability of ocean circulation in the southeastern South Atlantic inferred from the terrigenous sediment record of a drift deposit in the southern Cape Basin (ODP Site 1089). Palaeogeography, Palaeoclimatology, Palaeoecology 182 (3–4), 287-303.

Locarnini, R.A., Mishonov, A.V., Antonov, J.I., Boyer, T.P., Garcia, H.E., Baranova, O.K., Zweng, M.M., Johnson, D.R., 2010. World Ocean Atlas 2009. Volume 1: Temperature. S. Levitus, Ed. NOAA Atlas NESDIS 68, U.S. Government Printing Office, Washington, D.C., 184 pp.

Lončarić, N., Peeters, F.J.C., Kroon, D., Brummer, G.-J.A., 2006. Oxygen isotope ecology of recent planktic foraminifera at the central Walvis Ridge (SE Atlantic). Paleoceanography 21 (3), PA3009.

Lumpkin, R., Garzoli, S., 2011. Interannual to decadal changes in the western South Atlantic's surface circulation. J. Geophys. Res. 116 (C1), C01014.

Marchès, E., Mulder, T., Cremer, M., Bonnel, C., Hanquiez, V., Gonthier, E., Lecroart, P., 2007. Contourite drift construction influenced by capture of Mediterranean Outflow Water deep-sea current by the Portimão submarine canyon (Gulf of Cadiz, South Portugal). Marine Geology 242 (4), 247-260.

McCartney, M.S., 1977. Subantarctic Mode Water. A Voyage of Discovery: George Deacon 70th Anniversary Volume (Suppl. to Deep-Sea Res.).

McCave, I.N., Manighetti, B., Robinson, S.G., 1995. Sortable Silt and Fine Sediment Size/Composition Slicing: Parameters for Palaeocurrent Speed and Palaeoceanography. Paleoceanography 10 (3), 593-610.

McCave, I.N., Kiefer, T., Thornalley, D.J.R., Elderfield, H., 2005. Deep flow in the Madagascar–Mascarene Basin over the last 150000 years. Philosophical Transactions of the Royal Society A: Mathematical, Physical and Engineering Sciences 363 (1826), 81-99.

Mechoso, C.R., Dias, P.S., Baethgen, W., Barros, V., Berbery, E.H., Clarke, R., Cullen, H., Ereño C., Grassi, B., Lettenmaier, D., 2001. Climatology and hydrology of the Plata Basin, a document of VAMOS Scientific Study Group on the Plata Basin. (Available at *http://www.clivar.org/science/vamos_pubs.htm*).

Molinelli, 1981. The Antarctic influence on Antarctic Intermediate Water. Journal of Marine Research 39, 267–293.

Mulder, T., Lecroart, P., Hanquiez, V., Marches, E., Gonthier, E., Guedes, J.C., Thiébot, E., Jaaidi, B., Kenyon, N., Voisset, M., Perez, C., Sayago, M., Fuchey, Y., Bujan, S., 2006. The western part of the Gulf of Cadiz: contour currents and turbidity currents interactions. Geo-Marine Letters 26 (1), 31-41.

Niebler, H.S., Gersonde, R., 1998. A planktic foraminiferal transfer function for the

southern South Atlantic Ocean. Marine Micropaleontology 34 (3–4), 213-234.

Oke, P.R., England, M.H., 2004. Oceanic Response to Changes in the Latitude of the Southern Hemisphere Subpolar Westerly Winds. Journal of Climate 17 (5), 1040-1054.

Olson, D.B., Podestá, G.P., Evans, R.H., Brown, O.B., 1988. Temporal variations in the separation of Brazil and Malvinas Currents. Deep Sea Research Part A. Oceanographic Research Papers 35 (12), 1971-1990.

Peterson, R.G., Stramma, L., 1991. Upper-level circulation in the South Atlantic Ocean. Progress In Oceanography 26 (1), 1-73.

Piola, A.R., Georgi, D.T., 1982. Circumpolar properties of Antarctic intermediate water and Subantarctic Mode Water. Deep Sea Research Part A. Oceanographic Research Papers 29 (6), 687-711.

Piola, A.R., Gordon, A.L., 1989. Intermediate waters in the southwest South Atlantic. Deep Sea Research Part A. Oceanographic Research Papers 36 (1), 1-16.

Piola , A.R., Matano, R.P., 2001. Brazil and Falklands (Malvinas) Currents. In: Steele JH, Thorpe SA, Turekian KK (eds) Encyclopedia of Ocean Sciences. Academic Press, (San Diego,), pp 340-349

Piola, A.R., Romero, S.I., Zajaczkovski, U., 2008. Space–time variability of the Plata plume inferred from ocean color. Continental Shelf Research 28 (13), 1556-1567.

Piola, A.R., Campos, E.J.D., Möller, O.O., Jr., Charo, M., Martinez, C., 2000. Subtropical Shelf Front off eastern South America. J. Geophys. Res. 105 (C3), 6565-6578.

Piola, A.R., Matano, R.P., Palma, E.D., Möller, O.O., Jr., Campos, E.J.D., 2005. The influence of the Plata River discharge on the western South Atlantic shelf. Geophys. Res. Lett. 32 (1), L01603.

Preu, B., Hernández-Molina, F.J., Violante, R., Piola, A., Paterlini, C.M., Schwenk, T., Voigt, I., Krastel, S., Spieß, V., 2012 Morphosedimentary and hydrographic features of the northern Argentine margin: the interplay between erosive, depositional and gravitational processes and its conceptual implications. Deep-Sea Research Part I.

Rebesco, M., Camerlenghi, A., Van Loon, A.J., 2008. Chapter 1 Contourite Research: A Field in Full Development. In: Rebesco, M., Camerlenghi, A. (Eds.), Developments in Sedimentology. Elsevier, pp. 1-10.

Reid, J.L., 1994. On the total geostrophic circulation of the North Atlantic Ocean: Flow patterns, tracers, and transports. Progress in Oceanography 33 (1), 1-92.

Ribbe, J., 2001. Intermediate water mass production controlled by southern hemisphere winds. Geophys. Res. Lett. 28 (3), 535-538.

Rintoul, S.R., 1991. South Atlantic Interbasin Exchange. J. Geophys. Res. 96 (C2), 2675-2692.

Saenko, O.A., Weaver, A.J., 2001. Importance of wind‐driven sea ice motion for the formation of Antarctic Intermediate Water in a global climate model. Geophys. Res. Lett. 28 (21), 4147-4150.

Santoso, A., England, M.H., 2004. Antarctic Intermediate Water Circulation and Variability in a Coupled Climate Model. Journal of Physical Oceanography 34 (10), 2160-2179.

Shackleton, N., 1974 Attainment of isotopic equilibrium between ocean water and the benthonic foraminifera genus Uvigerina: Isotopic changes in the ocean during the last glacial. Colloq. Int. C.N.R.S. 219, 203-209.

Sijp, W.P., England, M.H., 2008. The effect of a northward shift in the southern hemisphere westerlies on the global ocean. Progress in Oceanography 79 (1), 1-19.

Stramma, L., England, M., 1999. On the water masses and mean circulation of the South Atlantic Ocean. J. Geophys. Res. 104 (C9), 20863-20883.

Toggweiler, J.R., 2009. Shifting Westerlies. Science 323 (5920), 1434-1435.

Tsuchiya, M., 1989. Circulation of the Antartic Intermediate Water in the North Atlantic Ocean. Journal of Marine Research 47, 747-755.

Urey, H.C., 1947. The thermodynamic properties of isotopic substances. Journal of the Chemical Society 562-581

Urien, C.M., Ewing, M., 1974. Recents sediments and environment of Southern Brasil, Uruguay, Buenos Aires and Rio Negro continental shelf. In: Burk, C.A., Drake, C. (Eds.), Geology of continental margins. Springer-Verlag, Berlin

Vivier, F., Provost, C., 1999. Volume transport of the Malvinas Current: Can the flow be monitored by TOPEX/POSEIDON? J. Geophys. Res. 104 (C9), 21105-21122.

Wanner, H., Solomina, O., Grosjean, M., Ritz, S.P., Jetel, M., 2011. Structure and origin of Holocene cold events. Quaternary Science Reviews 30 (21–22), 3109-3123.

Wilke, I., Bickert, T., Peeters, F.J.C., 2006. The influence of seawater carbonate ion concentration [CO32−] on the stable carbon isotope composition of the planktic foraminifera species Globorotalia inflata. Marine Micropaleontology 58 (4), 243-258.

Wüst, G., 1935. Die Stratosphäre. Wissenschaftliche Ergebnisse der Deutschen Atlantischen Expedition auf dem Vermessungs- und Forschungsschiff "Meteor" 1925-1924, 6:109-288.

Chapter 1

Chapter 2: A submarine canyon as a climate archive- Interaction of the Antarctic Intermediate Water with the Mar del Plata Canyon (Southwest Atlantic)

Ines Voigt[1], Ruediger Henrich[1], Benedict M. Preu[1], Alberto R. Piola[2], Till J.J. Hanebuth[1], Tilmann Schwenk[2], Cristiano M. Chiessi[3]

[1]MARUM –Center for Marine Environmental Sciences and Faculty of Geosciences, University of Bremen, D-28359 Bremen, Germany

[2] Servicio de Hidrografia Naval (SHN), Buenos Aires, Argentina

[3]School of Arts, Sciences and Humanities, University of São Paulo, Brazil

(*Manuscript submitted to Marine Geology*)

2.3. Abstract

The Mar del Plata Canyon is located at the continental margin off northern Argentina in a key intermediate and deep-water oceanographic setting. In this region, strong contour currents shape the continental margin by eroding, transporting and depositing sediments. They generate various depositional and erosive features, which together are described as a Contourite Depositional System (CDS). The Mar del Plata Canyon intersects the CDS, and does not have any obvious connection to the shelf or to an onshore sediment source. Here we present the dynamics, dispersal and accumulation processes of sediments in the canyon and show that continuous Holocene sedimentation is related to deep-water current activity. The Holocene deposits in the canyon are strongly bioturbated and consist mainly of coarse silt (i.e. "sortable silt" fraction, 10–63 μm) without primary structures, similarly to drift deposits. We propose that the Mar del Plata Canyon interacts with an intermediate-depth nepheloid layer generated by the northward-flowing Antarctic Intermediate Water (AAIW). This interaction results in rapid and continuous deposition of coarse silt sediments inside the canyon with an average sedimentation rate of 160cm/kyr during the Holocene. We conclude that the presence of the Mar del Plata Canyon decreases the transport capacity of AAIW, in particular of its deepest portion that is associated

with the nepheloid layer which in turn generates a change in the contourite deposition pattern around the canyon. Due to the highly energetic current regime, high temporal-resolution sediment records are rare in the Southwest Atlantic. Since sedimentation processes in the Mar del Plata Canyon indicate a response to changes of AAIW contour-current strength related to Late Glacial/Holocene variability, the sediments deposited within the canyon are a great climate archive for paleoceanographic reconstructions. Moreover, an additional involvement of (hemi) pelagic sediments indicate episodic productivity events in response to changes in upper ocean circulation possibly associated with Holocene changes in intensity of El Niño /Southern Oscillation.

2.4. Introduction

Submarine canyons are common morphological features at continental margins worldwide (*Harris and Whiteway, 2011*). They are important natural conduits for the transfer of terrigenous sediments to the deep sea, but also represent considerable (temporary) sinks for enhanced accumulation of modern sediments (*Carson et al., 1986*). The traditional approach of submarine canyons implies that sediment discharged by a nearby river system and/or by sediment movement across the continental shelf is carried down the canyon by gravitational processes and is deposited as mass transport deposits (MTDs). However, as most of the world's canyons (*Harris and Whiteway, 2011*), the Mar del Plata Canyon at the continental margin off northern Argentina does not have any obvious connection to the shelf or an onshore river system (e.g., La Plata River) (*Krastel et al., 2011*), and is therefore isolated from shelf-originated down-slope processes. The canyon is incorporated into a significant Contourite Depositional System (CDS) extensively present at the continental margin off northern Argentina, whose sedimentation processes are primarily controlled by northward-flowing Antarctic water masses, in particular by the Antarctic Intermediate Water (AAIW) (*Hernández-Molina et al., 2009, Preu et al., 2013*) (**Fig. 7**). Drift deposits (typical deposits formed within CDSs) have been comprehensively described from (sub)-recent deposits throughout the world's deep ocean environments (*Rebesco et al., 2008*), whereas submarine canyons incorporated into CDSs have not long been perceived. Although recent studies propose that submarine canyons significantly alter the hydrodynamics of contour currents, thereby leading to significant changes in contourite drift construction by capturing deep-sea currents (*Marchès et al., 2007*); the sedimentary processes in these submarine canyons remain poorly understood. Here we investigate the Holocene sedimentary records from the Mar del Plata Canyon, and consider the sedimentary processes and sediment characteristics of a submarine canyon that intersects a CDS. The deposits in the Mar del Plata Canyon yield insights into the interaction of a submarine canyon with an intermediate nepheloid layer (INL) as well as into the role of a canyon as a considerable (temporary) sink for Late Glacial/Holocene sediments. In highly energetic regions like the Southwest Atlantic the sedimentary records found in canyons may provide high temporal-resolution climate archives which can be used for paleoclimate and/or paleoceanographic reconstructions.

2.5. Regional setting

The Southwest Atlantic is a key location in the global intermediate and deep-water circulation (*Piola and Gordon, 1989; Peterson and Stramma, 1991; Stramma and England, 1999; Piola and Matano, 2001*) (**Fig. 7**). Different water masses formed in remote areas of the world extend into the Southwest Atlantic and generate a highly complex vertical stratification along the western boundary, where the circulation is focused to (Deep) Western Boundary Currents (*Stommel,*

1958). The main water masses include (from top to bottom) the Antarctic Intermediate Water (AAIW, ~500 - 1000 m), the Circumpolar Deep Water (CDW, ~1000 - 4000 m) and the Antarctic Bottom Water (AABW, >4000 m). By penetrating into the CDW, the North Atlantic Deep Water (NADW 2000 - 3000 m) vertically divides this water mass into two layers: the upper CDW (UCDW) and the lower CDW (LCDW). Deep Western Boundary Currents (also referred to as contour currents) are able to significantly shape the continental margin by eroding, transporting and depositing sediments at the sea floor (*Stow et al., 2002; Rebesco et al., 2008; Stow et al., 2008*). Along the Argentine margin they generate various depositional (drifts) and erosional features (terraces), which together form a Contourite Depositional System (CDS) (*Hernández-Molina et al., 2009*). The Mar del Plata Canyon, a relatively straight, deeply incised bathymetric feature, is incorporated into this CDS at around 38°S (**Figs. 7 & 8B**) (*Krastel et al., 2011*). The whole canyon is confined to the continental slope forming a so-called "blind" canyon that does not have any obvious connection to the shelf or to modern terrestrial

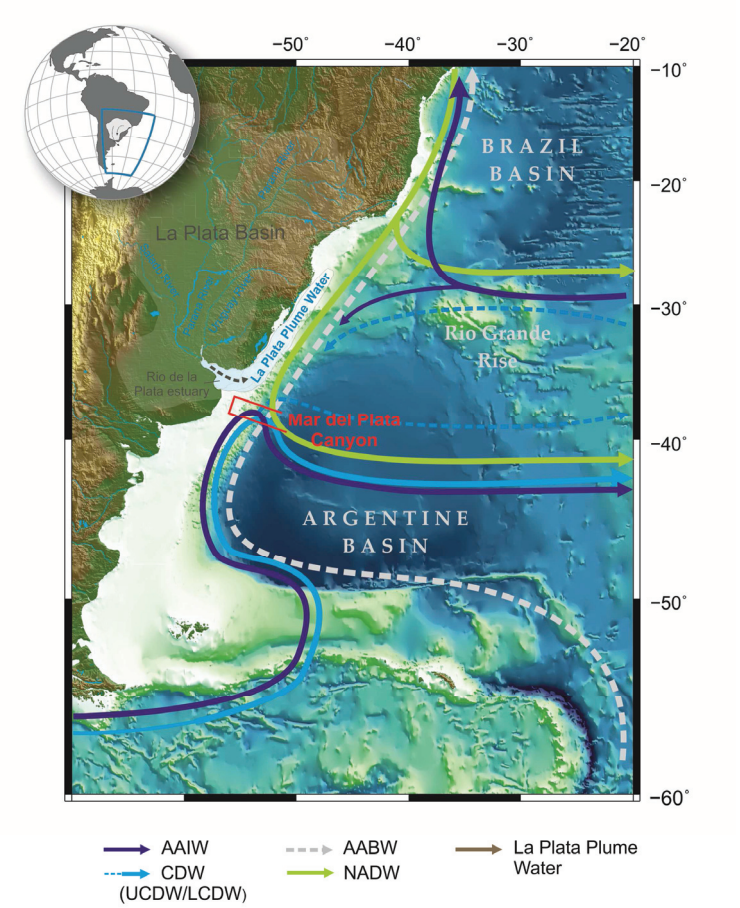

Figure 7 Schematic intermediate and deep-water circulation in the Southwest Atlantic (*Stramma and England 1999*). Northern- and southern-sourced water masses flow as Deep Western Boundary Currents along the western boundary. The La Plata River discharges into the ocean waters from La Plata basin that covers a large area of South America. Its plume extends along the Uruguay and southern Brazil shelf, thereby strongly influencing the ecosystems. AAIW – Antarctic Intermediate Water; CDW – Circumpolar Deep Water; UCDW – Upper Circumpolar Deep Water; NADW – North Atlantic Deep Water; LCDW – Lower Circumpolar Deep Water; AABW – Antarctic Bottom Water

fluvial systems (e.g., La Plata River) (*Krastel et al., 2011*). The mouth of the La Plata River is located at 35 °S (**Fig. 7**). The La Plata basin covers about 3.6 million km² thus being the second largest drainage basin in South America. It drains nearly 20 % of the surface area of South America and discharges about 23,000 m³/s of freshwater on the western South Atlantic shelf (*Mechoso et al., 2001*). This discharge influences the pelagic ecosystems by injecting nutrients and promoting an increase in phytoplankton biomass mainly over the continental shelf (*Hubold, 1980a; Hubold 1980b; Carreto et al., 1995*). On the annual mean the present-day La Plata plume is directed northward (*Piola et al., 2000*) which is also recognized in the sediment distribution off the La Plata estuary, where fluviomarine sediments have been traced on the Uruguayan middle shelf (e.g., along the northern river margin) (*Urien and Ewing 1974*). However, the La Plata plume undergoes large interannual variations related to changes in river discharge and wind pattern (*Piola et al., 2005; Piola et al., 2008*). During El Niño years the region is characterized by anomalously strong northeasterly winds and increased freshwater discharge when the La Plata plume spreads rather offshore. The Mar del Plata Canyon is not connected to the La Plata River from where sediment material could be delivered directly to the canyon by gravitational mass-wasting processes (*Krastel et al., 2011*) (**Fig. 8B**). The Mar del Plata canyon head is situated on the upper continental slope at a water depth

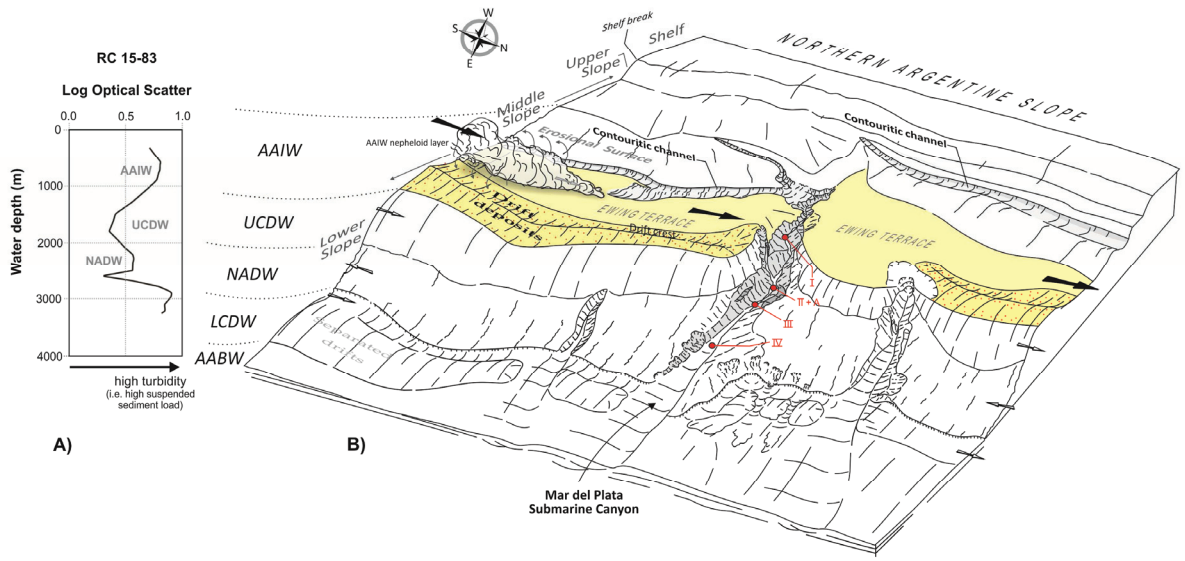

Figure 7 A: Measurements of high turbidity at the southern flank of the Mar del Plata Canyon suggest a very pronounced intermediate nepheloid layer testifying to strong current activity in the depth range of AAIW. **B:** Morpho-sedimentary map of the NE Argentine margin after *Preu et al., 2013* shows that the Mar del Plata Canyon is incorporated into a Contourite Depositional System. Yellow-colored surfaces indicate the Ewing terrace that is located at the lower boundary of the AAIW. Erosion/non-deposition takes place at the inner part of the Ewing terrace while drift deposition takes place at the outer part of the terrace. Drift deposits occur south of the Mar del Plata Canyon, but are missing directly north of it. Sediment cores: I - GeoB13832-2, II - GeoB13833-2, III - GeoB13862-1, IV - GeoB13861-1 (for more information about the sediment cores see Table. 1). CTD station: A – GeoB13833-3. AAIW – Antarctic Intermediate Water; UCDW – Upper Circumpolar Deep Water; NADW – North Atlantic Deep Water; LCDW – Lower Circumpolar Deep Water; AABW – Antarctic Bottom Water

of ~1000 m. The canyon extends for ~110 km downslope to a water depth of ~3900 m. The upper part of the Mar del Plata Canyon incises the Ewing contourite terrace, a pronounced bathymetric feature along the northern Argentine continental slope (*Krastel et al., 2011*). Contourite terraces at the depth of ~1000 m are observed along the entire continental margin off Argentina, and have been developed in depositional and erosive phases over time caused by the interaction of northward-flowing AAIW and UCDW (*Hernández-Molina et al., 2009; Hernández-Molina et al., 2010; Lastras et al., 2011*). At present, turbulent processes at the lower boundary of the AAIW inhibit sediment deposition over large areas on the Ewing terrace (*Preu et al., 2013*) (**Fig. 8B**). The hypothesis of strong AAIW in the study area is also supported by the OCCAM Global Ocean Model (*Gwilliam, 1996*) indicating flow velocities of ~15-20 cm/s at 1000 m water depth. Measurements of high turbidity which are part of the world ocean nepheloid layer composition data based assembled by the Lamont-Doherty Earth Observatory (**Fig. 8A**) indicate a very pronounced intermediate nepheloid layer (INL) testifying to strong current activity in the depth range of AAIW. The amount of suspended sediments decreases drastically toward the UCDW, and indicates the lower transport capacity of the UCDW, as well as the necessary conditions to form drift deposits. Nepheloid layers contain significant amounts of suspended sediment, and have been inferred to play an important role in the formation of drift deposits (*Rebesco et al., 2008*). Thus, drift deposits on the outer parts of the Ewing terrace are primarily influenced by sediment transported by the AAIW, and particularly by its deepest portion associated with the nepheloid layer (*Preu et al., 2013*) (**Figs. 8A,B**). A marked change in contourite drift construction occurs around the Mar del Plata Canyon. Accordingly, drift deposits are present south of the canyon, but are missing directly north of it (**Fig. 8A**).

2.6. Material & methods

This study is based on the stratigraphic, sedimentological and geochemical analyses of four gravity cores (i.e., GeoB13832-2, GeoB13833-2, GeoB13862-1 and GeoB13861-1) recovered from the thalweg of the Mar del Plata Canyon (**Figure 8B, Table 1**). The cores were collected during research cruise M78/3 a,b with the German RV METEOR (Krastel et al., 2012).

Table. 1 Location of sediment cores used in this study

Cruise	Core	Latitude	Longitude	Water depth (m)	Recovery (cm)
M78/3a	GeoB13832-2	37°90.23' S	54°14.12' W	2205	556
M78/3a	GeoB13833-2	37°95.20' S	53°83.68' W	3405	796
M78/3b	GeoB13862-1	38°09.18' S	53°60.98' W	3588	1016
M78/3b	GeoB13861-1	38°01.85' S	53°74.50' W	3715	668

2.6.1. Stratigraphy

Dating of the sedimentary sequences was performed using AMS-^{14}C measurements on 12 samples of planktonic foraminifera *Globorotalia inflata* (>150 µm fraction) (**Table 2**, Poznan Radiocarbon Laboratory, Poland). Foraminiferal radiocarbon ages are assumed as the most reliable source of information about the time of sediment deposition since these tests are less susceptible to lateral transport due to their large grain-size (*Fok-Pun and Komar, 1983; Ohkouchi et al., 2002; Mollenhauer et al., 2006*). The radiocarbon dates were calibrated with the CALIB 6.0 radiocarbon calibration program (*Stuiver and Reimer, 1993*) by applying the Marine09 calibration curve (*Reimer et al., 2009*). All ages are given in calibrated thousands of years before present (ka B.P.).

Stratigraphic correlation between the four sediment cores was based on ^{14}C ages and X-ray fluorescence (XRF) down-core records of Ca and Fe (**Fig. 9**).

2.6.2. X-ray radiographies and grain-size analysis

The sedimentary facies from each core were characterized by visual core descriptions and X-ray radiographies. Bulk and terrigenous grain-size distributions for GeoB13832-2, GeoB13833-2 and GeoB13862-1 were measured with a Coulter Laser Particle Sizer LS200. In order to isolate the terrigenous fraction (i.e., opal-, organic carbon- and carbonate-free) from the marine sediments, several pretreatment steps were undertaken to remove biogenic constituents (for methods see *Mulitza et al., 2008*).

Table.2 Radiocarbon dates and calibrated ages.

Sample Code	Depth (cm)	Species	Radiocarbon age ± 1σ error (yr B.P.)	Calibrated age (cal ka B.P.)	2σ calibrated age range (cal ka B.P)
Core GeoB13862-1					
Poz-38071	143	*G. inflata*	1790 ± 140	1.36	1.05 - 1.68
Poz-42354	258	*G. inflata*	4000 ± 50	4.00	3.85 - 4.15
Poz-38072	393	*G. inflata*	5380 ± 60	5.75	5.61 - 5.89
Poz-42355	490	*G. inflata*	5840 ± 80	6.25	6.06 - 6.43
Poz-42356	556	*G. inflata*	6140 ± 50	6.57	6.44 - 6.70
Poz-38074	669	*G. inflata*	8530 ± 70	9.18	8.99 - 9.36
Poz-38075	793	*G. inflata*	9740 ± 70	10.64	10.46 - 10.83
Poz-38076	913	*G. inflata*	10020 ± 130	10.91	10.61 - 11.22
Poz-42353	1007	*Mixed planktic foraminifera**	11210 ± 60	12.72	12.58 - 12.86
Core GeoB13832-2					
Poz-36053	50	*G. inflata*	1335 ± 35	0.87	0.78 - 0.95
Poz-36055	535	*G. inflata*	4750 ± 50	5.03	4.85 - 5.20
Core GeoB13832-2					
Poz-42357	777	*G. inflata*	5910 ± 50	6.33	6.22 - 6.43

*Mixed planktic foraminifera contained *G. inflata, G. bulloides* and *N. pachyderma*

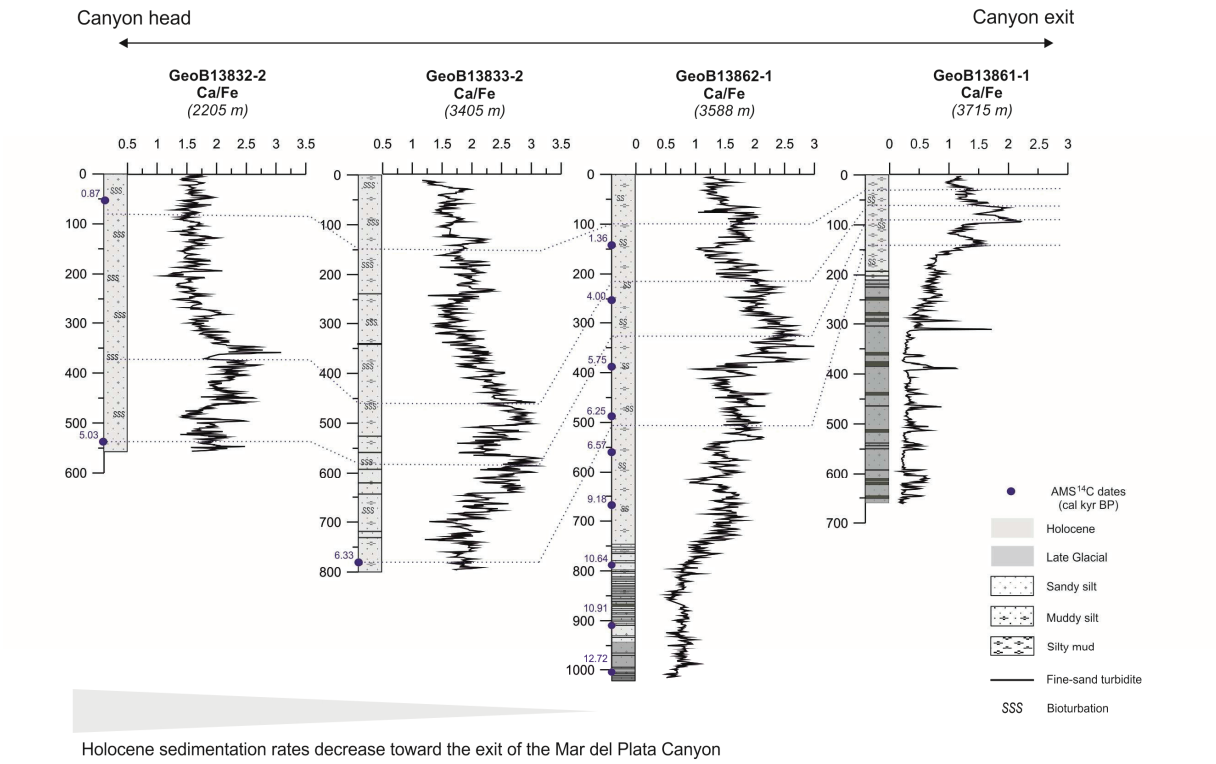

Figure 9 Stratigraphic correlation between the sediment cores recovered in the Mar del Plata Canyon. The correlation is based on both calibrated AMS-^{14}C ages and down-core Ca/Fe records. The highest average sedimentation rate is observed in GeoB13832-2 (190cm/kyr), followed by GeoB13833-2 (170cm/kyr), and GeoB13862-1 (140cm/kyr). Holocene depocentre is located in the upper part of the canyon.

2.6.3. Bulk geochemistry

Samples for bulk geochemical analyses were freeze dried and pulverised in an agate mortar. For the determination of organic carbon, calcium carbonate was removed by repeatedly adding aliquots of 0.25 NHCl. Total carbon (TC) and total organic carbon (TOC) were measured in homogenized sub-samples of bulk sediments, using a LECO CS-300 element analyzer. Carbonate was calculated from the difference between TC and TOC, and expressed as calcite [$CaCO_3$ = (TC-TOC) * 8.33]. Opal content was determined by the sequential leaching technique by *DeMaster* (*1981*), with modifications by *Müller and Schneider* (*1993*).

2.6.4. X-ray fluorescence (XRF) scanning

The XRF scanner is a nondestructive method for high resolution and relatively fast analyses of major and minor elements by scanning split sediment cores (*Jansen et al., 1998*). Element intensities, given as counts per second (cps), were measured on the split cores at 1-cm intervals. Prior and after analysis, the instrument was calibrated against a set of pressed powder standards. From the whole set of elements measured, we show here Ca/Fe and Si/Al. Calcium and Fe relative fluctuations trace the

relative abundance of biogenic carbonate and terrigenous material, respectively (*Govin et al., 2012*). Relative changes in Si and Al typically reflect changes in the input of biogenic opal or the strength of continental weathering.

2.6.5. CTD

A CTD cast was performed during the R/V Meteor cruise M78/3 a,b in the central part of the Mar del Plata Canyon at site GeoB13833-3. Additionally, an along-slope salinity and dissolved oxygen section in the vicinity of the Mar del Plata Canyon was constructed based on 36 historical hydrographic stations occupied on a relatively narrow strip between 37 and 39 °S roughly following the 1300 - 2000 m isobaths range.

2.7. Results

2.7.1. Holocene: Homogeneous coarse-silt sedimentary facies

All cores reveal remarkably high sedimentation rates during the Holocene (**Fig. 9**). The highest average sedimentation rate is observed in GeoB13832-2 (~190cm/kyr), followed by GeoB13833-2 (~170cm/kyr), and GeoB13862-1 (~140cm/kyr). Since sedimentation rates decrease toward the exit of the canyon, the thickest Holocene deposits appear to be concentrated in the upper part of the canyon (**Fig. 9**).

Sedimentary structures and characteristics

The typical sedimentary structures and characteristics of the Holocene facies are shown in **Figure 10** for GeoB13862-1. Accordingly, the Holocene sequence is defined by a coarse-silt dominated facies without any primary sedimentary structures. The most characteristic feature is the strong bioturbation present throughout all cores. The terrigenous fraction of the Holocene facies consist mainly of the "sortable-silt" fraction (10-63 μm), i.e., the portion of the fine fraction whose particle size sorting responds directly to hydrodynamic processes (*McCave et al., 1995; McCave, 2008*) (**Fig. 10A**). The analysis of X-ray radiographies and the visual core descriptions indicate no mass transport deposits (MTDs) in the Holocene sediments. The only exception is GeoB13833-2 that shows a few mm-thin bedded, dark grey fine-sand turbidites intercalated at distinct intervals (**Fig. 9**).

Bulk components

The Holocene sedimentary sequence is in general characterized by carbonate-rich (~15 %) and organic carbon-rich (~2.2 %) sediments (**Fig. 11**). TOC concentrations of up to 2.2 % indicate a preferred deposition of organic material in the Holocene, in particular between 8-5 and 3-1 ka B.P. (**Fig. 11**). Associated with these phases of generally enhanced accumulation of organic matter, the Holocene facies is intercalated by cm-thick layers enriched in biogenic opal (~15 %) (**Figs. 10B, 11**). These layers are composed of high percentages of marine phytoplankton (e.g., diatoms,

silicoflagellates) and, as a consequence, mark prominent peaks in the Si/Al records (**Fig. 11**).

Grain-size distribution

Variations in the bulk grain-size distribution also appear to be related to changes of TOC (**Fig. 11**). The additional influx of fine-grained material (10-20 µm) is associated to high TOC values, but is not observed in the terrigenous fraction which indicates a rather biogenic composition (**Fig. 10A**). The relative proportions of the sediment sub-fractions are similar in the sediment cores in which the coarse-silt fraction dominates the grain-size distribution during the Holocene (**Fig. 11**). GeoB13832-2 reveals average silt percentages of around 50 %, while GeoB13833-2 and GeoB13862 are characterized by higher

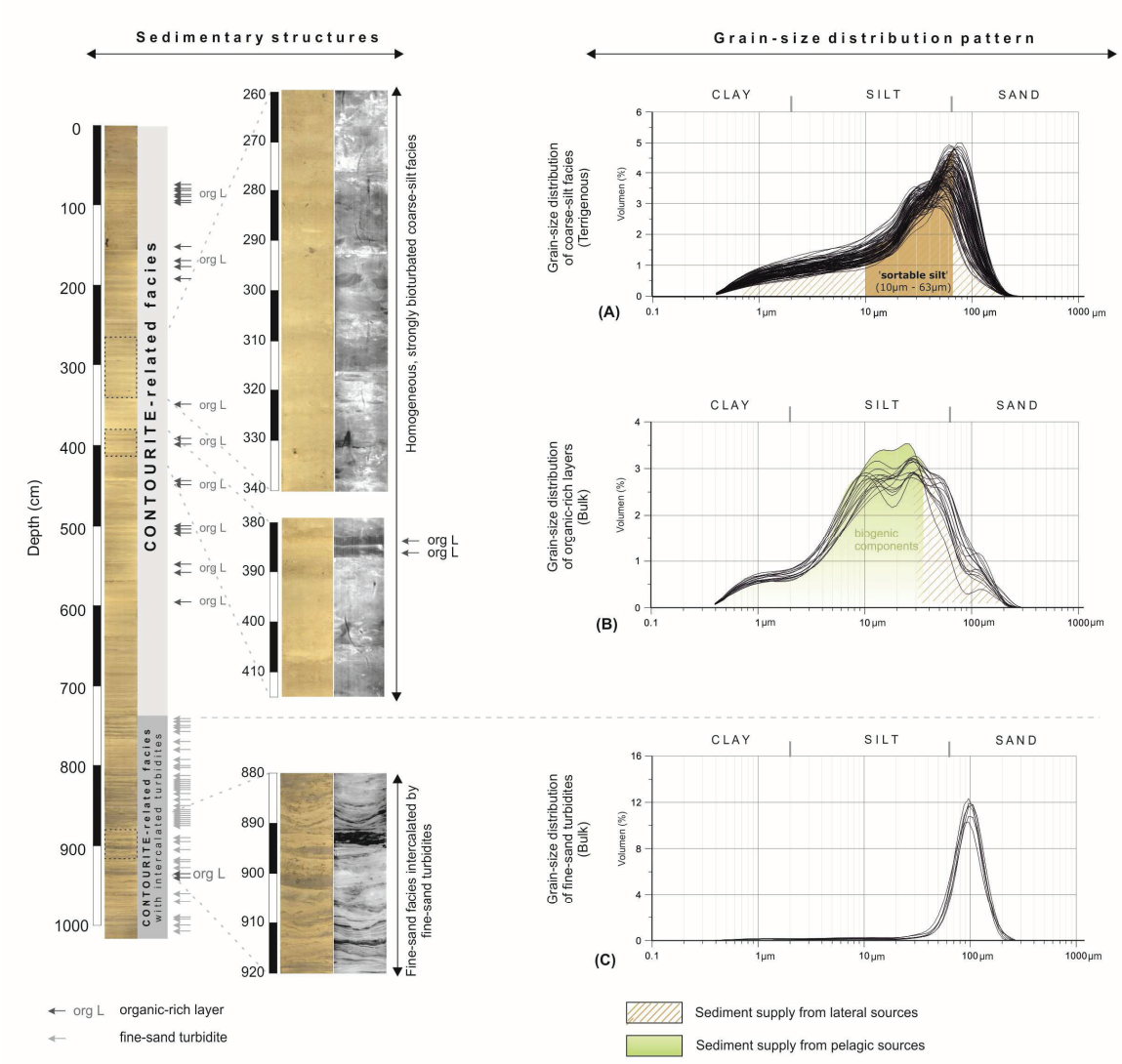

Figure 10 Left: Line-scan images and X-ray radiographies of the two different sedimentary facies in sediment core GeoB13862-1. The upper part of the core is characterized by homogenous, strongly bioturbated coarse-silt (i.e., "sortable silt" fraction, 10–63 µm) sediments. This facies is intercalated at distinct intervals by opal- and organic-rich layers. In contrast, the lower part of the core reveals fine-sand sediments intercalated by (partly) stacked fine-sand turbidites. Right: Grain-size distributions of the two sedimentary facies in sediment core GeoB13862-1. **A:** Terrigenous-sediment fraction of the coarse-silt facies dominated by the sortable-silt fraction (*McCave et al., 1995; McCave, 2008*). **B:** Bulk-grain-size distributions of opal- and organic-rich layers **C:** Bulk-grain-size distributions of intercalated fine-sand turbidites.

silt contents of around 70 % which indicates a fining trend in grain-size toward the exit of the canyon. In all sediment cores the variability in silt and sand percentages shows a twofold pattern, and clay makes up a minor fraction with continuous percentages of up to 10 %.

2.7.2. Transition Late Glacial to Holocene: Turbidite facies

Sedimentary structures and characteristics

The sedimentary facies at the transition from the Late Glacial to the Holocene is completely different to the Holocene facies because of the presence of mass transport deposits in the former. These deposits are characterized by intercalated thin-bedded, dark grey fine-sand turbidites (**Figs. 9 & 10C**). The turbidites are quartz-rich-upward sequences and show incomplete or so-called bottom/top cut-out sequences (*Bouma 1962*). Erosion by the turbidites is indicated by the radiograph observations, and is furthermore expected to be relevant, due to the predominantly coarse-grained type of turbidite deposits. With average sand percentages of ~ 40 % the sediments in between the turbidites are coarser in the Late Glacial/Holocene sedimentary sequence if compared to the Holocene sequence (**Fig. 11**).

Bulk components

According to the bulk geochemical composition, the Late Glacial/Holocene sequence is characterized by organic-poor and (≤ 0.7 %) carbonate-poor (≤ 3 %) sediments (**Fig. 11**).

2.8. Discussion

2.8.1. Holocene

Contour-current controlled sedimentation in the Mar del Plata Canyon

The depocenter of the Holocene facies is located in the upper part of the Mar del Plata Canyon (**Fig. 9**), next to the Ewing terrace which is primarily affected by northward-flowing AAIW and UCDW (*Hernández-Molina et al., 2009*). The remarkably high Holocene sedimentation rates in the canyon are coherent with sedimentation rates reported for drift deposits (*Howe et al., 1994; Howe et al., 2002*). Since contour currents are semi-permanent features in the ocean basins, they act almost continuously to affect sedimentation patterns. Therefore, we suggest that the rapidly accumulating and almost continuously deposited coarse-silt sediments in the Mar del Plata Canyon could be related to the activity of a near-bottom current. The dominance of the "sortable-silt" fraction over other particle sizes in the canyon cores also indicates a response to hydrodynamic processes (*McCave et al., 1995; McCave, 2008*) (**Figs. 10, 11**), and strongly supports the hypothesis of current-controlled sedimentation in the submarine canyon. Small-scale primary sedimentary structures (e.g., parallel and/or cross-laminae, ripples, internal erosional surfaces) are lacking in our sediment cores due to bioturbation. However, pervasive bioturbation itself could be an important diagnostic criterion for current-controlled sedimentation (*Stow and Faugères, 2008; Wetzel et al., 2008*).

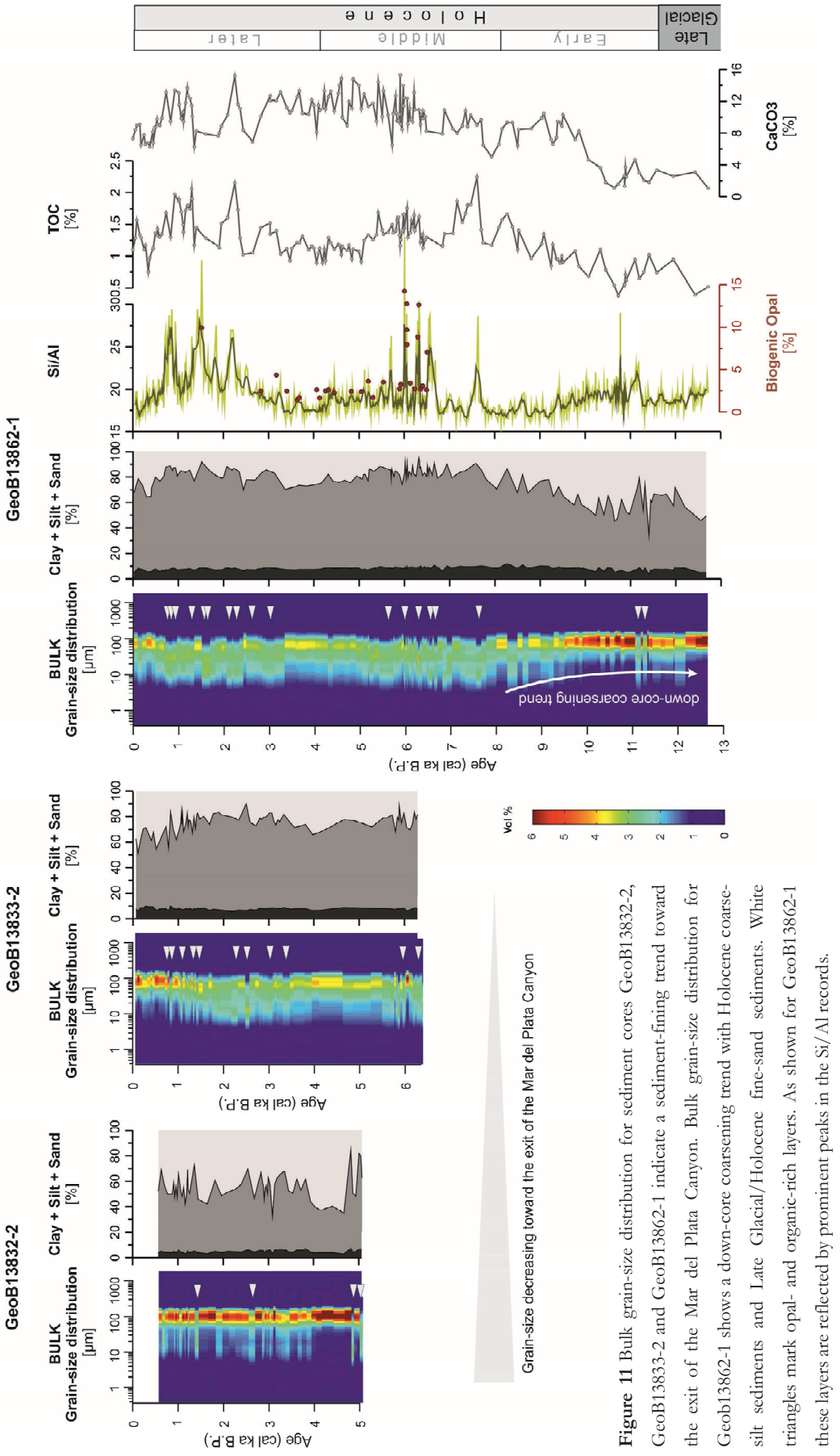

Figure 11 Bulk grain-size distribution for sediment cores GeoB13832-2, GeoB13833-2 and GeoB13862-1 indicate a sediment-fining trend toward the exit of the Mar del Plata Canyon. Bulk grain-size distribution for Geob13862-1 shows a down-core coarsening trend with Holocene coarse-silt sediments and Late Glacial/Holocene fine-sand sediments. White triangles mark opal- and organic-rich layers. As shown for GeoB13862-1 these layers are reflected by prominent peaks in the Si/Al records.

Because suspended organic matter is often adsorbed at the fine-grained material (*Mayer, 1994*) contour currents commonly supply food to deep-marine benthic organisms increasing their activity (Thistle et al., 1985; Lavaleye et al., 2002). Accordingly, the sedimentary characteristics of the Holocene facies in the Mar del Plata Canyon indicate contourite-related sediment deposits, and thus an influence of current-controlled sediment transport processes in the canyon. Due to the presence of the Mar del Plata Canyon in a CDS we propose that our Holocene sedimentary sequences were delivered to the canyon by the AAIW nepheloid layer which transported a considerable amount of sediments in suspension, and probably interacted with the canyon.

Interaction of the Mar del Plata Canyon with the AAIW nepheloid layer

McCave (*1986*) has demonstrated a clear relationship between regions of high deep-sea current velocity and the presence of nepheloid layers (i.e., layers with high suspended sediment load). Nepheloid layers can thus be useful indicators of strong current activity. Measurements of high turbidity south of the Mar del Plata Canyon suggest the presence of an intermediate nepheloid layer (INL) probably fed by erosive margin processes within the AAIW (**Fig. 8A**). Nepheloid layers at intermediate depths are well documented in various studies (e.g., *McCave and Carter, 1997*). Unconsolidated sediments can be winnowed from the sea floor and become resuspended, transported and redeposited by the AAIW. Thereby, the grain size and amount of sediments within the nepheloid layer depend in general on the intensity of the deep-sea current (*He et al., 2008*). The AAIW and more specifically its deepest portion associated with the nepheloid layer significantly influences the depositional pattern along the Ewing terrace (*Preu et al., 2013*). While the Mar del Plata Canyon is directly located at the Ewing terrace, the sedimentation processes in the canyon might also be strongly affected by the INL (**Figs. 8A,B**). *Preu et al., 2013* describe a change in contourite drift construction around the Mar del Plata Canyon (**Fig. 8B**). Drift deposits occur south of the canyon, but are not observed directly to the north of it. A change in depositional pattern around the canyon can also be interpreted by differences of modern sediments at the Ewing terrace (*Bozzano et al., 2011*). Accordingly, south of the canyon the water masses seem to be capable of winnowing and eroding the sea floor, thereby causing hiatuses and/or hardgrounds at the inner parts of the Ewing terrace; whereas deposition of sandy-silty contourites takes place at the outer parts of the Ewing terrace (*Bozzano et al., 2011*). The sedimentological data thus indicate a lateral change in the energetic environment south of the canyon, showing a gradient from erosion processes in the contourite channel to deposition processes at the drift's crest (**Fig. 8**). In contrast to the presence of both erosive and contourite depositional features south of the canyon, the modern sedimentation processes directly north of the canyon do not indicate such lateral change in depositional pattern, and are rather characterized by (hemi) pelagic sedimentation (*Bozzano et al., 2011*). These changes in depositional pattern indicate a

decrease of the flow energy between the southern and northern sides of the Mar del Plata Canyon. We thus propose that the canyon alters the circulation of the northward-flowing AAIW; in particular its deepest portion associated with the nepheloid layer, which primarily influences the depositional pattern along the Ewing terrace. The interaction of a deep-sea current with a submarine canyon has been described in the Gulf of Cadiz by *Marchès et al.,* (*2007*). Their observations present an erosional moat channel associated with high velocity upstream from the canyon and slow aggradation and a low sedimentation rate downstream. *Marchès et al.,* (*2007*) suggest that the sharp change in the erosion/deposition pattern across the canyon is due to the downslope deviation of Mediterranean Outflow Water. Along-slope salinity and dissolved oxygen sections from the vicinity of the Mar del Plata Canyon are presented in **Figs. 12A,B**. Two of the hydrographic stations used to produce the section were located inside the canyon. The salinity and oxygen sections suggest horizontally stratified water masses around and within the canyon. A similar picture emerges from the CTD cast performed inside the canyon during R/V Meteor cruise M78/3a,b (**Fig. 12C**). In contrast to the situation described in *Marchès et al.,* (*2007*), a horizontal stratification in our study area does not indicate that the Mar del Plata Canyon captures the AAIW. In general, the flow over canyons of complex topography and the role of stratification in the associated circulation are poorly understood (e.g., *Hickey, 1995; Haidvogel and Beckman, 1995*). Theoretical

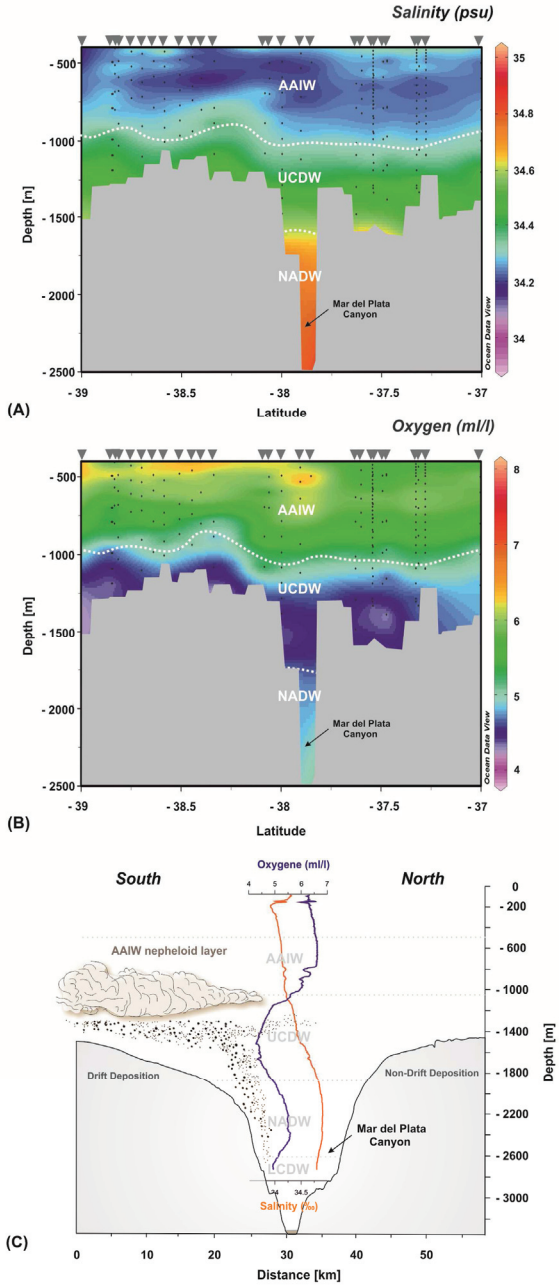

Figure 12 A+B: Along-slope salinity and dissolved oxygen section in the vicinity of the Mar del Plata Canyon showing horizontal water column stratification within the canyon. **C:** Schematic flow of the northward-flowing AAIW nepheloid layer over the Mar del Plata Canyon. Oxygen (blue line) and salinity (orange line) depth profiles from CTD at the location of sediment core GeoB13833-2 indicating that the Antarctic water masses are not flowing downslope the canyon. By crossing the canyon the suspended material of the AAIW nepheloid layer is released into the canyon which causes remarkably high sedimentation rates. AAIW – Antarctic Intermediate Water; UCDW – Upper Circumpolar Deep Water; NADW – North Atlantic Deep Water.

considerations based on potential vorticity conservation arguments and numerical simulations indicate that the flow tends to follow the isobaths. The flow over a canyon will thus describe a cyclonic loop and will tend to accelerate slightly along the canyon walls (e.g., *Klinck, 1996*). Along the canyon axis, however, the simulated circulation tends to be weaker, which may have a significant impact on the sedimentation processes at that location. As AAIW flows over the Mar del Plata Canyon the above described flow pattern may drastically decrease the transport capacity of the AAIW nepheloid layer. A decrease of the flow velocity and transport capacity will cause sedimentation of the suspended load from the INL. Thereby, a considerable amount of sediments will be released into the Mar del Plata canyon leading to the remarkably high sedimentation rates in the canyon. Thus, we assume that a change in hydrodynamic processes of AAIW is rather caused by 'crossing' the canyon, than by capturing and/or related down-canyon flowing of water masses as suggested by *Marchès et al., (2007)* (**Fig. 12C**).

Lateral differences in sedimentary pattern within the Mar del Plata Canyon

Lateral differences in sedimentary pattern across the Ewing terrace result from the differences in the flow of AAIW and UCDW (*Bozzano et al., 2011, Preu et al., 2013*). We also observe differences in the sediment cores collected in the Mar del Plata Canyon, with a decrease in sedimentation rates and a fining trend in grain-size toward the exit of the canyon (**Figs. 9,11**). Accordingly, our shallowest core (GeoB13832-2) reveals a much higher content of fine-sand than the other sediment cores. This core is located directly in front of the inner part of the Ewing terrace where erosion/non-deposition takes place (**Fig. 8B**). We assume that associated with the strong erosion within the AAIW the nepheloid layer is able to transport coarse-grained material, being responsible for the deposition of sediments with this grain-size in the upper part of the canyon. The higher sedimentation rates from GeoB13832-2 could also be explained by the high current activity of the AAIW resulting in high suspended sediment load of the nepheloid layer. In contrast, directly beneath the high velocity core of the AAIW, toward the interface of AAIW/UCDW, sediment material accumulates from the suspension of the nepheloid layer and leads to the formation of drift deposits on the Ewing terrace (*Preu et al., 2013*) (**Fig. 8B**). Through the gradual decrease of current velocities, the grain-size and the amount of suspended material within the INL decrease as well. Therefore, rather fine-grained material is delivered from the AAIW nepheloid layer into the canyon which would also explain the decrease in sedimentation rates. Accordingly, GeoB13833-2 and GeoB13862-1 located in front of the outer parts of Ewing terrace reveal higher contents of fine-grained material (**Fig. 11**). Our deepest sediment core (GeoB13861-1), however, shows a marked decrease in sedimentation rates (**Fig. 9**), which suggest that the lower parts of the canyon are not directly affected by AAIW and UCDW activity.

The Mar del Plata Canyon as a climate archive

The intercalated opal- and organic-rich layers described in all canyon cores (**Fig. 11**) are

probably related to enhanced accumulation of pelagic sediments, probably in response to positive productivity events in the upper water column above the Mar del Plata Canyon. The timing of these layers seems to be associated to the past variability of El Niño / Southern Oscillation (ENSO) (*Moy et al., 2002*) (**Fig. 13**). More specifically, anomalous positive productivity events above the Mar del Plata Canyon would be related to warm ENSO phases. Based on the current biogeographical setting in the Southwest Atlantic (e.g., *Longhurst 1998*) there are two possible sources of variability in the sedimentation rate of biogenic material in the Mar del Plata Canyon: one is associated with changes in the location of the Patagonian shelf break front (*Romero et al., 2006)* and the other with changes in the distribution of La Plata derived waters (*Piola et al., 2000*). The northernmost extension of the productive Patagonia shelf break front is associated with the northernmost extension of the Malvinas Current, which in the present reaches about 38 ºS (*Goni et al., 2011*). However, based on foraminiferal oxygen isotopic analyses performed on samples from different sediment cores obtained in- and outside the Mar del Plata Canyon (not shown here), we suggest that changes of the Malvinas Current are not correlated with the intercalated organic-rich layers throughout the Holocene. In contrast, below we show that there is strong evidence supporting the hypothesis that changes in the distribution of La Plata runoff mark the pace of the observed layering in the Mar del Plata Canyon. The La Plata derived waters influence nutrient distribution and, as a consequence, phytoplankton production of the adjacent coastal waters (*Ciotti et al., 1995*). Accordingly, primary production on the Southwest Atlantic shelf at 35 °S is enhanced by fertilization from the La Plata River. Recent studies indicate that

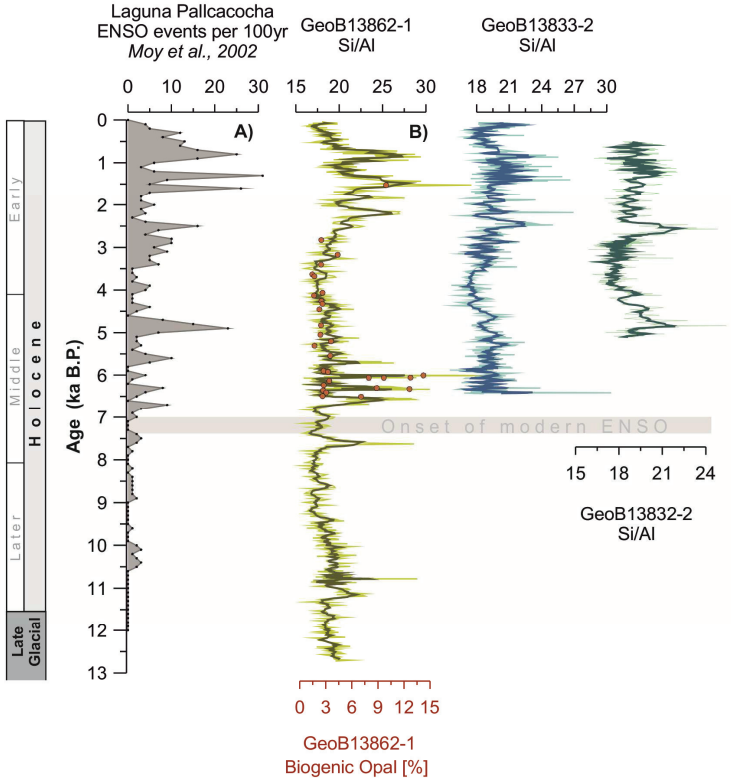

Figure 13 Comparison of geochemical parameters from the Mar del Plata Canyon cores with palaeoclimatic data from South America. **A:** Past variability of El Niño /Southern Oscillation (ENSO) during the Holocene (*Moy et al., 2002*). **B:** Si/Al peaks indicating a higher amount of biogenic opal and reflecting anomalous positive productivity events in the upper water column above the Mar del Plata Canyon.

on the annual mean the present-day La Plata plume is directed northward (e.g., *Piola et al., 2000*) (**Fig. 14A)**. The plume distribution sets the sediment distribution off the Rio de la Plata estuary, where fluviomarine facies have been traced on the Uruguayan middle shelf (e.g., along the northern river margin, *Urien and Ewing 1974*). Accordingly, surface sediments collected to the northeast of the estuary are characterized by organic carbon concentrations up to three times higher with values exceeding 2.5 % if compared to the adjacent areas (*Frenz et al., 2003*). Nevertheless, the La Plata plume undergoes large interannual variations related to changes in river discharge and wind pattern (*Piola et al., 2005; Piola et al., 2008*). There is strong evidence that large precipitation anomalies occur over most of the La Plata drainage basin during El Niño events (*Ropelewski and Halpert, 1987; Kiladis and Diaz, 1989*). This significantly increases the discharge of the major La Plata tributaries (*Mechoso and Iribarren, 1992; Depetris et al., 1996*) (**Fig. 14B**). El Niño events are also characterized by anomalously strong northeasterly winds that block an along-shore northward spreading of the La Plata plume and force the high-nutrient fluvial waters offshore (*Piola et al., 2005; Piola et al., 2008)* (**Fig. 14B**). Consequently, during modern times the La Plata outflow shows large interannual variability associated to ENSO. This variability also impacts the primary production in the upper water column as recorded in SeaWiFS-derived chlorophyll anomalies during strong El Niño events (*Ciotti et al., 1995; Garcia and Garcia, 2008*). Since the atmospheric circulation anomalies during El Niño events prevent the northward spreading of the La Plata plume forcing it offshore we assume that the enhanced La Plata outflow during anomalously strong El Niño events fertilizes the upper water column over the Mar del Plata Canyon which is recorded as enhanced accumulation of

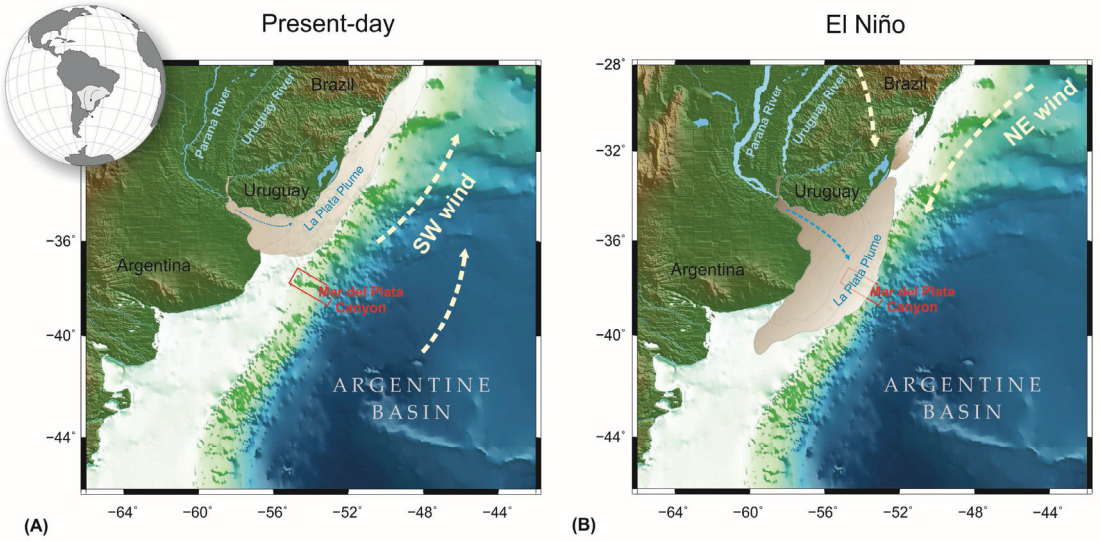

Figure 14 Schematic outflow pattern of the La Plata River plume depending on changes in wind circulation over South America (modified after *Piola et al., 2005, 2008*). **A:** Present-day plume extension is directed northward along the Uruguayan and Brazilian shelf. **B:** The combined effects of wind and precipitation anomalies during El Niño events in South America induce anomalously large outflow events of the La Plata River spreading offshore, thereby increasing phytoplankton biomass and production in the upper water column above the Mar del Plata Canyon.

particulate organic matter and planktonic primary producers (i.e., diatoms, silicoflagellates) (**Fig. 13**). The intercalated opal- and organic-rich layers in the canyon cores are thus probably related to a combination of conspicuously strong outflow events of the La Plata River and increased strength in northeasterly winds, both associated to El Niño events.

2.8.2. Transition Late Glacial/Holocene

Current-controlled mass-wasting processes in the Mar del Plata Canyon

Gravitational processes dominate the depositional pattern in the Mar del Plata Canyon during the transition Late Glacial/Holocene. The turbidites in the canyon reflect the same sedimentological characteristics as the drift deposits at the outer Ewing terrace which consist of dark grey, fine-sand with a siliciclastic composition (*Bozzano et al., 2011*). Therefore, we assume that turbidity-current activity during the transition Late Glacial/Holocene is related to sediment instability of drift deposits at the southern flank of the canyon. Recent studies suggest that the formation and northward penetration of Antarctic water masses were enhanced during the last glacial termination (e.g., *Pahnke et al., 2008; Hendry et al., 2012*). Related to the change in flow strength and associated increase accumulation of sediments, the plastered drift deposits on the outer part of the Ewing terrace were probably rather growing during that period. Hence, a down-current migration/progradation of drift deposits would be possible (*Mulder et al., 2006*) and would lead to local instability near the southern flank of the canyon which in turn resulted in gravitational processes like turbidity-currents. This assumption is also supported by a general coarsening of the current-controlled sedimentation in the canyon during the transition phase indicating a general increase in the strength of AAIW (**Fig. 11**). A general decrease in current velocity of the Antarctic water masses during the Holocene (*Pahnke et al., 2008*) would not promote progradation of the drift deposits. Accordingly, the Holocene facies does not show any down-canyon transport processes, except for GeoB13833-2 which is located directly in front of the drift deposits on the Ewing terrace, and therefore preferably affected by instability events of the drift deposits.

2.9. Conclusion

The Mar del Plata Canyon located at the continental margin off northern Argentina intersects a CDS that is formed by the northward-flowing Antarctic water masses (i.e., AAIW and UCDW). The canyon interacts with the intermediate nepheloid layer of the AAIW which results in rapid and continuous deposition of coarse-silt material (i.e., "sortable silt", 10-63 μm) within the canyon with remarkably high sedimentation rates of around 160cm/kyr during the Holocene The sediment deposits inside the canyon reveal sediment characteristics similar to drift deposits, and are characterized by strongly bioturbated coarse-silt sediments without any primary structures. The sedimentary pattern in the canyon indicates a response to changes of

contour-current strength of AAIW most probably related to climate variability. Accordingly, we interpret stronger (weaker) circulation of the AAIW during the Late Glacial (Holocene). The influence of (lateral) current-controlled transport processes on the sedimentation pattern in a submarine canyon appears to be an important process at continental margins which are affected by deep-water current activity. In highly energetic current regions as the Southwest Atlantic, where contour currents rework significant amounts of sediment, a submarine canyon can act as a sink for enhanced accumulation of sediments, holding a great potential as a climate archive. Accordingly, the Mar del Plata Canyon recorded anomalously positive productivity events in the water column over the canyon that are correlated to periods of strong El Niño activity during the Holocene. Large precipitation anomalies over southeastern South America associated with El Niño events significantly increase the discharge of the La Plata River that enhances primary production. Due to atmospheric circulation and precipitation anomalies the La Plata plume spreads offshore leading to event like accumulation of organic- and opal-rich layers in the Mar del Plata Canyon.

2.10. Acknowledgements

We thank B. Kockisch and M. Klann for their lab work (MARUM, Bremen), and K.H. Baumann, G. Fischer and O. Romero for comments and discussion. This study was funded through DFG-Research Center / Cluster of Excellence „The Ocean in the Earth System“ and was supported by the Bremen International Graduate School for Marine Sciences (GLOMAR) that is funded by the German Research Foundation (DFG) within the frame of the Excellence Initiative by the German federal and state governments to promote science and research at German universities. ARP acknowledges the support from grant CRN2076 from the Inter-American Institute for Global Change Research and the U.S. National Science Foundation grant GEO-0452325. CMC acknowledges the support from FAPESP (2010/09983-9). Further, we thank the members of the shipboard and scientific crews of the RV Meteor cruise M78/3a,b.

2.11. References

Bouma, A.H., 1962. Sedimentology of Some Flysch Deposits Elsevier, Amsterdam (1962), p. 168

Bozzano, G., Violante, R., Cerredo, M., 2011. Middle slope contourite deposits and associated sedimentary facies off NE Argentina. Geo-Marine Letters 31 (5), 495-507.

Carreto, J., A. Lutz, V., Carignan, M.O., Cucchi Colleoni, A.D., De Marco, S.G., 1995. Hydrography and chlorophyll a in a transect from the coast to the shelf-break in the Argentinian Sea. Continental Shelf Research 15 (2–3), 315-336.

Carson, B., Baker, E.T., Hickey, B.M., Nittrouer, C.A., DeMaster, D.J., Thorbjarnarson,

K.W., Snyder, G.W., 1986. Modern sediment dispersal and accumulation in Quinault submarine canyon -- A summary. Marine Geology 71 (1-2), 1-13.

Ciotti, Á.M., Odebrecht, C., Fillmann, G., Moller Jr, O.O., 1995. Freshwater outflow and Subtropical Convergence influence on phytoplankton biomass on the southern Brazilian continental shelf. Continental Shelf Research 15 (14), 1737-1756.

DeMaster, D.J., 1981. The supply and accumulation of silica in the marine environment. Geochimica et Cosmochimica Acta 45 (10), 1715-1732.

Depetris, P.J., Kempe, S., Latif, M., Mook, W.G., 1996. ENSO-controlled flooding in the Paraná River (1904–1991). Naturwissenschaften 83 (3), 127-129.

Frenz, M., Höppner, R., Stuut, J-B.W., Wagner, T., Henrich, R., 2003. Surface sediment bulk geochemistry and grain-size composition related to the oceanic circulation along the South American continental margin in the Southwest Atlantic. In: Wefer G, Mulitza S, Ratmeyer V (eds) The South Atlantic in the Late Quaternary: reconstruction of material budgets and current systems. Springer, Berlin, pp 347–373

Fok-Pun, L., Komar, P.D., 1983. Settling velocities of planktonic foraminifera; density variations and shape effects. The Journal of Foraminiferal Research 13 (1), 60-68.

Garcia, C.A.E., Garcia, V.M.T., 2008. Variability of chlorophyll-a from ocean color images in the La Plata continental shelf region. Continental Shelf Research 28 (13), 1568-1578.

Goni, G.J., Bringas, F., DiNezio, P.N., 2011. Observed low frequency variability of the Brazil Current front. J. Geophys. Res. 116 (C10), C10037.

Govin, A., Holzwarth, U., Heslop, D., Ford Keeling, L., Zabel, M., Mulitza, S., Collins, J.A., Chiessi, C.M., 2012. Distribution of major elements in Atlantic surface sediments (36°N-49°S): Imprint of terrigenous input and continental weathering. Geochem. Geophys. Geosyst. 13, Q01013.

Gwilliam, C.S., 1996. Modelling the global ocean circulation on the T3D. In: Ecer, A., Periaux, J., Satdfuka, N., S. TaylorA2 - A. Ecer, J.P.N.S., Taylor, S. (Eds.), Parallel Computational Fluid Dynamics 1995. North-Holland, Amsterdam, pp. 33-40

Haidvogel, D.B., A. Beckman, 1995. Wind-driven residual currents over a coastal canyon. Proc. Hawaiian Winter Workshop on Topographic Effects in the Ocean, P. Müller and D. Henderson, Eds., School of Ocean and Earth Science and Technology, University of Hawaii, Honolulu, 219–224.

Harris, P.T., Whiteway, T., 2011. Global distribution of large submarine canyons: Geomorphic differences between active and passive continental margins. Marine Geology 285 (1–4), 69-86.

He, Y., Duan, T., Gao, Z., 2008. Chapter 7 Sediment Entrainment. In: Rebesco, M., Camerlenghi, A. (Eds.), Developments in Sedimentology. Elsevier, pp. 99-119.

Hendry, K.R., Robinson, L.F., Meredith, M.P., Mulitza, S., Chiessi, C.M., Arz, H., 2012. Abrupt changes in high-latitude nutrient supply to the Atlantic during the last glacial cycle. Geology 40 (2), 123-126.

Hernández-Molina, F.J., Paterlini, M., Violante, R., Marshall, P., de Isasi, M., Somoza, L., Rebesco, M., 2009. Contourite depositional system on the Argentine Slope: An exceptional record of the influence of Antarctic water masses. Geology 37 (6), 507-510.

Hernández-Molina, F.J., Paterlini, M., Somoza, L., Violante, R., Arecco, M.A., de Isasi, M., Rebesco, M., Uenzelmann-Neben, G., Neben, S., Marshall, P., 2010. Giant mounded drifts in the Argentine Continental Margin: Origins, and global implications for the history of thermohaline circulation. Marine and Petroleum Geology 27 (7), 1508-1530.

Hickey, B., 1995, Coastal submarine canyons. Proc. Hawaiian Winter Workshop on Topographic Effects in the Ocean, P. Müller and D. Henderson, Eds., School of Ocean and Earth Science and Technology, Univ. of Hawaii, Honolulu, 95–110.

Howe, J.A., Stoker, M.S., Stow, D.A.V., 1994. Late Cenozoic Sediment Drift Complex, Northeast Rockall Trough, North Atlantic. Paleoceanography 9 (6), 989-999.

Howe, J.A., Stoker, M.S., Stow, D.A.V., Akhurst, M.C., 2002. Sediment drifts and contourite sedimentation in the northeastern Rockall Trough and Faroe-Shetland Channel, North Atlantic Ocean. Geological Society, London, Memoirs 22 (1), 65-72.

Hubold, G. (1980a), Hydrography and plankton off southern Brazil and Rio de la Plata, spring cruise: August–November 1978, Atlântica, 4, 1– 22.

Hubold, G. (1980b), Second report on hydrography and plankton off southern Brazil and Rio de la Plata, autumn cruise: April– June 1978, Atlântica, 4, 23–42.

Jansen, J.H.F., Van der Gaast, S.J., Koster, B., Vaars, A.J., 1998. CORTEX, a shipboard XRF-scanner for element analyses in split sediment cores. Marine Geology 151 (1–4), 143-153.

Kiladis, G.N., Diaz, H.F., 1989. Global Climatic Anomalies Associated with Extremes in the Southern Oscillation. Journal of Climate 2 (9), 1069-1090.

Klinck, J.M., 1996. Circulation near submarine canyons: A modeling study. J. Geophys. Res. 101 (C1), 1211-1223.

Krastel, S., Wefer, G., Hanebuth, T., Antobreh, A., Freudenthal, T., Preu, B., Schwenk, T., Strasser, M., Violante, R., Winkelmann, D., party, M.s.s., 2011. Sediment dynamics and geohazards off Uruguay and the de la Plata River region (northern Argentina and Uruguay). Geo-Marine Letters 31 (4), 271-283.

Krastel, S., Wefer, G., 2012. Report and preliminary results of RV METEOR Cruise M78/3. Sediment transport off Uruguay and Argentina: from the shelf to the deep sea; 19.05.2009 – 06.07.2009, Montevideo (Uruguay) – Montevideo (Uruguay) Berichte aus dem Fachbereich Geowissenschaften, 285 . Fachbereich Geowissenschaften, Bremen.

Lastras, G., Acosta, J., Muñoz, A., Canals, M., 2011. Submarine canyon formation and evolution in the Argentine Continental Margin between 44°30'S and 48°S. Geomorphology 128 (3–4), 116-136.

Lavaleye, M.S.S., Duineveld, G.C.A., Berghuis, E.M., Kok, A., Witbaard, R., 2002. A comparison between the megafauna communities on the N.W. Iberian and Celtic continental margins—effects of coastal upwelling? Progress In Oceanography 52 (2–4), 459-476.

Longhurst, A., 1998. Ecological Geography of the Sea, Elsevier, New York.

Marchès, E., Mulder, T., Cremer, M., Bonnel, C., Hanquiez, V., Gonthier, E., Lecroart, P., 2007. Contourite drift construction influenced by capture of Mediterranean Outflow Water deep-sea current by the Portimão submarine canyon (Gulf of Cadiz, South Portugal). Marine Geology 242 (4), 247-260.

Mayer, L.M., 1994. Surface area control of organic carbon accumulation in continental shelf sediments. Geochimica et Cosmochimica Acta 58 (4), 1271-1284.

McCave, I.N., 1986. Local and global aspects of the bottom nepheloid layers in the world ocean. Netherlands Journal of Sea Research 20 (2–3), 167-181.

McCave, I.N., Manighetti, B., Robinson, S.G., 1995. Sortable Silt and Fine Sediment Size/Composition Slicing: Parameters for Palaeocurrent Speed and Palaeoceanography. Paleoceanography 10 (3), 593-610.

McCave, I.N., Carter, L., 1997. Recent sedimentation beneath the Deep Western Boundary Current off northern New Zealand. Deep Sea Research Part I: Oceanographic Research Papers 44 (7), 1203-1237.

McCave, I.N., 2008. Chapter 8 Size Sorting During Transport and Deposition of Fine Sediments: Sortable Silt and Flow Speed. In: Rebesco, M., Camerlenghi, A. (Eds.), Developments in Sedimentology. Elsevier, pp. 121-142.

Mechoso, C.R., Iribarren, G.P., 1992. Streamflow in Southeastern South America and the Southern Oscillation. Journal of Climate 5 (12), 1535-1539.

Mechoso, C.R., Dias, P.S., Baethgen, W., Barros, V., Berbery, E.H., Clarke, R., Cullen, H., Ereño C., Grassi, B., Lettenmaier, D., 2001. Climatology and hydrology of the Plata Basin, a document of VAMOS Scientific Study Group on the Plata Basin, 56 pp. (Available at *http://www.clivar.org/science/vamos_pubs.htm*)

Mollenhauer, G., McManus, J.F., Benthien, A., Müller, P.J., Eglinton, T.I., 2006. Rapid

lateral particle transport in the Argentine Basin: Molecular 14C and 230Thxs evidence. Deep Sea Research Part I: Oceanographic Research Papers 53 (7), 1224-1243.

Moy, C.M., Seltzer, G.O., Rodbell, D.T., Anderson, D.M., 2002. Variability of El Nino/Southern Oscillation activity at millennial timescales during the Holocene epoch. Nature 420 (6912), 162-165.

Mulder, T., Lecroart, P., Hanquiez, V., Marches, E., Gonthier, E., Guedes, J.C., Thiébot, E., Jaaidi, B., Kenyon, N., Voisset, M., Perez, C., Sayago, M., Fuchey, Y., Bujan, S., 2006. The western part of the Gulf of Cadiz: contour currents and turbidity currents interactions. Geo-Marine Letters 26 (1), 31-41.

Mulitza, S., Prange, M., Stuut, J.-B., Zabel, M., von Dobeneck, T., Itambi, A.C., Nizou, J., Schulz, M., Wefer, G., 2008. Sahel megadroughts triggered by glacial slowdowns of Atlantic meridional overturning. Paleoceanography 23 (4), PA4206.

Müller, P.J., Schneider, R., 1993. An automated leaching method for the determination of opal in sediments and particulate matter. Deep Sea Research Part I: Oceanographic Research Papers 40 (3), 425-444.

Ohkouchi, N., Eglinton, T.I., Keigwin, L.D., Hayes, J.M., 2002. Spatial and Temporal Offsets Between Proxy Records in a Sediment Drift. Science 298 (5596), 1224-1227.

Pahnke, K., Goldstein, S.L., Hemming, S.R., 2008. Abrupt changes in Antarctic Intermediate Water circulation over the past 25,000[thinsp]years. Nature Geosci 1 (12), 870-874.

Peterson, R.G., Stramma, L., 1991. Upper-level circulation in the South Atlantic Ocean. Progress In Oceanography 26 (1), 1-73.

Piola, A.R., Gordon, A.L., 1989. Intermediate waters in the southwest South Atlantic. Deep Sea Research Part A. Oceanographic Research Papers 36 (1), 1-16.

Piola, A.R., Campos, E.J.D., Möller, O.O., Jr., Charo, M., Martinez, C., 2000. Subtropical Shelf Front off eastern South America. J. Geophys. Res. 105 (C3), 6565-6578.

Piola, A.R., Matano, R.P., 2001. Brazil And Falklands (malvinas) Currents. In: Editor-in-Chief: John, H.S. (Ed.) Encyclopedia of Ocean Sciences. Academic Press, Oxford, pp. 340-349.

Piola, A.R., Matano, R.P., Palma, E.D., Möller, O.O., Jr., Campos, E.J.D., 2005. The influence of the Plata River discharge on the western South Atlantic shelf. Geophys. Res. Lett. 32 (1), L01603.

Piola, A.R., Romero, S.I., Zajaczkovski, U., 2008. Space–time variability of the Plata plume inferred from ocean color. Continental Shelf Research 28 (13), 1556-1567.

Preu, B., Hernández-Molina, F.J., Violante, R., Piola, A., Paterlini, C.M., Schwenk, T., Voigt, I., Krastel, S., Spieß, V., 2013. Morpho-sedimentary characteristics of

the northern Argentine margin: the interplay between erosive, depositional and gravitational processes. Journal of Geophysical Research – Earth Surface (accepted)

Rebesco, M., Camerlenghi, A., Van Loon, A.J., 2008. Chapter 1 Contourite Research: A Field in Full Development. In: Rebesco, M., Camerlenghi, A. (Eds.), Developments in Sedimentology. Elsevier, pp. 1-10.

Reimer, P.J., Baillie, M.G.L., Bard, E., Bayliss, A., Beck, J.W., Blackwell, P.G., Bronk Ramsey, C. Buck, C.E., Burr, G.S., Edwards, R.L., Friedrich, M., Grootes, P.M., Guilderson, T.P., Hajdas, I., Heaton, T.J., Hogg, A.G., Hughen, K.A., Kaiser, K.F., Kromer, B., McCormac, F.G., Manning, S.W., Reimer, R.W., Richards, D.A., Southon, J.R., Talamo, S., Turney, C.S.M., van der Plicht, J., Weyhenmeyer ,C.E., 2009. IntCal09 and Marine09 radiocarbon age calibrationcurves, 0–50,000 years cal BP. Radiocarbon, 51, pp. 1111–1150.

Romero, S.I., Piola, A.R., Charo, M., Garcia, C.A.E., 2006. Chlorophyll-a variability off Patagonia based on SeaWiFS data. J. Geophys. Res. 111 (C5), C05021.

Ropelewski, C.F., Halpert, M.S., 1987. Global and Regional Scale Precipitation Patterns Associated with the El Niño/Southern Oscillation. Monthly Weather Review 115 (8), 1606-1626.

Stommel, H., 1958. The abyssal circulation. Deep Sea Research (1953) 5 (1), 80-82.

Stow, D.A.V., Faugères, J.-C., Howe, J.A., Pudsey, C.J., Viana, A.R., 2002. Bottom currents, contourites and deep-sea sediment drifts: current state-of-the-art. Geological Society, London, Memoirs 22 (1), 7-20.

Stow, D.A.V., Faugères, J.C., 2008. Chapter 13 Contourite Facies and the Facies Model. In: Rebesco, M., Camerlenghi, A. (Eds.), Developments in Sedimentology. Elsevier, pp. 223-256.

Stow, D.A.V., Hunter, S., Wilkinson, D., Hernández-Molina, F.J., 2008. Chapter 9 The Nature of Contourite Deposition. In: Rebesco, M., Camerlenghi, A. (Eds.), Developments in Sedimentology. Elsevier, pp. 143-156.

Stramma, L., England, M., 1999. On the water masses and mean circulation of the South Atlantic Ocean. J. Geophys. Res. 104 (C9), 20863-20883.

Stuiver, M., Reimer, P.J., 1993. Extended ^{14}C data base and revised CALIB 3.0 ^{14}C age calibration program. Radiocarbon, 35 , pp. 215–230 Radiocarbon, 35 (1993), pp. 215–230

Thistle, D., Yingst, J.Y., Fauchald, K., 1985. A deep-sea benthic community exposed to strong near-bottom currents on the Scotian Rise (western Atlantic). Marine Geology 66 (1–4), 91-112.

Urien, C.M., Ewing, M., 1974. Recents sediments and environment of Southern Brasil, Uruguay, Buenos Aires and Rio Negro continental shelf Burk, C.A., Drake, C., (Eds.), Geology of

continental margins, Springer-Verlag, Berlin (1974), p. 157

Wetzel, A., Werner, F., Stow, D.A.V., 2008. Chapter 11 Bioturbation and Biogenic Sedimentary Structures in Contourites. In: Rebesco, M., Camerlenghi, A. (Eds.), Developments in Sedimentology. Elsevier, pp. 183-202.

Chapter 3: Holocene millennial-scale oscillations of Antarctic Intermediate Water strength

Ines Voigt[1], Cristiano M. Chiessi[2], Alberto R. Piola[3], Rüdiger Henrich[1]

[1]MARUM –Center for Marine Environmental Sciences and Faculty of Geosciences, University of Bremen, D-28359 Bremen, Germany

[2]School of Arts, Sciences and Humanities, University of São Paulo, Brazil

[3]Servicio de Hidrografia Naval (SHN), Buenos Aires, Argentina

(Ready for submission to Nature Geoscience)

3.1. Abstract

Antarctic Intermediate Water (AAIW) formation in the Southern Ocean is an essential component of the Atlantic meridional overturning circulation (AMOC). However, the role of AAIW in Holocene abrupt climate changes remains poorly understood. Here we present a Holocene high-resolution sedimentary record from the Southwest Atlantic to reconstruct changes in the strength of AAIW. Our data reveal millennial-and orbital-scale perturbations in AAIW with enhanced (reduced) northward advection of AAIW during periods of reduced (enhanced) North Atlantic Deep Water (NADW) circulation. This provides strong evidence for a Holocene AAIW-NADW see-saw. The variations in AAIW circulation indicate a tight coupling to Southern Hemisphere climate oscillations. Thereby, increased formation of AAIW closely corresponded to Southern Hemisphere cold events and poleward shifts of the Southern Westerly Winds (SWW) that favored higher ice-ocean freshwater fluxes toward regions of AAIW renewal. Our data show that the SWW-Southern Ocean coupled system is essential in driving changes in AMOC during the Holocene, and indicate that the trigger for abrupt climate change in the Holocene may reside in the Southern Hemisphere.

3.2. Main text

The circulation of Antarctic Intermediate Water (AAIW) is thought to make an important contribution to the global ocean-climate system. In the present-day climate, the formation of North Atlantic Deep Water (NADW) in the high latitudes of the North Atlantic is fed by upper-thermocline water and, in part, by modified less dense AAIW. AAIW supplies a large fraction of the northward flow required to balance the southward export of NADW, and thus represents an active player in the Atlantic meridional overturning circulation (AMOC). The potential role the AAIW plays in contributing changes in the AMOC is suggested by paleoproxy reconstructions (*Pahnke and Zahn, 2005; Pahnke et al., 2008*) and climate model simulations *(Saenko et al., 2003b; Weaver et al., 2003*) providing strong evidence for a NADW–AAIW see-saw during the last deglaciation. However, a possible link between AAIW and NADW circulation during the Holocene remains speculative. Hence, understanding the natural variability in the AAIW overturning circulation along with forcing- and feedback mechanisms is a significant challenge in Holocene climate research.

Here we present a high-resolution Holocene paleocurrent record from the Southwest Atlantic that documents millennial-to orbital-scale changes in the flow strength of AAIW. Our record provides a detailed documentation of the history of AAIW circulation and renewal in response to climate oscillations in Southern Hemisphere high latitudes, and it's linking to changes of the NADW overturning circulation during the Holocene.

We studied gravity core GeoB13862-1 (38°09.18' S / 53°60.98' W / 3588 m water depth) recovered in the Mar del Plata Canyon at the continental margin off northern Argentina (**Fig. 15**). The canyon is incorporated into a Contourite Depositional System induced by northward-flowing Antarctic intermediate and deep water masses (*Hernández-Molina et al., 2009*). Holocene sedimentation rates (~150 cm/kyr) are greatly enhanced in the canyon owning to the interaction of the canyon with the AAIW (*Voigt et al., (submitted)*). Thereby, sediments transported with the AAIW are released into the canyon producing a continuous ~750 cm long Holocene record. Details of the ^{14}C-based age model are provided in the *Supplementary Information, Table S1*. We used the "sortable silt" percentage (SS%) and the "sortable silt" mean size ($\overline{SS}$) (*McCave et al., 1995*) to reconstruct relative changes in intermediate-depth contour-current strength, i.e., AAIW. Both "sortable silt" parameters refer to the fraction of the sediment (i.e., terrigenous 10-63 μm) whose size sorting varies in response to hydrodynamic processes, where higher values reflect stronger near-bottom flow and vice versa. Grain-size distributions of the terrigenous fraction were measured with a Coulter Laser Particle Sizer LS13320. In order to isolate the terrigenous fraction (i.e., opal-, organic carbon- and carbonate-free), several pretreatment steps were undertaken to remove biogenic constituents (for methods, see *Mulitza et al., 2008*).

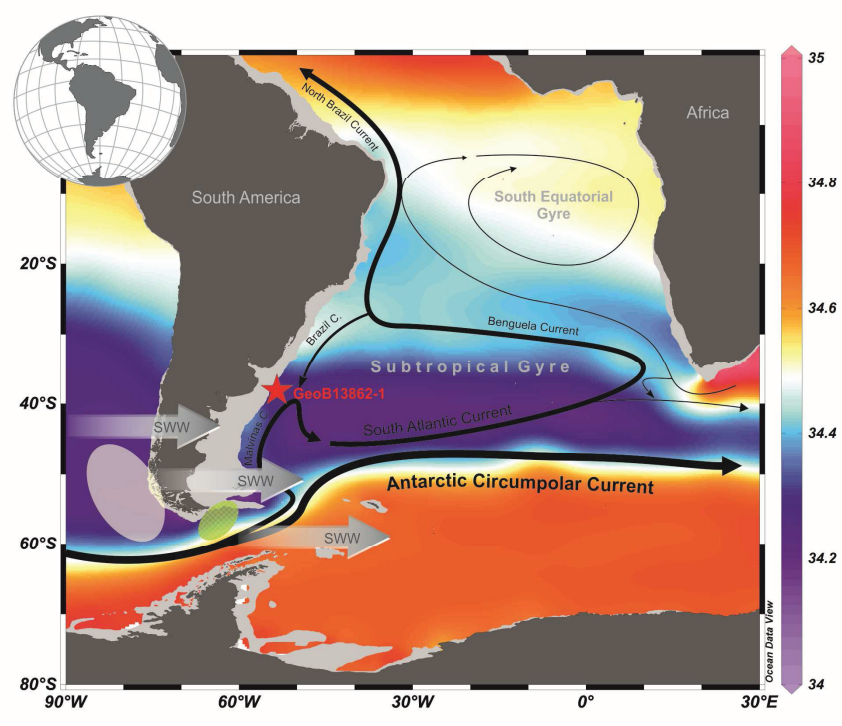

Figure 15 Present-day annual mean salinity at 700 m water depth in the South Atlantic (WOA09; *Locarnini et al. 2010*). Black arrows indicate Antarctic Intermediate Water (AAIW) circulation (*Stramma and England, 1999*). Main AAIW source region is indicated by the white ellipse, and the region of strong mixing by the green ellipse. Grey arrows mark the prevailing Southern Westerly Winds (SWW).

Superimposed on a slight increase in AAIW strength at ~5.5 ka B.P., a succession of millennial-scale AAIW variations is recognized in the "sortable silt" paleocurrent record of GeoB13862-1 indicating a highly variable intermediate water circulation throughout the Holocene (**Fig. 16D**) (see *Supplementary Information,* SF1). Spectral analysis was performed with the software REDFIT (*Schulz and Mudelsee, 2002*) and reveals a statistically significant periodicity with a strong 1441 (±250) year cycle (*Supplementary Information,* SF2).

We interpret variations in the high-resolution "sortable silt" paleocurrent record of GeoB13862-1 as millennial- to orbital-scale changes in AAIW formation and circulation throughout the Holocene. In the modern ocean, AAIW mainly forms in the southeast Pacific and southwest Atlantic (e.g., *McCartney, 1977; Piola and Georgi, 1982; Piola and Gordon, 1989*). Around the tip of South America intermediate water is originated by isopycnal exchange of cold and fresh Antarctic Surface Water across the Antarctic Polar Front, and by contributions of Sub-Antarctic Mode Water that originates from deep winter convection along the Subantarctic Zone (*Piola and Gordon, 1989*) **(Fig. 15)**. Variations in the strength/position of the Southern Westerly Winds (SWW) and associated ice-ocean freshwater fluxes are proposed to greatly influence the formation and circulation of AAIW. Westerly winds induce ocean cooling and freshening by favoring the northward

Ekman freshwater transport; with increase AAIW renewal during periods of intensified SWW (*Ribbe, 2001; Saenko and Weaver, 2001; Santoso and England, 2004*) and/or poleward shifted SWW (*Oke and England, 2004*). Antarctic sea-ice melting that occurs predominately away from the Antarctic continent due to the effect of prevailing westerly winds and intense precipitation adds freshwater to the regions where AAIW isopycnal surfaces outcrop, and thereby contribute to AAIW renewal (e.g. *Duffy et al., 2001; Saenko and Weaver, 2001; Santoso and England, 2004*). The correlation to wind stress implies that natural variability of AAIW strongly depends upon wind-forcing of the SWW and thus indicates a high sensitivity to Southern Hemisphere climate changes.

Coupling to Southern Hemisphere climate oscillations

Past perturbations in AAIW strength are consistent to Southern Hemisphere climate changes during the Holocene (**Fig. 16**). The long-term increase in AAIW circulation correlated to orbital-scale Holocene cooling (~2 °C) and freshening in the Southern Hemisphere recorded in ice cores around Antarctica that show a widespread early Holocene climatic optimum followed by cooler, more glaciated conditions (*Masson et al., 2000; Vimeux et al., 2001; Masson-Delmotte et al., 2004*). A substantial surface water cooling was recorded in the southeast Pacific (2-4 °C) (*Kaiser et al., 2008; Shevenell et al., 2011*) and the South Atlantic (*Hodell et al., 2001*) with associated changes in Antarctic sea-ice conditions, e.g., advanced sea-ice distribution and/or iceberg delivery (**Fig. 16H,I**)(*Domack et al., 2001; Kanfoush et al., 2002*). The abrupt response in AAIW strength at around 5.5 ka BP is synchronous to the general increase in IRD deposition, therefore providing evidence that overall increased ice-ocean freshwater fluxes toward regions where AAIW isopycnal surfaces outcrop might had directly contributed to enhanced AAIW formation (*Duffy et al., 2001; Saenko and Weaver, 2001; Saenko et al., 2003a*). The good correspondence to the onset of Patagonian glacier advances at ~5.0 ka BP (*Glasser et al., 2004*) further supports this hypothesis. The increase in AAIW strength is consistent with decreasing austral winter-spring insolation at 60 °S (*Renssen et al., 2005*) (**Fig. 16C**). The sensitivity to 60 °S winter-spring insolation is because AAIW renewal occurs in austral late winter and early spring when the cool atmospheric temperatures and deep mixed layers are conducive to deep convection. An overall poleward shift of the SWW throughout the Holocene as suggest by several proxy-based reconstructions (*Moros et al., 2009; Moreno et al., 2010; Fletcher and Moreno, 2011, Voigt et al., (in prep)*) and climate model simulations (*Varma et al., 2012*) might had also contributed to enhanced AAIW formation (*Oke and England, 2004*).

Superimposed on the Holocene orbital-scale cooling in the Southern Hemisphere high latitudes a succession of millennial-scale Antarctic cold events was recognized in the Pacific sector of Antarctica (*Masson et al., 2000*).

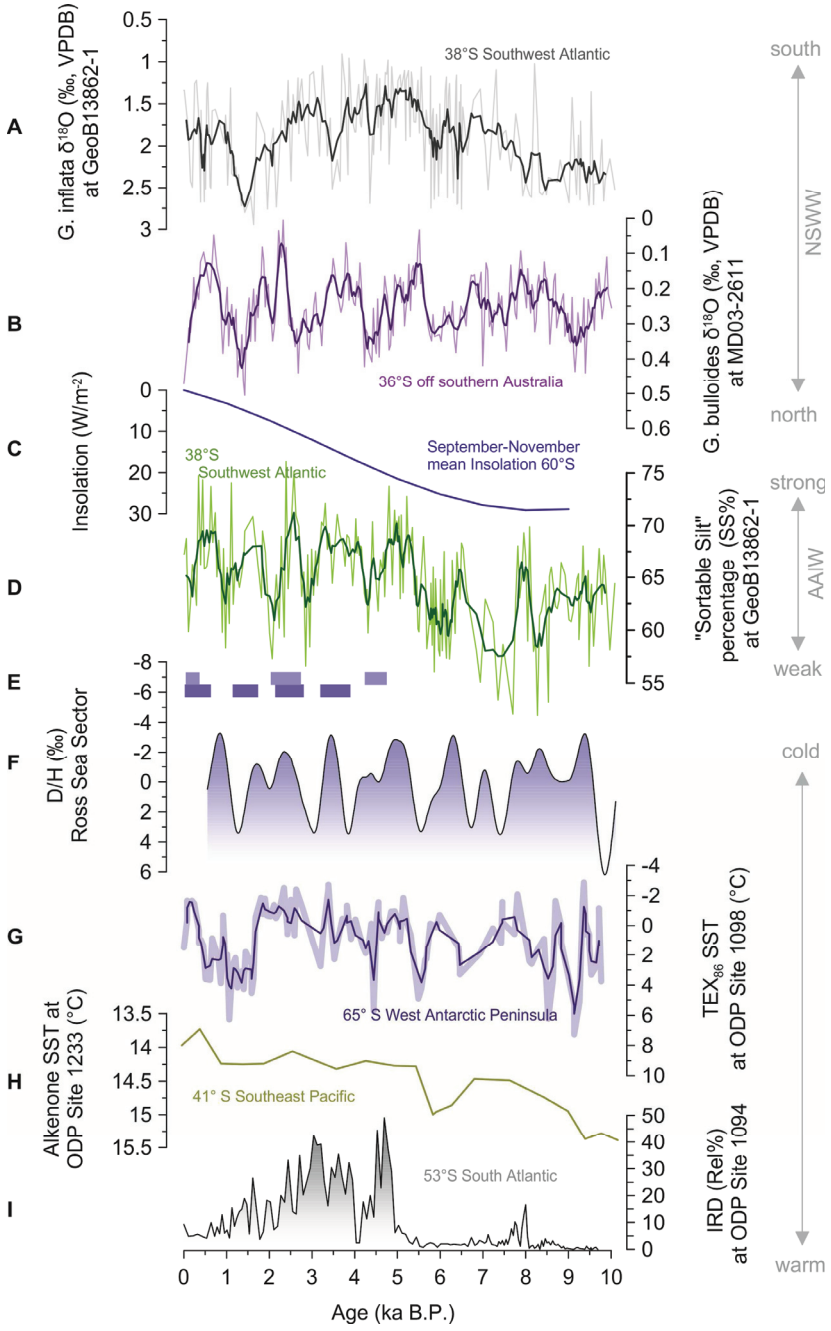

Figure 2 Millennial- and orbital- scale trends in the AAIW overturning circulation compared with Holocene Southern Hemisphere high-latitude climate records. Note that plots A, B, C, F, G and H have reversed y-axis. **A+B:** Latitudinal shifts of the northern boundary of the Southern Westerly Winds (NSWW) indicated by **(A)** planktonic foraminifer (G. inflata) $\delta^{18}O$ record from the Soutwest Atlantic (*Voigt et al.,(in prep)*, and **(B)** planktonic foraminifer (G. bulloides) $\delta^{18}O$ record off South Australia (*Moros et al., 2009*)(both plotted with a five-point running average). **C:** Austral spring (September-November) mean insolation at 60 °S, plotted as deviations from present-day mean (*Renssen et al., 2005)*. **D:** "Sortable silt" percentage (SS%) of GeoB13862-1 (plotted with a five-point running average). **E:** Blue boxes denote Neoglacial glacier advances in Patagonia (*Glasser et al., 2004*). **F:** Antarctic temperature (*Masson et al., 2000*). First component of an EOF analysis iscalculated from (detrended) isotopic records from the Ross-Sea sector (Byrd-Taylor Dome). **G:** TEX_{86}-derived SST in the sub-Antarctic Pacific (plotted with a three-point running average) (*Shevenell et al., 2011*). **H:** Alkenone-derived SST in the Southeast Pacific (*Kaiser et al., 2008*). **I:** Relative percentage of IRD in the South Atlantic (*Kanfoush et al., 2002*).

Millennial-scale variability in AAIW strength correlates to Antarctic temperature changes with increased strength in AAIW during abrupt Antarctic climate cooling (**Fig. 16F**). Coincident to these Antarctic cold events significant millennial-scale fluctuations are recorded in TEX_{86} sea surface temperature (SST) proxy west of Antarctic Peninsula (*Shevenell et al., 2011*)(**Fig. 16G**). Significant glacier and icefield advances in throughout Patagonia (*Glasser et al., 2004*) (**Fig. 16E**) associated with cool-temperate and wet conditions in southwest Patagonia (*Moreno et al., 2009*) coincided with abrupt increases in AAIW circulation. These observations support the hypothesis that intense precipitation and/or advanced sea-ice cover associated to Southern Ocean surface water cooling might have reinforced the freshwater flux towards regions where AAIW isopycnal surfaces outcrop. The freshwater subducted to intermediate depths and thereby contributed to the formation of cold, fresh AAIW (*Duffy et al., 2001*). Evidence for millennial-scale variability of the SSW comes from $\delta^{18}O$ records of planktonic foraminifer off South America (**Fig. 16A**) (*Voigt et al. (in prep)*) and off South Australia (**Fig. 16B**) (*Moros et al., 2009*) that both indicate surface oceanic circulation changes in response to latitudinal shifts of the SWW. Within age-model uncertainties the timing of millennial-scale variability in the SWW is synchronous with the abrupt changes in the AAIW overturning circulation; with poleward (equatorward) shifts of the SWW correspond to increased (decreased) AAIW strength (**Fig. 16A,B**). The SWW-AAIW linkage is supported by climate model studies (*Oke and England, 2004*) suggesting that poleward shifts of SWW would have the effect of shifting the Ekman-driven flow poleward, thereby favoring colder Antarctic Surface Water being transported northward toward the regions where AAIW is formed. This in turn could have contributed to increased renewal of AAIW, resulting in cooling and freshening at intermediate depths of the South Atlantic. Intensified SWW may have further contributed to increased formation of AAIW by inducing ocean cooling and freshening via (respectively) air-sea and ice-ocean fluxes (*Ribbe, 2001; Saenko and Weaver, 2001; Santoso and England, 2004*). Here we note that significant changes in intermediate water circulation during the Holocene correlated to changes in the SWW-Southern Ocean coupled system; with increased AAIW strength corresponded to millennial-scale cold anomalies in the Southern Hemisphere in conjunction with poleward shifted and strengthened SWW.

Interhemispheric NADW–AAIW Coupling

The injection of cool, fresh AAIW into the South Atlantic subtropical gyre is thought to have important implications for the Atlantic heat and salinity budget and possibly the rate of NADW formation (*Graham et al., 2011*). A high-resolution Holocene $\overline{SS}$ record from the North Atlantic (*Hall et al., 2004*) indicates the presence of a highly variable deep Iceland Scotland Overflow (ISOW) flow throughout the Holocene - a precursor water mass of NADW **(Fig. 17**). Significant parts of NADW perturbations during the Holocene have been associated to millennial-scale Northern Hemisphere cold events; with reductions in

NADW production triggered by the impact of increased freshwater inflow to the North Atlantic (*Bond et al., 2001*). The changes in AAIW circulation are antiphased with perturbations in NADW circulation; with abruptly increased AAIW northward advection correlating to periods of reduced North Atlantic overturning circulation and vice versa (**Fig. 17B,C**). The spectral analysis of our records shows a periodicity of ~1500-yr in AAIW circulation which is coherent with quasi-periodic ISOW/NADW fluctuations (*Bianchi and McCave, 1999*) (*see Supplementary Information,* SF3). The inverse relationship of millennial-scale changes in NADW formation and the northward penetration of AAIW provides strong evidence for a NADW–AAIW see-saw operating during the Holocene. Abrupt changes in the northward flow of AAIW associated with AMOC reduction have also been suggested by paleoproxy reconstructions (*Pahnke et al., 2008*) and climate model simulations (*Saenko et al., 2003b; Weaver et al., 2003*) during the last deglaciation. Thereby, NADW-AAIW coupling was maintained by opposite density gradients at the high latitudes formation regions as a response to freshwater anomalies which resulted in reversals in water-mass formation and related changes in the AMOC. However, it still is questionable if these underlying mechanisms work during the Holocene due to generally larger NADW-AAIW density gradient (*Saenko et al., 2003b*). If increased AAIW renewal were forced by cold and fresh anomalies in the Southern Hemisphere, as suggested by simultaneous AAIW and Southern Hemisphere climate

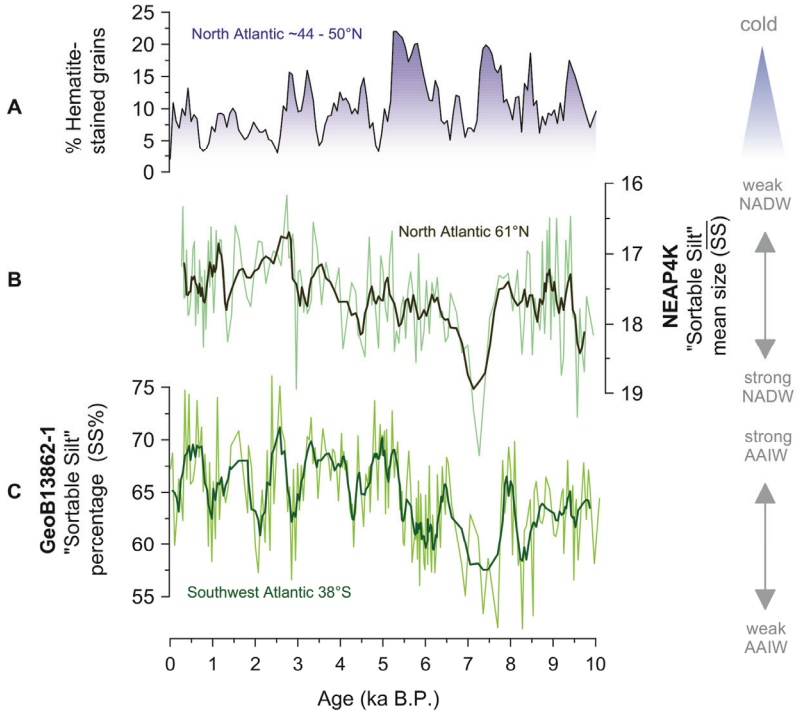

Figure 17 Comparison of Holocene paleocurrent records from the North- and South Atlantic. Note that plot B has reversed y-axis. **A:** Ice-rafting proxy record from North Atlantic marine core (MC52-MD29191-CMC21-GGC22) (*Bond et al., 2001*). **B:** NEAP4K $\overline{SS}$ (*Hall et al., 2004*). **C:** GeoB13862-1 SS%. Five-point running average is shown for B and C.

changes, incursions of cool, fresh AAIW into the North Atlantic could have had a dampening effect on the formation of NADW. Recent climate simulations support our interpretation of a pervasive link between formation of AAIW and NADW for the Holocene (*Graham et al., 2011*), and demonstrate that initial changes in AMOC strength may be related to perturbations in AAIW. The incursions of cool, fresh AAIW to the upper water column in the North Atlantic may have been involved in cooling and freshening of the North Atlantic during Northern Hemisphere cold events and thereby contributed to the reduction of NADW formation. *Graham et al., 2011* also show that the ventilation timescale for AAIW in the Atlantic ranges from 50-150 years, consistent with recent observations (*Holzer et al., 2010*), thus supporting the hypothesis of a synchronous AAIW-NADW coupling.

Atlantic cooling and freshening as a direct response to wind shifts in the Southern Hemisphere would indicate that the SWW-Southern Ocean coupled system is essential in driving millennial-scale changes in the AMOC providing evidence that the trigger for abrupt climate change in the Holocene may reside in the Southern Hemisphere. Recent observations show significant cooling and freshening of intermediate waters in the Southern Ocean over the last 50 yr (*Bindoff and McDougall, 1994; Johnson and Orsi, 1997; Wong et al., 1999*) probably in response to a recent poleward shift of the SWW (*Oke and England, 2004*), thereby supporting our interpretation of a SWW-AAIW linkage. Yet, considering the recent changes in AAIW circulation clarifies that even small changes may be sufficient for the mid-depth competition between northern and southern source waters in the Atlantic and could be an additional source of modern climate variability.

3.3. Acknowledgements

We thank J. Groeneveld and G. Martínez-Méndez for comments and discussion. This study was funded through DFG-Research Center / Cluster of Excellence „The Ocean in the Earth System“ and was supported by the Bremen International Graduate School for Marine Sciences (GLOMAR) that is funded by the German Research Foundation (DFG) within the frame of the Excellence Initiative by the German federal and state governments to promote science and research at German universities. ARP acknowledges the support from grant CRN2076 from the Inter-American Institute for Global Change Research and the U.S. National Science Foundation grant GEO-0452325. CMC acknowledges the support from FAPESP (2010/09983-9).

3.4. References

Bianchi, G.G., McCave, I.N., 1999. Holocene periodicity in North Atlantic climate and deep-ocean flow south of Iceland. Nature 397 (6719), 515-517.

Bindoff, N.L., McDougall, T.J., 1994. Diagnosing Climate Change and Ocean Ventilation Using Hydrographic Data.

Journal of Physical Oceanography 24 (6), 1137-1152.

Bond, G., Kromer, B., Beer, J., Muscheler, R., Evans, M.N., Showers, W., Hoffmann, S., Lotti-Bond, R., Hajdas, I., Bonani, G., 2001. Persistent Solar Influence on North Atlantic Climate During the Holocene. Science 294 (5549), 2130-2136.

Domack, E., Leventer, A., Dunbar, R., Taylor, F., Brachfeld, S., Sjunneskog, C., 2001. Chronology of the Palmer Deep site, Antarctic Peninsula: a Holocene palaeoenvironmental reference for the circum-Antarctic. The Holocene 11 (1), 1-9.

Duffy, P.B., Eby, M., Weaver, A.J., 2001. Climate Model Simulations of Effects of Increased Atmospheric CO_2 and Loss of Sea Ice on Ocean Salinity and Tracer Uptake. Journal of Climate 14 (4), 520-532.

Fletcher, M.-S., Moreno, P.I., 2011. Zonally symmetric changes in the strength and position of the Southern Westerlies drove atmospheric CO_2 variations over the past 14 k.y. Geology 39 (5), 419-422.

Glasser, N.F., Harrison, S., Winchester, V., Aniya, M., 2004. Late Pleistocene and Holocene palaeoclimate and glacier fluctuations in Patagonia. Global and Planetary Change 43 (1–2), 79-101.

Graham, J., Stevens, D., Heywood, K., Wang, Z., 2011. North Atlantic climate responses to perturbations in Antarctic Intermediate Water. Climate Dynamics 37 (1-2), 297-311.

Hall, I.R., Bianchi, G.G., Evans, J.R., 2004. Centennial to millennial scale Holocene climate-deep water linkage in the North Atlantic. Quaternary Science Reviews 23 (14–15), 1529-1536.

Hernández-Molina, F.J., Paterlini, M., Violante, R., Marshall, P., de Isasi, M., Somoza, L., Rebesco, M., 2009. Contourite depositional system on the Argentine Slope: An exceptional record of the influence of Antarctic water masses. Geology 37 (6), 507-510.

Hodell, D.A., Kanfoush, S.L., Shemesh, A., Crosta, X., Charles, C.D., Guilderson, T.P., 2001. Abrupt Cooling of Antarctic Surface Waters and Sea Ice Expansion in the South Atlantic Sector of the Southern Ocean at 5000 cal yr B.P. Quaternary Research 56 (2), 191-198.

Holzer, M., Primeau, F.W., Smethie, W.M., Jr., Khatiwala, S., 2010. Where and how long ago was water in the western North Atlantic ventilated? Maximum entropy inversions of bottle data from WOCE line A20. J Geophys. Res. 115 (C7), C07005.

Johnson, G.C., Orsi, A.H., 1997. Southwest Pacific Ocean Water-Mass Changes between 1968/69 and 1990/91. Journal of Climate 10 (2), 306-316.

Kaiser, J., Schefuß, E., Lamy, F., Mohtadi, M., Hebbeln, D., 2008. Glacial to Holocene changes in sea surface temperature and coastal vegetation in north central Chile: high versus low latitude forcing. Quaternary Science Reviews 27 (21–22), 2064-2075.

Kanfoush, S.L., Hodell, D.A., Charles, C.D., Janecek, T.R., Rack, F.R., 2002. Comparison of ice-rafted debris and physical properties in ODP Site 1094 (South Atlantic) with the Vostok ice core over the last four climatic cycles. Palaeogeography, Palaeoclimatology, Palaeoecology 182 (3–4), 329-349.

Locarnini, R.A., Mishonov, A.V., Antonov, J.I., Boyer, T.P., Garcia, H.E., Baranova, O.K., Zweng, M.M., Johnson, D.R., 2010. World Ocean Atlas 2009. Volume 1: Temperature. S. Levitus, Ed. NOAA Atlas NESDIS 68, U.S. Government Printing Office, Washington, D.C., 184 pp.

Masson-Delmotte, V., Stenni, B., Jouzel, J., 2004. Common millennial-scale variability of Antarctic and Southern Ocean temperatures during the past 5000 years reconstructed from the EPICA Dome C ice core. The Holocene 14 (2), 145-151.

Masson, V., Vimeux, F., Jouzel, J., Morgan, V., Delmotte, M., Ciais, P., Hammer, C., Johnsen, S., Lipenkov, V.Y., Mosley-Thompson, E., Petit, J.-R., Steig, E.J., Stievenard, M., Vaikmae, R., 2000. Holocene Climate Variability in Antarctica Based on 11 Ice-Core Isotopic Records. Quaternary Research 54 (3), 348-358.

McCartney, M.S., 1977. Subantarctic Mode Water. A Voyage of Discovery: George Deacon 70th Anniversary Volume (Suppl. to Deep-Sea Res.).

McCave, I.N., Manighetti, B., Robinson, S.G., 1995. Sortable Silt and Fine Sediment Size/Composition Slicing: Parameters for Palaeocurrent Speed and Palaeoceanography. Paleoceanography 10 (3), 593-610.

Moreno, P.I., François, J.P., Villa-Martínez, R.P., Moy, C.M., 2009. Millennial-scale variability in Southern Hemisphere westerly wind activity over the last 5000 years in SW Patagonia. Quaternary Science Reviews 28 (1–2), 25-38.

Moreno, P.I., Francois, J.P., Moy, C.M., Villa-Martínez, R., 2010. Covariability of the Southern Westerlies and atmospheric CO_2 during the Holocene. Geology 38 (8), 727-730.

Moros, M., De Deckker, P., Jansen, E., Perner, K., Telford, R.J., 2009. Holocene climate variability in the Southern Ocean recorded in a deep-sea sediment core off South Australia. Quaternary Science Reviews 28 (19–20), 1932-1940.

Mulitza, S., Prange, M., Stuut, J.-B., Zabel, M., von Dobeneck, T., Itambi, A.C., Nizou, J., Schulz, M., Wefer, G., 2008. Sahel megadroughts triggered by glacial slowdowns of Atlantic meridional overturning. Paleoceanography 23 (4), PA4206.

Oke, P.R., England, M.H., 2004. Oceanic Response to Changes in the Latitude of the Southern Hemisphere Subpolar Westerly Winds. Journal of Climate 17 (5), 1040-1054.

Pahnke, K., Zahn, R., 2005. Southern Hemisphere Water Mass Conversion

Linked with North Atlantic Climate Variability. Science 307 (5716), 1741-1746.

Pahnke, K., Goldstein, S.L., Hemming, S.R., 2008. Abrupt changes in Antarctic Intermediate Water circulation over the past 25,000 years. Nature Geoscience 1 (12), 870-874.

Piola, A.R., Georgi, D.T., 1982. Circumpolar properties of Antarctic intermediate water and Subantarctic Mode Water. Deep Sea Research Part A. Oceanographic Research Papers 29 (6), 687-711.

Piola, A.R., Gordon, A.L., 1989. Intermediate waters in the southwest South Atlantic. Deep Sea Research Part A. Oceanographic Research Papers 36 (1), 1-16.

Renssen, H., Goosse, H., Fichefet, T., Masson-Delmotte, V., Koç, N., 2005. Holocene climate evolution in the high-latitude Southern Hemisphere simulated by a coupled atmosphere-sea ice-ocean-vegetation model. The Holocene 15 (7), 951-964.

Ribbe, J., 2001. Intermediate water mass production controlled by southern hemisphere winds. Geophys. Res. Lett. 28 (3), 535-538.

Saenko, O.A., Weaver, A.J., 2001. Importance of wind-driven sea ice motion for the formation of Antarctic Intermediate Water in a global climate model. Geophys. Res. Lett. 28 (21), 4147-4150.

Saenko, O.A., Weaver, A.J., England, M.H., 2003a. A Region of Enhanced Northward Antarctic Intermediate Water Transport in a Coupled Climate Model. Journal of Physical Oceanography 33 (7), 1528-1535.

Saenko, O.A., Weaver, A.J., Gregory, J.M., 2003b. On the Link between the Two Modes of the Ocean Thermohaline Circulation and the Formation of Global-Scale Water Masses. Journal of Climate 16 (17), 2797-2801.

Santoso, A., England, M.H., 2004. Antarctic Intermediate Water Circulation and Variability in a Coupled Climate Model. Journal of Physical Oceanography 34 (10), 2160-2179.

Schulz, M., Mudelsee, M., 2002. REDFIT: estimating red-noise spectra directly from unevenly spaced paleoclimatic time series. Computers & Geosciences 28 (3), 421-426.

Shevenell, A.E., Ingalls, A.E., Domack, E.W., Kelly, C., 2011. Holocene Southern Ocean surface temperature variability west of the Antarctic Peninsula. Nature 470 (7333), 250-254.

Stramma, L., England, M., 1999. On the water masses and mean circulation of the South Atlantic Ocean. J. Geophys. Res. 104 (C9), 20863-20883.

Varma, V., Prange, M., Merkel, U., Kleinen, T., Lohmann, G., Pfeiffer, M., Renssen, H., Wagner, A., Wagner, S., Schulz, M., 2012. Holocene evolution of the Southern Hemisphere westerly winds in transient simulations with global climate models. Clim. Past 8 (2), 391-402.

Vimeux, F., Masson, V., Jouzel, J., Petit, J.R., Steig, E.J., Stievenard, M., Vaikmae, R., White, J.W.C., 2001. Holocene hydrological cycle changes in the Southern Hemisphere documented in East Antarctic deuterium excess records. Climate Dynamics 17 (7), 503-513.

Voigt, I., Henrich, R., Preu, P., Piola, A.R., Hanebuth, T.J.J., Schwenk, T., Chiessi, C.M., 2012. A submarine canyon as a climate archive- Interaction of the Antarctic Intermediate Water with the Mar del Plata Canyon (Southwest Atlantic). Marine Geology (submitted).

Voigt, I., Chiessi, C.M., Mulitza, S., Prange, M., Groeneveld, J., Henrich, R., 2013. Holocene oscillations of Southern Westerly Winds in response to North Atlantic climate perturbations (in preparation for Nature Geoscience).

Weaver, A.J., Saenko, O.A., Clark, P.U., Mitrovica, J.X., 2003. Meltwater Pulse 1A from Antarctica as a Trigger of the Bølling-Allerød Warm Interval. Science 299 (5613), 1709-1713.

Wong, A.P.S., Bindoff, N.L., Church, J.A., 1999. Large-scale freshening of intermediate waters in the Pacific and Indian oceans. Nature 400 (6743), 440-443.

3.5. Supplementary Information

3.5.1. Age model

Age model for GeoB13862-1 is are based on a published age model (*Voigt et al., (submitted*). The age model for the Holocene sequence of GeoB13862-1 is based on 7 Accelerator Mass Spectrometry (AMS) ^{14}C dates determined on monospecific samples of the planktonic foraminifer Globigerina inflata (>150 mm fraction). The radiocarbon dates were calibrated with the CALIB 6.0 software (*Stuiver et al., 2010*) applying the Marine09 calibration curve (*Reimer et al., 2009*).

Table S1

Sample Code	Depth (cm)	Species	Radiocarbon age ± 1σ error (a B.P.)	2σ calibrated age range (cal a B.P	Calibrated age, interpolated from 2σ range (cal ka BP)
Core GeoB13862-2					
Poz-38071	143	*G. inflata*	1790 ± 140	1050-1668	1,36
Poz-42354	258	*G. inflata*	4000 ± 50	3852-4152	4,00
Poz-38072	393	*G. inflata*	5380 ± 60	5612-5886	5,75
Poz-42355	490	*G. inflata*	5840 ± 80	6057-6434	6,25
Poz-42356	556	*G. inflata*	6140 ± 50	6440-6700	6,57
Poz-38074	669	*G. inflata*	8530 ± 70	8994-9363	9,18
Poz-38075	793	*G. inflata*	9740 ± 70	10460-10827	10,64

3.5.2. Paleocurrent proxy record of GeoB13862-1

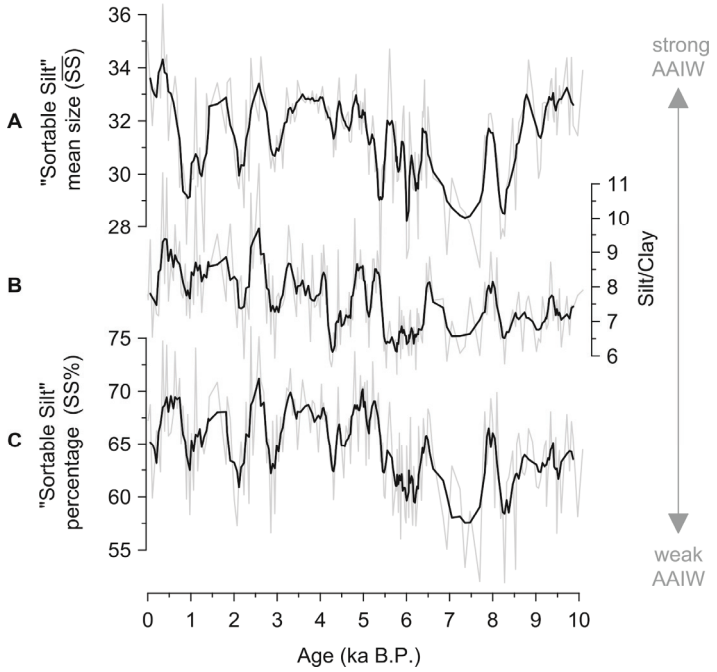

Supplementary Figure SF1. Proxies for the strength of Antarctic Intermediate Water (AAIW) flow in the western South Atlantic from core GeoB13862-1. **A:** "Sortable silt" mean size ($\overline{SS}$). **B:** Silt/clay ratio. **C:** "Sortable silt" percentage (SS%). Original data (grey line) and a five-point running average (black line) is shown for all plots.

3.5.3. Spectralanalysis

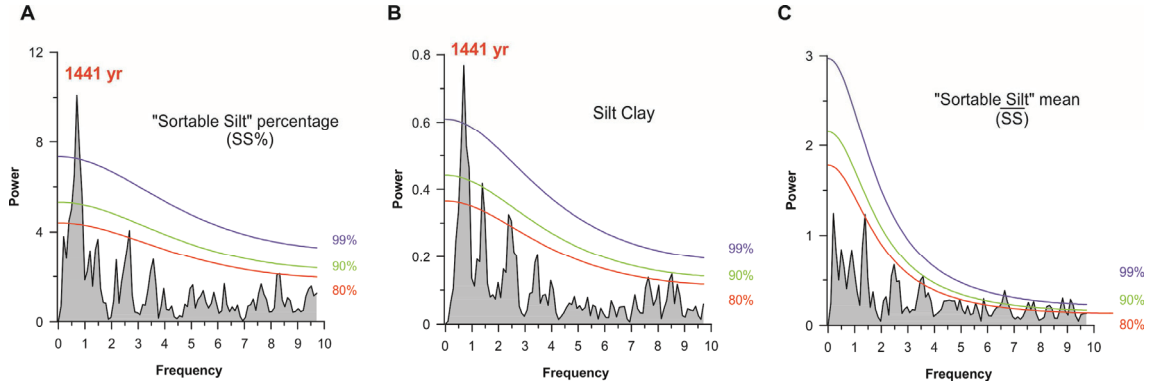

Supplementary Figure SF2. Spectral analyses of GeoB13862-1 **(A)** SS% - "Sortable Silt" percentage **(B)** Silt/Clay and **(C)** $\overline{SS}$- "Sortable Silt" mean. Peaks that exceed the 95% confidence level are labeled with their periods (in years). Analyses were performed with the software REDFIT (*Schulz and Mudelsee, 2002*). The number of overlapping segments chosen was 3, and a Rectangle type window was used.

3.5.4. Interhemispheric NADW–AAIW Coupling

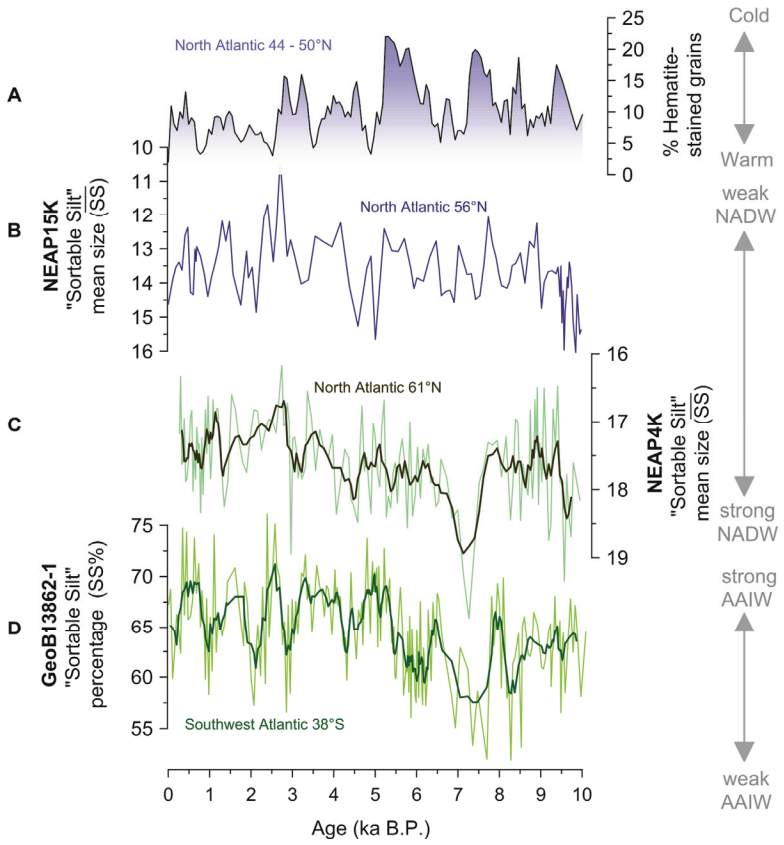

Supplementary Figure SF3. Comparison of Holocene paleocurrent records from the North- and South Atlantic. Note that plot B and C have reversed y-axis. **A:** Ice-rafting proxy record from North Atlantic marine core (MC52-MD29191-CMC21-GGC22) (*Bond et al., 2001*). **B:** NEAP15K $\overline{SS}$ (*Bianchi and McCave, 1999*). **C:** NEAP4K $\overline{SS}$ (*Hall et al., 2004*). **D:** GeoB13862-1 SS%. Five-point running average is shown for B and C.

Bianchi, G.G., McCave, I.N., 1999. Holocene periodicity in North Atlantic climate and deep-ocean flow south of Iceland. Nature 397 (6719), 515-517.

Bond, G., Kromer, B., Beer, J., Muscheler, R., Evans, M.N., Showers, W., Hoffmann, S., Lotti-Bond, R., Hajdas, I., Bonani, G., 2001. Persistent Solar Influence on North Atlantic Climate During the Holocene. Science 294 (5549), 2130-2136.

Hall, I.R., Bianchi, G.G., Evans, J.R., 2004. Centennial to millennial scale Holocene climate-deep water linkage in the North Atlantic. Quaternary Science Reviews 23 (14–15), 1529-1536.

Reimer, P.J., Baillie, M.G.L., Bard, E., Bayliss, A., Beck, J.W., Blackwell, P.G., Bronk Ramsey, C. Buck, C.E., Burr, G.S., Edwards, R.L., Friedrich, M., Grootes, P.M., Guilderson, T.P., Hajdas, I., Heaton, T.J., Hogg, A.G., Hughen, K.A., Kaiser, K.F., Kromer, B.,

McCormac, F.G., Manning, S.W., Reimer, R.W., Richards, D.A., Southon, J.R., Talamo, S., Turney, C.S.M., van der Plicht, J., Weyhenmeyer ,C.E., 2009. IntCal09 and Marine09 radiocarbon age calibrationcurves, 0–50,000 years cal BP. Radiocarbon 51, pp. 1111–1150.

Schulz, M., Mudelsee, M., 2002. REDFIT: estimating red-noise spectra directly from unevenly spaced paleoclimatic time series. Computers & Geosciences 28 (3), 421-426.

Stuiver, M., Reimer, P.J., 1993. Extended ^{14}C data base and revised CALIB 3.0 ^{14}C age calibration program. Radiocarbon, 35 , pp. 215–230.

Voigt, I., Henrich, R., Preu, P., Piola, A.R., Hanebuth, T.J.J., Schwenk, T., Chiessi, C.M., 2012. A submarine canyon as a climate archive- Interaction of the Antarctic Intermediate Water with the Mar del Plata Canyon (Southwest Atlantic). Marine Geology (submitted).

Chapter 4: Holocene oscillations of Southern Westerly Winds in response to North Atlantic climate perturbations

Ines Voigt[1], Cristiano M. Chiessi[2], Stefan Mulitza[1], Matthias Prange[1], Jeroen Groeneveld[1], Rüdiger Henrich[1]

[1]MARUM –Center for Marine Environmental Sciences and Faculty of Geosciences, University of Bremen, D-28359 Bremen, Germany

[2]School of Arts, Sciences and Humanities, University of São Paulo, Brazil

(*In preparation for Nature Geoscience*)

4.1. Abstract

The Southern Westerly Winds (SWW) are an important component of the global climate system. However, understanding Holocene variability of the SWW along with forcing- and feedback mechanisms remains a significant challenge in climate research. Here, we present high-resolution planktonic foraminifera oxygen isotope records from the western South Atlantic that reveal Holocene millennial-scale migrations of the Brazil- Malvinas Confluence - a highly sensitive feature for changes in the position and strength of the northern boundary of the SWW. Our results demonstrate that latitudinal shifts of the SWW were part of synchronous and systematic changes in westerly winds over both hemispheres during North Atlantic cold events. We propose that an initial forcing within the North Atlantic was transmitted to the Southern Hemisphere via large-scale reorganizations of the atmospheric circulation. This provides strong evidence for a tight atmospheric teleconnection operating during the Holocene that is conceptually different to the mechanism proposed to control modern and future changes in the westerlies.

4.2. Main Text

The Southern Westerly Winds (SWW) play an important role in the global climate system through the wind-driven upwelling of deep water in the Southern Ocean and the potentially resulting atmospheric CO_2 variations. Although the Holocene (11,700 cal yr B.P. to the present) was a period of abrupt climate fluctuations on millennial-to-centennial time scales (*Bond et al., 2001*) there is surprisingly little systematic knowledge about Holocene changes in the strength and position of the SWW. Recent studies suggested a synchronous poleward shift of the global westerlies for the twentieth century (*Gillett et al., 2003, Wu et al., 2012*). The possibility that this systematic change in winds over both hemispheres might occur under greenhouse-gas forcing has raised significant concerns (*Saenko et al., 2005*), thereby pointing to a need for proxy-based reconstructions of Holocene natural variability of the SWW.

Previous studies suggested a vital role for large amplitude changes in deglacial North Atlantic sea surface temperatures (SST) in regulating changes in the SWW via large-scale reorganizations of the atmospheric circulation (e.g., *Anderson et al., 2009; Toggweiler 2009; Lee at al., 2011*). They inferred that southward shifts of the Intertropical Convergence Zone (ITCZ) induced by North Atlantic cooling led to a strengthening and southward shift of the SWW. Ice-rafted debris (IRD) deposited in the North Atlantic reveal millennial-scale climate variability in the North Atlantic also during the Holocene (*Bond et al. 2001*), rising a major question: to what extent were the SWW affected by remote North Atlantic cooling during the Holocene? Here, we validate the underlying mechanisms for abrupt reorganizations of the SWW belt during North Atlantic cold events, and provide detailed insights into an atmospheric see-saw operating during the Holocene.

The BMC as a reliable proxy for SWW variability

The Brazil-Malvinas Confluence (BMC), a prominent feature in the upper-level circulation in the western South Atlantic, is considered a highly sensitivity feature for changes in the strength and position of the SWW (*Sijp and England, 2008; Lumpkin and Garzoli, 2011*). The BMC is characterized by the encounter of southward-flowing Brazil Current (BC) and northward-flowing Malvinas (Falkland) Current (MC) (*Peterson and Stramma 1991*)(**Fig. 18**). This encounter takes place at approximately 38 °S, generating one of the most energetic regions of the world ocean (*Gordon, 1989*). The subantarctic waters of the MC and the subtropical waters of the BC collide in the upper 800 m of the water column which make the BMC a major ventilation area for much of the South Atlantic thermocline (*Gordon, 1981*). The combined flow of the two currents causes a strong thermohaline frontal zone (e.g., *Olson et al., 1988*) characterized by sharp horizontal and vertical temperature and salinity gradients. After the confluence, both currents turn eastward and flow offshore in a series of large-scale meanders and eddies. A marked seasonal and interannual variability in the location of the confluence is governed by the maximum of the wind stress curl (i.e., the northern boundary of the SWW, N-SWW)

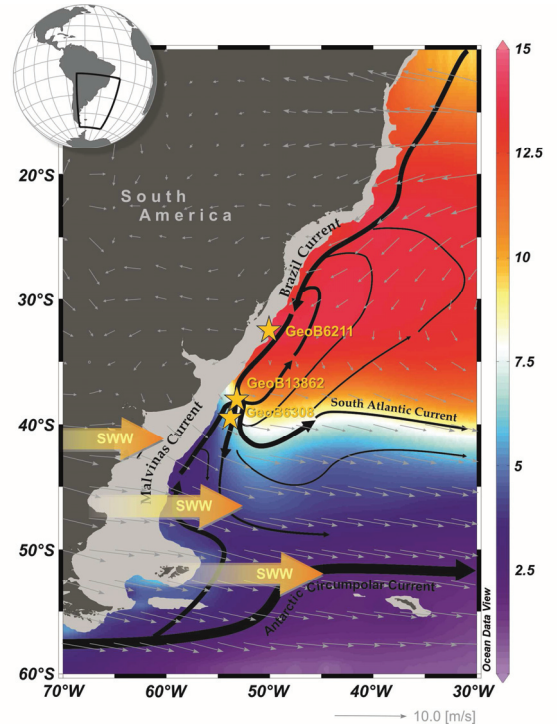

Figure 18 Modern annual mean temperature in the western South Atlantic at 350 m water depth (*Locarnini et al., 2010*). Black arrows indicate the upper-ocean circulation of the western South Atlantic (*Piola and Matano, 2001*). Grey arrows indicate present-day annual mean zonal wind (m s^{-1}) at 850 hPa based on NCEP/NCAR reanalysis data (*Kalnay et al., 1996*). Yellow stars show the position of the sediment cores investigated in this study. Site GeoB13862-1 is well situated to monitor past changes in upper-ocean circulation because it is located beneath the modern mean position of the Brazil-Malvinas Confluence that separates cooler subpolar waters to the south from warmer subtropical waters to the north.

across the South Atlantic (see *Supplementary Information,* SF4) (*Matano et al., 1993; Lumpkin and Garzoli, 2011*). The tight coupling between the BMC and the local wind field makes the confluence ideal for reconstruction of past variability of the N-SWW.

We investigated a north–south transect of three marine sediment cores from the mid-latitudes of the western South Atlantic (**Fig. 18; Table 3**) covering the present extent of the BMC. This enables us to record time-space oscillations of the BMC in response to changes in the position of the N-SWW throughout the Holocene (0–11 kyr; all ages given as calibrated ages before present). Details of the ^{14}C-based age models for all cores are provided in the *Supplementary Information,* Table S2. We used the stable oxygen isotope composition ($\delta^{18}O$) of the deep dwelling planktonic foraminifera *Globorotalia inflata* (see *Supplementary Information*). This species occurs in high amounts at subtropical to subpolar conditions, and shows an apparent calcification depth of 350-400 m in the South Atlantic (*Groeneveld and Chiessi, 2011*) which qualifies it for reconstructions of the BMC (*Chiessi et al., 2007*). We expressed our $\delta^{18}O$ values as continental ice volume–corrected (ivc) in order to compare our downcore $\delta^{18}O$ values to modern BC and MC $\delta^{18}O$ values. We calculated $\delta^{18}O$ (ivc) by the updated version of the sea-level curve of *Lambeck and Chappell (2001)* multiplied by a constant coefficient of 1.0 ‰/130 m (*Schrag et al., 2002*).

Table 3| Sediment core transect

Core ID	Latitude	Longitude	Water depth (m)
GeoB6211	32.5052° S	50.2427° W	657
GeoB13862-1	38.0918° S	53.6098° W	3588
GeoB6308	39.3017° S	53.9650° W	3620

Time-space variability of the BMC

Similar to recent observations (*Chiessi et al., 2007*), our northernmost core shows low $\delta^{18}O$ values (~1.09 ‰) typical of the BC, whereas our southernmost core shows high $\delta^{18}O$ values (~2.78 ‰) characteristic of the MC (**Fig. 19**).

The $\delta^{18}O$ record of GeoB6211 (GeoB6308) thus indicate a sustained influence of the BC (the MC) throughout the Holocene. Moreover, both records show low amplitude millennial-scale oscillations (≤1 ‰). On the other hand, the $\delta^{18}O$ record of GeoB13862-1 shows high amplitude (up to 2 ‰) millennial-scale changes throughout the Holocene, clearly indicating altered phases of BC and MC influence (**Fig. 19**). We interpret the abrupt shifts in the $\delta^{18}O$ record of GeoB13862-1 as representative of millennial-scale N-S shifts of the BMC. The low amplitude variability of the $\delta^{18}O$ records of our northernmost and southernmost cores indicate that the BMC never extrapolated ~32.5 and 39.3 °S but rather oscillated between these latitudes.

Spectral analyses of the $\delta^{18}O$ records performed with the software REDFIT (*Schulz and Mudelsee, 2002*) revealed statistically significant oscillations (99 % confidence level) in the southern cores (i.e., GeoB13862-1 and GeoB6308) and the lack of it in the northern core (GeoB6211)(see *Supplementary Information,* SF5). The spectra depict a pronounced peak with period of ~2500 yr (1900-3600 yr in GeoB13862), and ~2200 yr (1700-2900 yr in GeoB6308).

Millennial-scale variations of the N-SWW

Through the tight coupling of the BMC to the northern boundary of the SWW (*Matano et al., 1993; Lumpkin and Garzoli, 2011*) reconstructions of the confluence latitude enable a reliable proxy for changes in the position and strength of N-SWW (*Oke and England, 2004; Sijp and England, 2008*). We suggest that millennial-scale N-S shifts of the BMC during the Holocene were intimately linked to latitudinal shifts of the N-SWW: southward (northward) shifts of the BMC indicate decreases (increases) in the strength of the northern edge of the westerlies, consistent with poleward (equatorward) shifts of the N-SWW. Statistically significant oscillations with similar period in the southern sediment cores of our transect (i.e., GeoB13862-1, GeoB6308) and the lack of it in the northern core of our transect (i.e., GeoB6211) indicate a southern forcing for

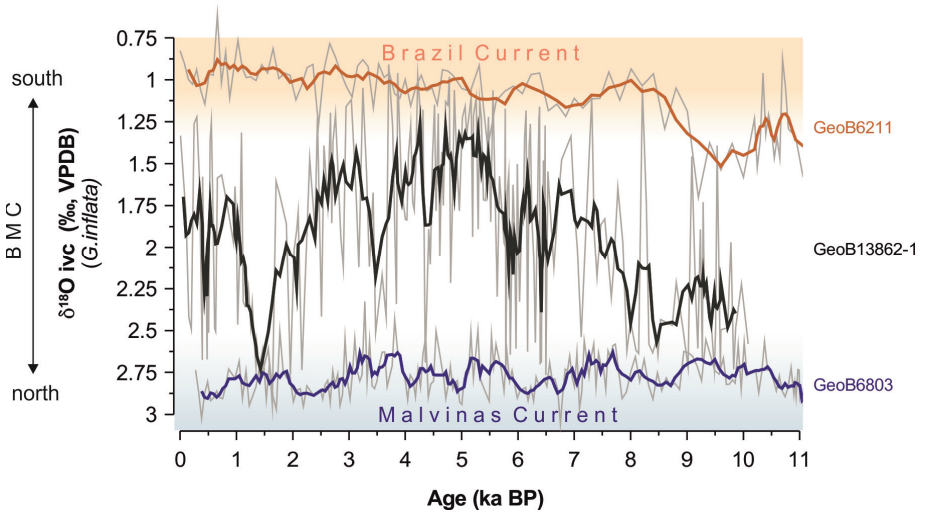

Figure 19 Ice volume corrected *Globorotalia inflata* $\delta^{18}O$ ($\delta^{18}O$ ivc) records along the N-S transect in the western South Atlantic (thin grey curves), plotted together with a 5-point running average (bold curves). Red (blue) background indicate the modern $\delta^{18}O$ signature of the Brazil Current (Malvinas Current) (*Chiessi et al., 2007*).

the oscillations in N-SWW (*Supplementary Information,* SF5).

Within age-model uncertainties the timing of millennial-scale variability in the N-SWW is synchronous with significant iceberg discharge events in the North Atlantic (*Bond et al., 2001*), providing striking evidence that poleward shifts of the N-SWW corresponded to remote North Atlantic cooling (**Fig. 20C**). Wavelets analyses of our $\delta^{18}O$ records from GeoB13862-1 and GeoB6308 show a relatively stationary ~2000-year period throughout the Holocene (*Supplementary Information,* SF6). A similar periodicity was described for the North Atlantic IRD record during the Holocene (*Obrochta et al., 2012*). This may indicate a pervasive link between North Atlantic climate perturbations and structural changes of SWW during the Holocene. Previous studies have suggested that large-scale changes in the North Atlantic surface ocean circulation (*deMenocal et al., 2000; Thornalley et al., 2009*) were closely linked to changes in the strength and position of Northern Hemisphere westerly winds (*Sorrel et al., 2012*). Hereby, westward, reduced extensions of the subpolar gyre in the North Atlantic demonstrate a response to weaker and southward-shifted westerlies during North Atlantic cold events (*Sorrel et al., 2012*). Consistent with a westward contraction of the subpolar gyre, most of the poleward shifts of N-SWW coincide with weaker and southward shifted Northern Hemisphere westerlies (**Fig. 20A,B**). The synchronous southward shifts of the westerly winds over both hemispheres indicate large-scale reorganizations of the atmospheric circulation during Holocene cold events.

North Atlantic trigger and atmospheric teleconnection

A recent model study provide a rapid mechanism by which North Atlantic cooling would be teleconnected to the SWW (*Lee et al., 2011*), and hence to the position of the BMC. Initial North Atlantic cooling would shift the ITCZ southward along with an alteration of the Hadley circulation; a weakening of the southern branch of the Hadley circulation and subsequent weakening of the Southern Hemisphere subtropical jet would in turn modify the structure of SWW belt and lead to a strengthening and southward shifting of the SWW (*Lee et al., 2011*). A similar atmospheric teleconnection was suggested to operate during the last deglaciation (e.g., *Anderson et al., 2009; Toggweiler, 2009*). Our results indicate that the atmospheric teleconnection from the North Atlantic to the SWW was also active during the Holocene even if the surface temperature forcing in the North Atlantic was significantly smaller compared to the magnitude of the temperature changes typical for the last deglaciation.

The linkage between North Atlantic temperature changes and the mean position the ITCZ is well established (*Zhang and Delworth, 2005; Broccoli et al., 2006*). Holocene paleoclimate reconstructions generally agree that southward shifts of the ITCZ along with an asymmetric response of the Hadley circulation caused a seesaw pattern of rainfall distribution between the southern and northern low latitudes. Abrupt increases (decreases) in South American monsoon (Asian and Indian monsoon) during North Atlantic cold events were linked to

southward (northward) displacements of the ITCZ (*Fleitmann et al., 2003; Wang et al., 2005; Stríkis et al., 2011*). The observed latitudinal shifts of N-SWW seem to closely correspond to abrupt variations in South American monsoon rainfall (*Stríkis et al., 2011*): poleward (equatorward) shifts of N-SSW correlated to increased (decreased) precipitation in central-eastern Brazil (**Fig. 20D**). The coincident timing of the observed millennial-scale variations in N-SSW and the South America monsoon indicates large-scale atmospheric reorganizations in the Southern Hemisphere supporting the Holocene operation of the teleconnection proposed by *Lee et al.* (*2011*). Moreover, these millennial-scale oscillations were closely related to abrupt climate

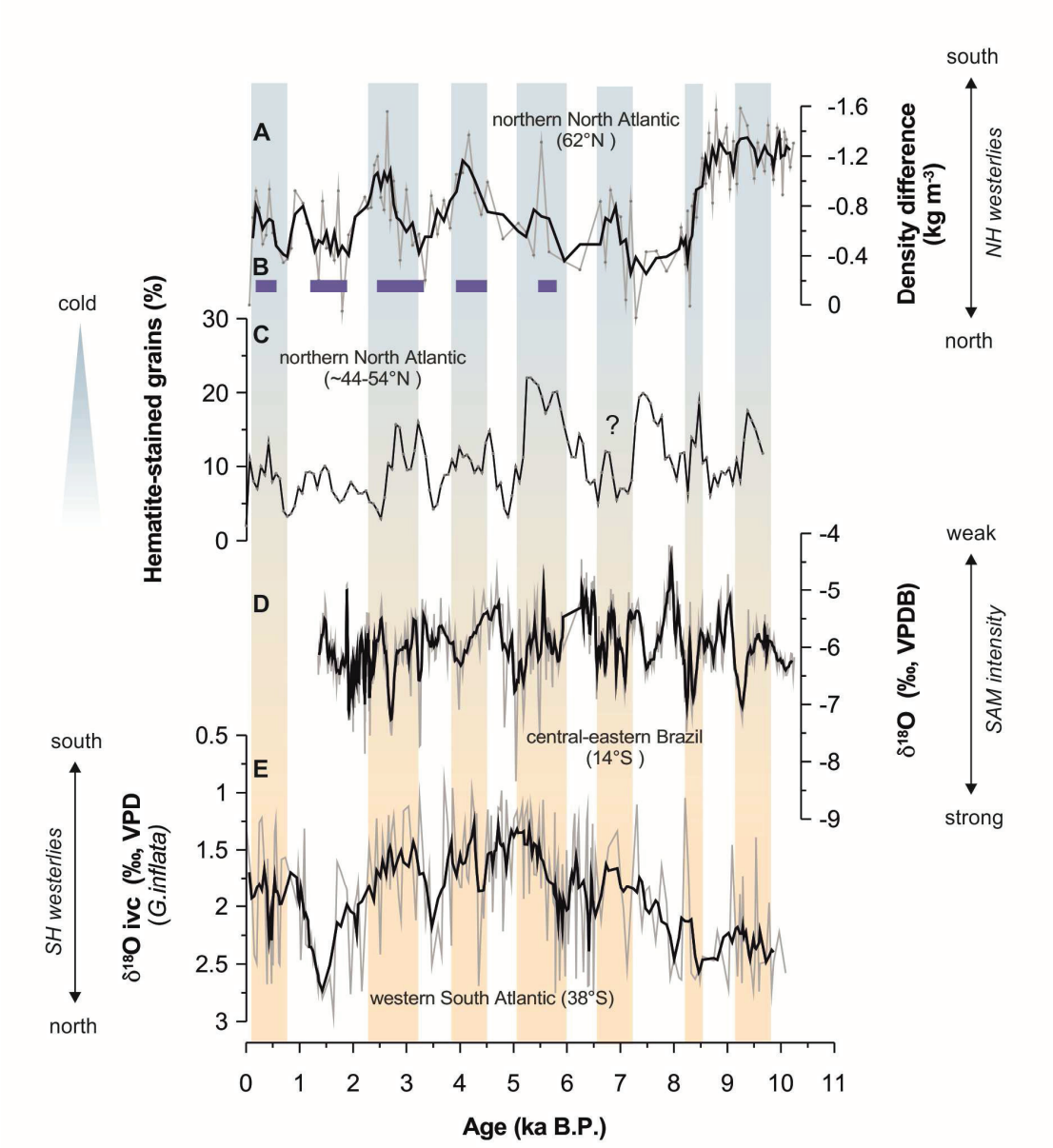

Figure 20 A: Water density difference (stratification increases upwards) between *Globigerina bulloides* and *Globorotalia inflata* (*Thornalley et al., 2009*). **B:** Holocene storm periods to northern Europe (*Sorrel et al., 2012*). **C:** Hematite-stained grain record from North Atlantic marine core (MC52 - MD29191 - CMC21 - GGC22)(*Bond et al., 2001*). **D:** Stalagmite $\delta^{18}O$ record from Lapa Grande Cave, central-eastern Brazil (*Stríkis et al., 2011*). **E:** Ice volume corrected *Globorotalia inflata* $\delta^{18}O$ ($\delta^{18}O$ ivc) record from site GeoB13862-1.

changes in the North Atlantic region (**Fig. 20A,B,C**).

The reorganizations in the SWW belt during Holocene cold events highlight that this millennial-scale mode of Holocene climate instability appears to have been roughly synchronous across the Earth atmosphere, including southward shifts of the Northern Hemisphere westerlies (*Sorrel et al., 2012*), the ITCZ (*Fleitmann et al., 2003; Wang et al., 2005; Stríkis et al., 2011*) and the Southern Hemisphere westerlies, thereby providing strong evidence for a Holocene atmospheric see-saw. Our data thus indicates a north-to-south atmospheric teleconnection operating during the Holocene and emphasize the importance of the tropical atmosphere (i.e., ITCZ/Hadley circulation) for transmitting millennial-scale Holocene climate variability between both hemispheres.

We further conclude that the recent synchronous poleward shift of the global westerlies (i.e., opposite directions in both hemispheres) (*Wu et al., 2012*) seems not to be consistent with natural variability of the westerlies during the Holocene. Our findings show that the unique character of the changes described by *Wu et al., 2012* indicates that a forcing not active during the Holocene may indeed be responsible for the recent changes observed in the global westerlies, and might be attributed to anthropogenic greenhouse-gas forcing (*Saenko et al., 2005*).

4.3. Acknowledgements

We thank M. Segl for help with the isotope analyses. This study was funded through DFG-Research Center / Cluster of Excellence „The Ocean in the Earth System“ and was supported by the Bremen International Graduate School for Marine Sciences (GLOMAR) that is funded by the German Research Foundation (DFG) within the frame of the Excellence Initiative by the German federal and state governments to promote science and research at German universities. CMC acknowledges the support from FAPESP (2010/09983-9).

4.4. References

Anderson, R.F., Ali, S., Bradtmiller, L.I., Nielsen, S.H.H., Fleisher, M.Q., Anderson, B.E., Burckle, L.H., 2009. Wind-Driven Upwelling in the Southern Ocean and the Deglacial Rise in Atmospheric CO_2. Science 323 (5920), 1443-1448.

Bond, G., Kromer, B., Beer, J., Muscheler, R., Evans, M.N., Showers, W., Hoffmann, S., Lotti-Bond, R., Hajdas, I., Bonani, G., 2001. Persistent Solar Influence on North Atlantic Climate During the Holocene. Science 294 (5549), 2130-2136.

Broccoli, A.J., Dahl, K.A., Stouffer, R.J., 2006. Response of the ITCZ to Northern Hemisphere cooling. Geophys. Res. Lett. 33 (1), L01702.

Chiessi, C.M., Ulrich, S., Mulitza, S., Pätzold, J., Wefer, G., 2007. Signature of the Brazil-

Malvinas Confluence (Argentine Basin) in the isotopic composition of planktonic foraminifera from surface sediments. Marine Micropaleontology 64 (1–2), 52-66.

deMenocal, P., Ortiz, J., Guilderson, T., Sarnthein, M., 2000. Coherent High- and Low-Latitude Climate Variability During the Holocene Warm Period. Science 288 (5474), 2198-2202.

Fleitmann, D., Burns, S.J., Mudelsee, M., Neff, U., Kramers, J., Mangini, A., Matter, A., 2003. Holocene Forcing of the Indian Monsoon Recorded in a Stalagmite from Southern Oman. Science 300 (5626), 1737-1739.

Gillett, N.P., Thompson, D.W.J., 2003. Simulation of Recent Southern Hemisphere Climate Change. Science 302 (5643), 273-275.

Gordon, A.L., 1981. South Atlantic thermocline ventilation. Deep Sea Research Part A. Oceanographic Research Papers 28 (11), 1239-1264.

Gordon, A.L., 1989. Brazil-Malvinas Confluence–1984. Deep Sea Research Part A. Oceanographic Research Papers 36 (3), 359-384.

Groeneveld, J., Chiessi, C.M., 2011. Mg/Ca of Globorotalia inflata as a recorder of permanent thermocline temperatures in the South Atlantic. Paleoceanography 26 (2), PA2203.

Kalnay, E., Kanamitsu, M., Kistler, R., Collins, W., Deaven, D., Gandin, L., Iredell, M., Saha, S., White, G., Woollen, J., Zhu, Y., Leetmaa, A., Reynolds, R., Chelliah, M., Ebisuzaki, W., Higgins, W., Janowiak, J., Mo, K.C., Ropelewski, C., Wang, J., Jenne, R., Joseph, D., 1996. The NCEP/NCAR 40-Year Reanalysis Project. Bulletin of the American Meteorological Society 77 (3), 437-471.

Lambeck, K., Chappell, J., 2001. Sea Level Change Through the Last Glacial Cycle. Science 292 (5517), 679-686.

Lee, S.-Y., Chiang, J.C.H., Matsumoto, K., Tokos, K.S., 2011. Southern Ocean wind response to North Atlantic cooling and the rise in atmospheric CO2: Modeling perspective and paleoceanographic implications. Paleoceanography 26 (1), PA1214.

Locarnini, R.A., Mishonov, A.V., Antonov, J.I., Boyer, T.P., Garcia, H.E., Baranova, O.K., Zweng, M.M., Johnson, D.R., 2010. World Ocean Atlas 2009. Volume 1: Temperature. S. Levitus, Ed. NOAA Atlas NESDIS 68, U.S. Government Printing Office, Washington, D.C., 184 pp.

Lumpkin, R., Garzoli, S., 2011. Interannual to decadal changes in the western South Atlantic's surface circulation. J. Geophys. Res. 116 (C1), C01014.

Matano, R.P., Schlax, M.G., Chelton, D.B., 1993. Seasonal Variability in the Southwestern Atlantic. J. Geophys. Res. 98 (C10), 18027-18035.

Obrochta, S.P., Miyahara, H., Yokoyama, Y., Crowley, T.J., 2012. A re-examination of evidence for the North Atlantic "1500-year cycle" at Site 609. Quaternary Science Reviews 55 (0), 23-33.

Oke, P.R., England, M.H., 2004. Oceanic Response to Changes in the Latitude of the Southern Hemisphere Subpolar Westerly Winds. Journal of Climate 17 (5), 1040-1054.

Olson, D.B., Podestá, G.P., Evans, R.H., Brown, O.B., 1988. Temporal variations in the separation of Brazil and Malvinas Currents. Deep Sea Research Part A. Oceanographic Research Papers 35 (12), 1971-1990.

Peterson, R.G., Stramma, L., 1991. Upper-level circulation in the South Atlantic Ocean. Progress In Oceanography 26 (1), 1-73.

Piola, A.R., Matano, R.P., 2001. Brazil and Falklands (Malvinas) Currents. In: Steele JH, Thorpe SA, Turekian KK (eds) Encyclopedia of Ocean Sciences. Academic Press, (San Diego,), pp 340-349

Saenko, O., Fyfe, J., England, M., 2005. On the response of the oceanic wind-driven circulation to atmospheric CO_2 increase. Climate Dynamics 25 (4), 415-426.

Schrag, D.P., Adkins, J.F., McIntyre, K., Alexander, J.L., Hodell, D.A., Charles, C.D., McManus, J.F., 2002. The oxygen isotopic composition of seawater during the Last Glacial Maximum. Quaternary Science Reviews 21 (1–3), 331-342.

Schulz, M., Mudelsee, M., 2002. REDFIT: estimating red-noise spectra directly from unevenly spaced paleoclimatic time series. Computers & Geosciences 28 (3), 421-426.

Sijp, W.P., England, M.H., 2008. The effect of a northward shift in the southern hemisphere westerlies on the global ocean. Progress in Oceanography 79 (1), 1-19.

Sorrel, P., Debret, M., Billeaud, I., Jaccard, S.L., McManus, J.F., Tessier, B., 2012. Persistent non-solar forcing of Holocene storm dynamics in coastal sedimentary archives. Nature Geoscience 5 (12), 892-896.

Stríkis, N.M., Cruz, F.W., Cheng, H., Karmann, I., Edwards, R.L., Vuille, M., Wang, X., de Paula, M.S., Novello, V.F., Auler, A.S., 2011. Abrupt variations in South American monsoon rainfall during the Holocene based on a speleothem record from central-eastern Brazil. Geology 39 (11), 1075-1078.

Thornalley, D.J.R., Elderfield, H., McCave, I.N., 2009. Holocene oscillations in temperature and salinity of the surface subpolar North Atlantic. Nature 457 (7230), 711-714.

Toggweiler, J.R., 2009. Shifting Westerlies. Science 323 (5920), 1434-1435.

Wang, Y., Cheng, H., Edwards, R.L., He, Y., Kong, X., An, Z., Wu, J., Kelly, M.J., Dykoski, C.A., Li, X., 2005. The Holocene Asian Monsoon: Links to Solar Changes and North Atlantic Climate. Science 308 (5723), 854-857.

Wu, L., Cai, W., Zhang, L., Nakamura, H., Timmermann, A., Joyce, T., McPhaden, M.J., Alexander, M., Qiu, B., Visbeck, M., Chang, P., Giese, B., 2012. Enhanced warming over the global subtropical western boundary currents. Nature Clim. Change 2 (3), 161-166.

Zhang, R., Delworth, T.L., 2005. Simulated Tropical Response to a Substantial Weakening of the Atlantic Thermohaline Circulation. Journal of Climate 18 (12), 1853-1860.

4.5. Supplementary Information

4.5.1. Variability of the Brazil-Malvinas Confluence in the instrumental record

A marked seasonal variability in the location of the Brazil-Malvinas Confluence (BMC), up to 900 km along the continental shelf break, has been observed from satellite observations (*Olson et al., 1988; Goni and Wainer, 2001; Saraceno et al., 2004*) and (sub)surface observations (*Garzoli and Bianchi, 1987; Olson et al., 1988; Garzoli and Garraffo, 1989*). Seasonal migration shifts of the can be explained by out-of-phase changes in the mass transport of both the MC and the BC, coupled with a latitudinal displacement of the local wind stress patterns (*Provost et al., 1992; Matano et al., 1993; Garzoli and Giulivi, 1994; Wainer et al., 2000*). Numerical studies *Matano et al. (1993)* indicate that the seasonality of the position of the BMC is governed by the curl of wind stress (i.e., the northern boundary of the Southern Westerly Winds, N-SWW), which has maximum values following a similar annual cycle governs. Accordingly, during austral summer (DJF) the confluence reaches its southernmost extent; during austral winter (JJA) it reaches its northernmost extent (**Fig. SF4**). In addition to the seasonal variability, strong interannual variability

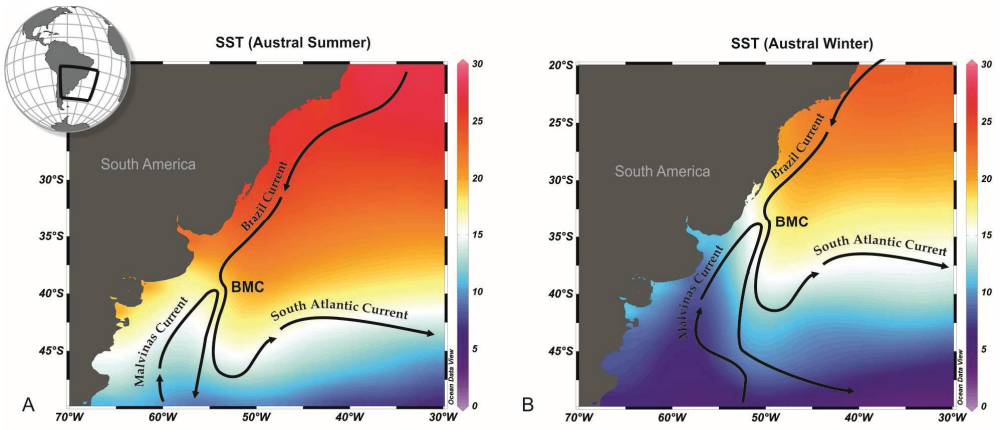

Supplementary Figure SF4 Seasonal mean sea surface temperature in the western South Atlantic with emphasis to the Brazil-Malvinas Confluence (BMC) (*Locarnini et al., 2010*)). A: southward shift of the BMC during austral summer (January-March). B: northward shift of the BMC during austral winter (July –September).

forced by anomalous wind patterns south of the confluence has also been described (*Garzoli and Giulivi, 1994*). Since the mid-1960s the atmosphere of the Southern Hemisphere (SH) has undergone pronounced changes in response to a sustained shift toward the positive phase of the Southern Annular Mode (SAM) (*Marshall, 2003*). This trend entails a southward movement of the SH major pressure systems accompanied by a poleward intensification of the SWW (*Hartmann and Lo, 1998*). A recent southward shift of −0.6 to −0.9° decade^{-1} in the confluence latitude is suggested as a direct response to a poleward shift in the maximum of the wind stress curl across the South Atlantic basin (i.e., reduction in the strength of the northern boundary of the SWW)(*Lumpkin and Garzoli, 2011*). The tight coupling between the latitude of

the confluence and the SWW on seasonal and interannual timescales makes the BMC a highly sensitivity region to record past shifts of the SWW (*Oke and England, 2004; Sijp and England, 2008; Lumpkin and Garzoli, 2011*).

4.5.2. Age models

Age models for GeoB13862-1 and GeoB6211 are based on age models previously published by *Voigt et al. (submitted)* and *Razik et al. (accepted)*, respectively (Supplementary Table S1). However, the composite record of GeoB6211 is for the first time presented here and produced by the gravity core GeoB6211-2 and the companion multicore GeoB6211-2 1 (*Schulz et al., 2001*). Composite record of GeoB6308 is produced by the gravity core GeoB6308-3 and the companion multicore GeoB6308-1 (*Bleil et al., 2001*). The age model for GeoB6308 is based on new AMS ^{14}C ages performed on monospecific samples of planktonic foraminifera *Globorotalia inflata* (Supplementary Table S2). Calibration of the conventional radiocarbon ages was performed with CALIB 6.0 radiocarbon calibration program (*Stuiver and Reimer, 1993*) by applying the Marine09 calibration curve (*Reimer et al., 2009*) and no ΔR. Age models were obtained by linear interpolation of calibrated ages.

Sample Code	Depth (cm)	Species	Radiocarbon age ± 1σ error (a BP)	2σ calibrated age range (cal a BP)	Calibrated age, interpolated from 2σ range (cal ka BP)
Core GeoB13862-2					
Poz-38071	143	*G. inflata*	1790 ± 140	1050-1668	1,36
Poz-42354	258	*G. inflata*	4000 ± 50	3852-4152	4,00
Poz-38072	393	*G. inflata*	5380 ± 60	5612-5886	5,75
Poz-42355	490	*G. inflata*	5840 ± 80	6057-6434	6,25
Poz-42356	556	*G. inflata*	6140 ± 50	6440-6700	6,57
Poz-38074	669	*G. inflata*	8530 ± 70	8994-9363	9,18
Poz-38075	793	*G. inflata*	9740 ± 70	10460-10827	10,64
Core GeoB6211					
KIA30528	18	*G. ruber* / *G. sacculifer*	1685 ± 30	1169-1299	1,23
KIA35166	35	*G. ruber* / *G. sacculifer*	3170 ± 40	2839-3105	2,97
KIA35165	55	*G. ruber* / *G. sacculifer*	4625 ± 45	4763-4973	4,87
KIA30527	73	*G. ruber*	7145 ± 55	7506-7730	7,62
NOSAMS75186	86	*G. ruber* / *G. sacculifer*	9370 ± 40	10136-10324	10,25

KIA35163	95	*G. ruber* / *G. sacculifer*	9920 ± 70	10630-11097	10,85
KIA35162	101	*G. ruber* / *G. sacculife4*	9810 ± 110	10493-11084	10,80
KIA30526	123	*G. ruber* / *G. sacculifer*	12600 ± 70	13812-14254	14,05
Core GeoB6308					
Poz-42364	2	*G. inflata*	750 ± 70	270-499	0,38
Poz-42363	11	*G. inflata*	1310 ± 30	769-924	0,85
Poz-43433	4	*G. inflata*	1500 ± 30	958-1142	1,05
Poz-43435	16	*G. inflata*	2770 ± 30	2358-2618	2,49
Poz-43436	28	*G. inflata*	3645 ± 30	3445-3637	3,54
Poz-43437	40,5	*G. inflata*	4490 ± 35	4564-4803	4,68
Poz-43438	52	*G. inflata*	5240 ± 25	5552-5672	5,61
Poz-43439	64	*G. inflata*	6290 ± 40	6642-6861	6,75
Poz-43440	76	*G. inflata*	7310 ± 40	7667-7873	7,77
Poz-43441	88	*G. inflata*	8970 ± 40	9518-9776	9,65
Poz-43442	100	*G. inflata*	9930 ± 50	10676-11087	10,9
Poz-43443	107	*G. inflata*	10130 ± 50	11050-11227	11,15

4.5.3. Methods

The apparent calcification depth of dwelling planktonic foraminifera *G. inflata* in the western South Atlantic is constant (350-400 m) even under different upper water column structures and lies within the permanent thermocline (*Chiessi et al., 2007; Groeneveld and Chiessi, 2011*). Evidences for changes in shell chemistry by addition of secondary calcite during the end phase of their ontogenetic cycle highlights the importance of a careful selection of individual *G. inflata* specimens when producing downcore geochemical records with *G. inflata* (*Lončarić et al., 2009; Groeneveld and Chiessi, 2011*). To reduce the potential bias caused by different size fractions and states of encrustation (*Groeneveld and Chiessi, 2011*) we selected only non-encrusted specimens of *G. inflata* in the size range between 315-400 μm and with three chambers in the final whorl.

Stable oxygen isotopes were measured with a Finnigan MAT 251 mass spectrometer with an automated carbonate preparation device at the Department of Geosciences, University of Bremen. For each sample, approximately 10 specimens of *G. inflata* were hand-picked from the 315-400 μm size fraction. The isotopic composition of the carbonate sample was measured on the CO_2 gas produced by the reaction of foraminiferal carbonate with phosphoric acid at a constant temperature of 75°C. For all stable oxygen isotope measurements a working standard (Burgbrohl CO_2 gas) was used, which was calibrated against

Vienna Pee Dee Belemnite (VPDB) by using the NBS 18, 19 and 20 standards. Consequently, all $\delta^{18}O$ data given here are relative to the VPDB standard. Analytical standard deviation is about 0.07 ‰.

4.5.4. Spectral analysis in the frequency domain

Spectral analyses in the frequency domain were performed with the software REDFIT (*Schulz and Mudelsee, 2002*). The program works directly from unevenly spaced data avoiding the introduction of bias during interpolation. Prior to analysis, the data were linearly detrended with PAST.

Spectral analyses of the $\delta^{18}O$ records revealed statistically significant oscillations (99 % confidence level) in the southern cores (i.e., GeoB13862-1 and GeoB6308) and the lack of it in the northern core (GeoB6211). The spectra depict a pronounced peak with period of ~2500 yr (1900-3600 yr in GeoB13862), and ~2200 yr (1700-2900 yr in GeoB6308).

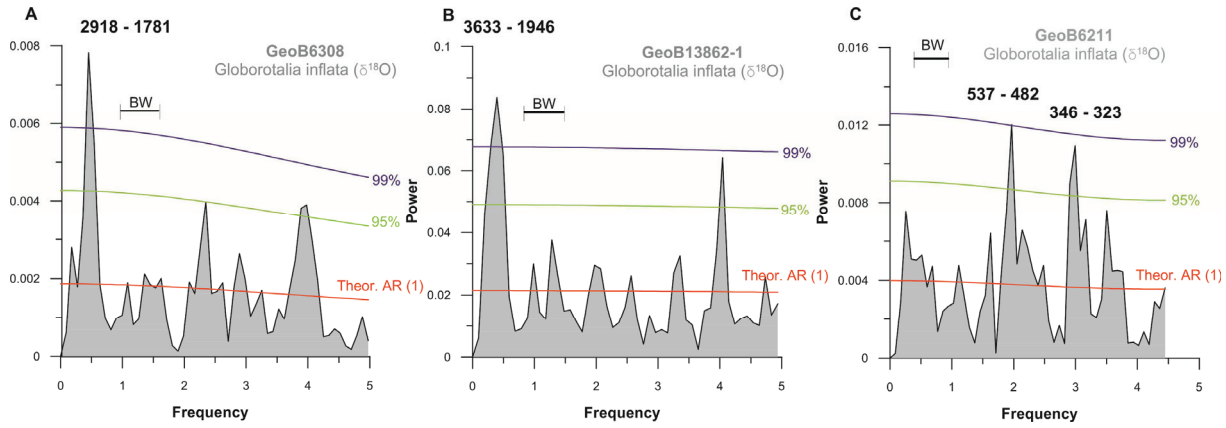

Supplementary Figure SF5 Spectral analyses of *Globorotalia inflata* $\delta^{18}O$ records from **(A)** GeoB6308 **(B)** GeoB13862-1 and **(C)** GeoB6211. Peaks that exceed the 95 % confidence level are labeled with their periods (in years). The number of overlapping segments chosen was 3, and a Rectangle type window was used. The bandwidth (BW) indicates the frequency resolution. Blue and green depict the 99 and 95 % confidence level, respectively. Red lines depict the red-noise spectrum.

4.5.5. Spectral analyses in the time-frequency domain

Morlet wavelet analyses were performed using the online facility of the Program in Atmospheric and Oceanographic Science at the University of Colorado (*http://ion.researchsystems.com/* (*Torrence and Compo, 1998*)). Prior to analysis, the data were first linearly detrended and then linearly interpolated. The intervals selected for linear interpolation are similar to the mean temporal resolution of the records (i.e., 50, 50 and 100yrs for GeoB6308, GeoB13862-1 and GeoB6211, respectively).

The wavelet analysis indicates that a ~2000-year period is relatively stationary on both the GeoB13862-1 and the GeoB6308 indicating that the (quasi) cyclicities are significant throughout the Holocene. The ~2000-year period present in both cores reflect a tight coupling between changes in the mass transport of the MC (GeoB6308) and latitudinal shifts of the BMC (GeoB13862-1). The lack of ~2000-year period in GeoB6211 (for the interval <7 cal kyr BP) confirms that changes in the mass transport of the BC are not primarily affecting the dynamics of the BMC. Hence, we interpret that latitudinal shifts of the BMC were primarily controlled by a forcing from the Southern Westerly Winds, consistently to the mechanism proposed by *Lee et al.* (*2011*).

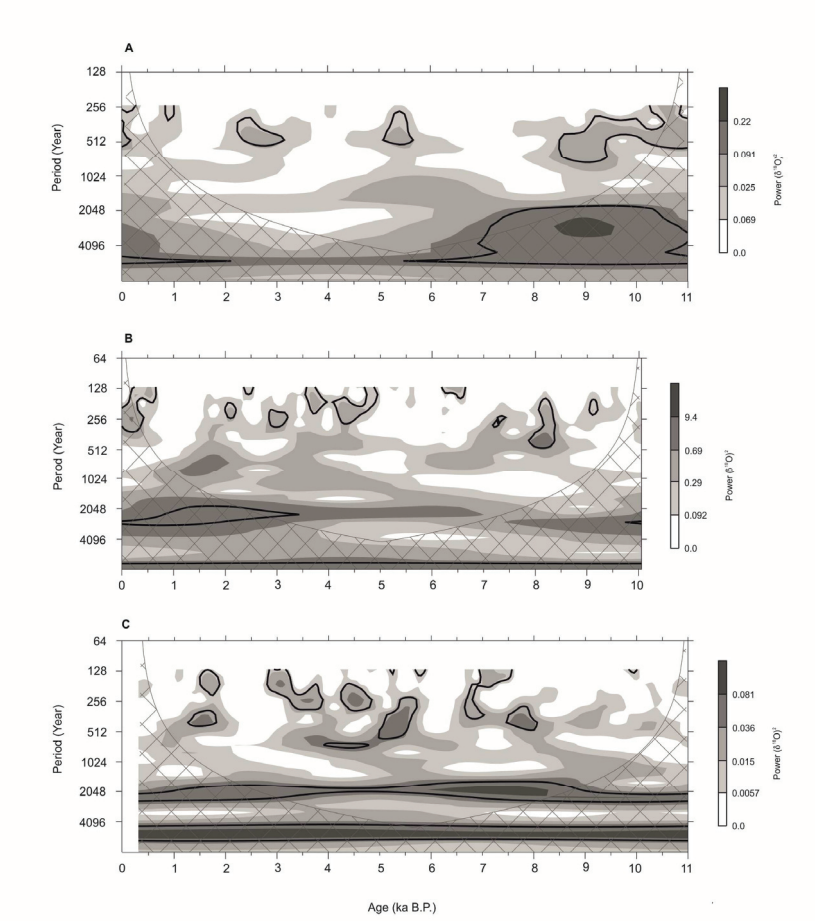

Supplementary Figure SF6 Wavelet power spectra of the *Globoroalia inflata* $\delta^{18}O$ records of **(A)** GeoB6308 **(B)** GeoB13862-1 and **(C)** GeoB6211. The wavelet analyses of all records were performed using a Morlet wavelet, a frequency parameter of 5, a starting scale of 2, a scale width of 0.25 and a 10 % significance level (black contour) with a red-noise background spectrum.

4.5.6. Holocene variability of Malvinas (Falkland) Current

Within age-model uncertainties the timing of millennial-scale variability in the Malvinas Current (GeoB6308) is synchronous with significant iceberg discharge events in the North Atlantic (*Bond et al., 2001*). Since the Malvinas Current is primarily affected by prevailing westerlies, the data from GeoB6308

support our hypothesis of a tight coupling between the remote North Atlantic and southward shift of the westerlies, consistently to the mechanism proposed by *Lee et al.* (*2011*).

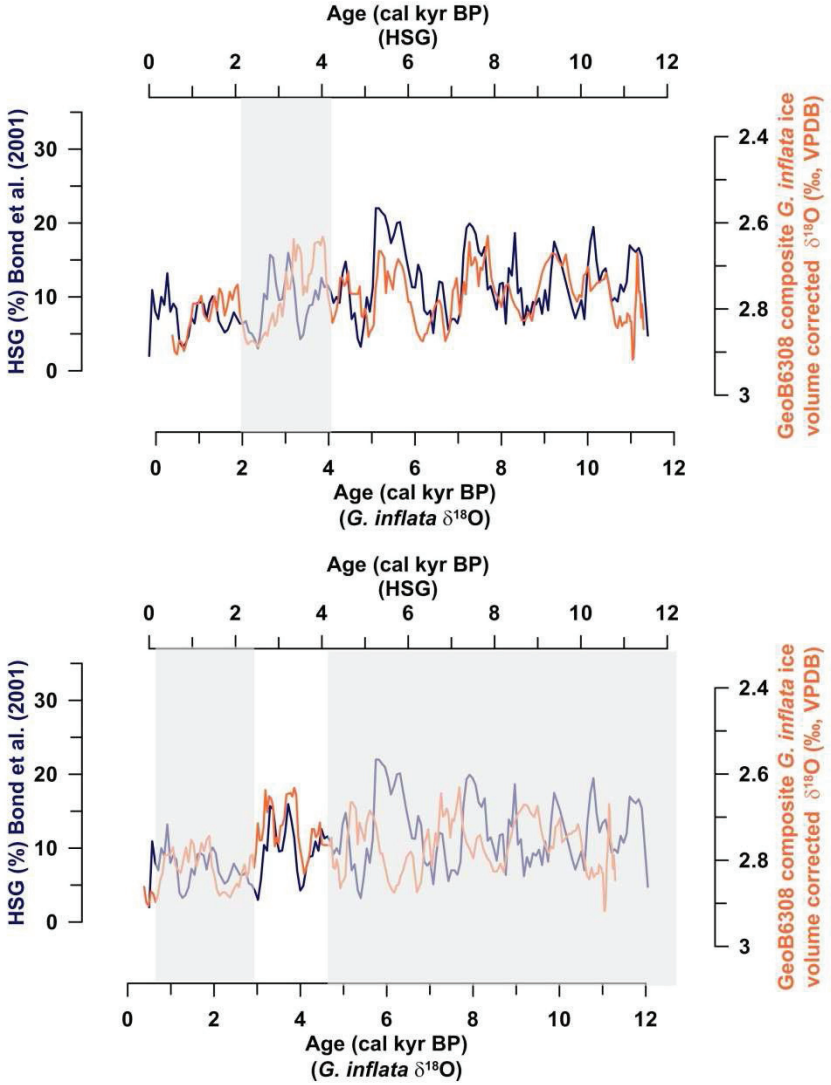

Supplementary Figure SF7 Comparison between Hematite-stained grain record from North Atlantic marine core (MC52 - MD29191 - CMC21 - GGC22)(*Bond et al., 2001*) with ice volume corrected *Globorotalia inflata* $\delta^{18}O$ ($\delta^{18}O$ ivc) record from site GeoB6308. The difference in both plots lies in the alignment of both x-axis with the aim of synschronizing the time-window between ca. 2 and 4 cal kyr BP.

Bleil, U., and Cruise Participants, 2001. Report and preliminary results of Meteor Cruise M46/3, Montevideo - Mar del Plata. January 4 - February 7, 2000. Berichte, Fachbereich Geowissenschaften, 172. Universität Bremen, Bremen, 161 pp.

Bond, G., Kromer, B., Beer, J., Muscheler, R., Evans, M.N., Showers, W., Hoffmann, S., Lotti-Bond, R., Hajdas, I., Bonani, G., 2001. Persistent Solar Influence on North Atlantic Climate During the Holocene. Science 294 (5549), 2130-2136.

Chiessi, C.M., Ulrich, S., Mulitza, S., Pätzold, J., Wefer, G., 2007. Signature of the Brazil-Malvinas Confluence (Argentine Basin) in the isotopic composition of planktonic foraminifera from surface sediments. Marine Micropaleontology 64 (1–2), 52-66.

Garzoli, S.L., Bianchi, A., 1987. Time-Space Variability of the Local Dynamics of the Malvinas-Brazil Confluence as Revealed by Inverted Echo Sounders. J. Geophys. Res. 92 (C2), 1914-1922.

Garzoli, S.L., Garraffo, Z., 1989. Transports, frontal motions and eddies at the Brazil-Malvinas currents confluence. Deep Sea Research Part A. Oceanographic Research Papers 36 (5), 681-703.

Garzoli, S.L., Giulivi, C., 1994. What forces the variability of the southwestern Atlantic boundary currents? Deep Sea Research Part I: Oceanographic Research Papers 41 (10), 1527-1550.

Goni, G.J., Wainer, I., 2001. Investigation of the Brazil Current front variability from altimeter data. J. Geophys. Res. 106 (C12), 31117-31128.

Groeneveld, J., Chiessi, C.M., 2011. Mg/Ca of Globorotalia inflata as a recorder of permanent thermocline temperatures in the South Atlantic. Paleoceanography 26 (2), PA2203.

Hartmann, D.L., Lo, F., 1998. Wave-Driven Zonal Flow Vacillation in the Southern Hemisphere. Journal of the Atmospheric Sciences 55 (8), 1303-1315.

Lee, S.-Y., Chiang, J.C.H., Matsumoto, K., Tokos, K.S., 2011. Southern Ocean wind response to North Atlantic cooling and the rise in atmospheric CO2: Modeling perspective and paleoceanographic implications. Paleoceanography 26 (1), PA1214.

Locarnini, R.A., Mishonov, A.V., Antonov, J.I., Boyer, T.P., Garcia, H.E., Baranova, O.K., Zweng, M.M., Johnson, D.R., 2010. World Ocean Atlas 2009. Volume 1: Temperature. S. Levitus, Ed. NOAA Atlas NESDIS 68, U.S. Government Printing Office, Washington, D.C., 184 pp.

Lončarić, N., Peeters, F.J.C., Kroon, D., Brummer, G.-J.A., 2006. Oxygen isotope ecology of recent planktic foraminifera at the central Walvis Ridge (SE Atlantic). Paleoceanography 21 (3), PA3009.

Lumpkin, R., Garzoli, S., 2011. Interannual to decadal changes in the western South Atlantic's surface circulation. J. Geophys. Res. 116 (C1), C01014.

Marshall, G.J., 2003. Trends in the Southern Annular Mode from Observations and Reanalyses. Journal of Climate 16 (24), 4134-4143.

Matano, R.P., Schlax, M.G., Chelton, D.B., 1993. Seasonal Variability in the Southwestern Atlantic. J. Geophys. Res. 98 (C10), 18027-18035.

Oke, P.R., England, M.H., 2004. Oceanic Response to Changes in the Latitude of the Southern Hemisphere Subpolar

Westerly Winds. Journal of Climate 17 (5), 1040-1054.

Olson, D.B., Podestá, G.P., Evans, R.H., Brown, O.B., 1988. Temporal variations in the separation of Brazil and Malvinas Currents. Deep Sea Research Part A. Oceanographic Research Papers 35 (12), 1971-1990.

Provost, C., Garcia, O., Garçon, V., 1992. Analysis of Satellite Sea Surface Temperature Time Series in the Brazil-Malvinas Current Confluence Region: Dominance of the Annual and Semiannual Periods. J. Geophys. Res. 97 (C11), 17841-17858.

Ratzik, S., Chiessi; C.M., Romero, O.E., von Dobeneck, T., 2013. Interaction of the South American Monsoon System and the Southern Westerly Wind Belt during the last 14 kyr. Palaeogeography, Palaeoclimatology, Palaeoecology (accepted).

Reimer, P.J., Baillie, M.G.L., Bard, E., Bayliss, A., Beck, J.W., Blackwell, P.G., Bronk Ramsey, C. Buck, C.E., Burr, G.S., Edwards, R.L., Friedrich, M., Grootes, P.M., Guilderson, T.P., Hajdas, I., Heaton, T.J., Hogg, A.G., Hughen, K.A., Kaiser, K.F., Kromer, B., McCormac, F.G., Manning, S.W., Reimer, R.W., Richards, D.A., Southon, J.R., Talamo, S., Turney, C.S.M., van der Plicht, J., Weyhenmeyer ,C.E., 2009. IntCal09 and Marine09 radiocarbon age calibrationcurves, 0–50,000 years cal BP. Radiocarbon, 51, pp. 1111–1150.

Saraceno, M., Provost, C., Piola, A.R., Bava, J., Gagliardini, A., 2004. Brazil Malvinas Frontal System as seen from 9 years of advanced very high resolution radiometer data. J. Geophys. Res. 109 (C5), C05027.

Schulz, H.D., and Cruise Participants, 2001. Report and preliminary results of Meteor Cruise M46/2, Recife (Brazil) – Montevideo (Uruguay). December 2 - December 29, 1999. Berichte, Fachbereich Geowissenschaften, 174. Universität Bremen, Bremen, 107 pp.

Schulz, M., Mudelsee, M., 2002. REDFIT: estimating red-noise spectra directly from unevenly spaced paleoclimatic time series. Computers & Geosciences 28 (3), 421-426.

Sijp, W.P., England, M.H., 2008. The effect of a northward shift in the southern hemisphere westerlies on the global ocean. Progress in Oceanography 79 (1), 1-19.

Stuiver, M., Reimer, P.J., 1993. Extended 14C data base and revised CALIB 3.0 14C age calibration program. Radiocarbon, 35 , pp. 215–230

Torrence, C., Compo, G.P., 1998. A Practical Guide to Wavelet Analysis. Bulletin of the American Meteorological Society 79 (1), 61-78.

Voigt, I., Henrich, R., Preu, P., Piola, A.R., Hanebuth, T.J.J., Schwenk, T., Chiessi, C.M., 2012. A submarine canyon as a climate archive- Interaction of the Antarctic Intermediate Water with the

Mar del Plata Canyon (Southwest Atlantic). Marine Geology (submitted).

Wainer, I., Gent, P., Goni, G., 2000. Annual cycle of the Brazil-Malvinas confluence region in the National Center for Atmospheric Research Climate System Model. J. Geophys. Res. 105 (C11), 26167-26177.

Chapter 5: Summary and Outlook

The main focus of this thesis was to determine the natural variability of the ocean circulation in the western South Atlantic during the Holocene, with special emphasis on the sedimentation processes in the Mar del Plata Canyon. The following chapter provides a summary of the conclusions for each specific objective stated in Chapter 1 and outlines perspectives for future work.

(1) To assess if the Mar del Plata Canyon interacts with the Antarctic Intermediate Water

A major outcome of this PhD project is a new conceptual model for sedimentation processes taking place in submarine canyons that are located at current-influenced continental margins. The presented data suggest that the Mar del Plata Canyon located at the continental margin off northern Argentina interacts with an intermediate-nepheloid layer (INL) generated by the northward-flowing Antarctic Intermediate Water (AAIW). Due to this interaction considerable amounts of sediment transported with the AAIW are released into the canyon, thereby leading to continuous high sedimentation rates of ~150cm/kyrs during the Holocene. We assume that a change in hydrodynamics of northward-flowing Antarctic water masses is caused by "crossing" the canyon associated with a drastically decrease of the flow energy, competency and capacity. Our results further indicate that the presence of the canyon generates a change in the contourite drift construction.

Sediment deposits in the canyon indicate a response to changes of contour-current strength of AAIW related to Late Glacial/Holocene climate variability, which provides that the canyon holds a great potential for a climate archive. We conclude that in particular in such highly dynamic current regions as the western South Atlantic where contour currents rework/redistribute significant amounts of sediment (*Hernández-Molina et al., 2009*), a submarine canyon can provide a great potential for reconstructing paleoceanographic and paleoclimatic changes with a high temporal resolution.

This contemplation is supported by the fact that due to an additional involvement of (hemi)pelagic sediments the canyon records productivity events in upper water column possibly associated with Holocene El Niño /Southern Oscillation (ENSO) variability in South America. We assume that due to the effects of wind and precipitation anomalies the La Plata River plume spread offshore during anomalously strong El Niño events (*Ciotti et al., 1995; Piola et al., 2005; Garcia and Garcia, 2008;*

Piola et al., 2008), which in turn led to fertilization of the upper water column over the Mar del Plata Canyon. Hence, layers enriched with particular organic matter and planktonic primary producers (i.e., diatoms, silicoflagellates) were accumulated in the canyon during strong Holocene El Niño events.

An important question that requires future work is whether other submarine canyon systems show an influence of (lateral) current-controlled transport processes on the sedimentation pattern. If the interaction with a deep-sea current appears to be an important process at current-influenced continental margins than other submarine canyon systems possibly provide a great potential as climate archives.

(2) To determine the response in AAIW formation and circulation to changes in the strength/position of SWW during the Holocene.

Our results show a highly variable intermediate water circulation throughout the Holocene. Superimposed on a slight increase in AAIW strength at ~ 5.5 ka B.P., a succession of millennial-scale variations in AAIW strength is recognized in the "sortable silt" paleoflow proxy record of the sediment core GeoB13862-1 retrieved from the Mar del Plata Canyon. Variations in AAIW strength are consistent to Southern Hemisphere climate oscillations and indicate a tight coupling to Southern Hemisphere cold events (*Masson et al., 2000; Glasser et al., 2004; Shevenell et al., 2011*) and poleward shifted Southern Westerly Winds (SWW) (*Moros et al., 2009*) that both favored higher ice-ocean freshwater fluxes toward regions of AAIW renewal (*Ribbe, 2001; Saenko and Weaver, 2001; Oke and England, 2004; Santoso and England, 2004*), and therefore contributed to an increase in AAIW formation and circulation strength.

3) Determine the response in AMOC to changes in AAIW formation and circulation patterns

The sensitivity of AAIW formation to atmosphere-ocean processes in the Southern Hemisphere permits the transfer of climate variability to the North Atlantic and thereby links AAIW and North Atlantic Deep Water (NADW) circulation on millennial timescales. An antiphase relationship in AAIW and NADW circulation provides strong evidence for a NADW-AAIW see-saw during the Holocene. The strengthening of the intermediate overturning branch of the AMOC may have contributed to a cooling and freshening of the North Atlantic and have led to reduction of NADW formation (*Graham et al., 2011*). We thus confirm a close coupling between atmosphere-ocean interactions in the Southern Hemisphere and the AMOC.

To assess the reliability of the presented forcing mechanisms in Chapters 3 future modeling experiments could investigate the response of AAIW formation and circulation to natural climate variability, for example with reconstructed Holocene values for total solar irradiance and other possibly forcing scenarios. It still remains unclear if significant changes occurred in the whole structure of the western

South Atlantic water column during the Holocene. Since the GeoB13862-1 is located at 3600 m water depth, measurements of paired Mg/Ca – $\delta^{18}O$ values on benthic foraminifera might provide important new insights into the impact and importance of the LCDW (Lower Circumpolar Deep Water) on the meridional heat exchange. By focusing on other Mar del Plata Canyon cores there is further potential to reconstruct deep-water variability during the Holocene. Specifically, sediment core GeoB13832-2 may be a potential candidate for measurements of paired Mg/Ca – $\delta^{18}O$ on benthic foraminifera because Holocene sedimentation rates are greatest, and therefore provide a high temporal resolution for the late Holocene (0 - 4 ka. B.P.).

4) Determine N-S shifts of Brazil- Malvinas Confluence in response to the local wind field

We record Holocene millennial-scale shifts of the Brazil- Malvinas Confluence (BMC) based on a N-S transect of high- resolution $\delta^{18}O$ records of planktonic foraminifer *G. inflata*. We conclude that N-S shifts of BMC are largely determined by latitudinal shifts of the northern boundary of the SWW (*Matano et al., 1993; Lumpkin and Garzoli, 2011*). Changes in the SWW belt were in phase with large-scale variations in the Southern Hemisphere atmospheric circulation (i.e., South America Monsoon System) that both indicate a tight coupling to North Atlantic climate perturbations. Therefore, we infer a vital role for the North Atlantic in regulating SWW belt changes (*Lee et al., 2011*). These results emphasize the importance of the meridional atmospheric circulation of the Hadley cells for the transmitting millennial-scale climate variability between both hemispheres and highlight its role in Holocene abrupt climate changes.

In the future, the presented record could be completed by measurements of Mg/Ca to accurately convert $\delta^{18}O$ to calcification temperature by using the paleotemperature equation for *G. inflata* from *Groeneveld and Chiessi, 2011*. Further, preliminary observations indicated that the planktonic foraminiferal assemblages from sediment core GeoB13862-1 show significant down-core changes. Planktonic foraminiferal assemblages are an important proxy for reconstructing changes in primary productivity, and hence could provide additional information on past N-S shifts of BMC (*Boltovskoy et al., 1996*).

Boltovskoy, E., Boltovskoy, D., Correa, N., Brandini, F., 1996. Planktic foraminifera from the southwestern Atlantic (30 °–60 °S): species-specific patterns in the upper 50 m. Marine Micropaleontology 28 (1), 53-72.

Ciotti, Á.M., Odebrecht, C., Fillmann, G., Moller Jr, O.O., 1995. Freshwater outflow and Subtropical Convergence influence on phytoplankton biomass on the southern Brazilian continental shelf. Continental Shelf Research 15 (14), 1737-1756.

Garcia, C.A.E., Garcia, V.M.T., 2008. Variability of chlorophyll-a from ocean color

images in the La Plata continental shelf region. Continental Shelf Research 28 (13), 1568-1578.

Glasser, N.F., Harrison, S., Winchester, V., Aniya, M., 2004. Late Pleistocene and Holocene palaeoclimate and glacier fluctuations in Patagonia. Global and Planetary Change 43 (1–2), 79-101.

Graham, J., Stevens, D., Heywood, K., Wang, Z., 2011. North Atlantic climate responses to perturbations in Antarctic Intermediate Water. Climate Dynamics 37 (1-2), 297-311.

Groeneveld, J., Chiessi, C.M., 2011. Mg/Ca of Globorotalia inflata as a recorder of permanent thermocline temperatures in the South Atlantic. Paleoceanography 26 (2), PA2203.

Hernández-Molina, F.J., Paterlini, M., Violante, R., Marshall, P., de Isasi, M., Somoza, L., Rebesco, M., 2009. Contourite depositional system on the Argentine Slope: An exceptional record of the influence of Antarctic water masses. Geology 37 (6), 507-510.

Lee, S.-Y., Chiang, J.C.H., Matsumoto, K., Tokos, K.S., 2011. Southern Ocean wind response to North Atlantic cooling and the rise in atmospheric CO_2: Modeling perspective and paleoceanographic implications. Paleoceanography 26 (1), PA1214.

Lumpkin, R., Garzoli, S., 2011. Interannual to decadal changes in the western South Atlantic's surface circulation. J. Geophys. Res. 116 (C1), C01014.

Masson, V., Vimeux, F., Jouzel, J., Morgan, V., Delmotte, M., Ciais, P., Hammer, C., Johnsen, S., Lipenkov, V.Y., Mosley-Thompson, E., Petit, J.-R., Steig, E.J., Stievenard, M., Vaikmae, R., 2000. Holocene Climate Variability in Antarctica Based on 11 Ice-Core Isotopic Records. Quaternary Research 54 (3), 348-358.

Matano, R.P., Schlax, M.G., Chelton, D.B., 1993. Seasonal Variability in the Southwestern Atlantic. J. Geophys. Res. 98 (C10), 18027-18035.

Moros, M., De Deckker, P., Jansen, E., Perner, K., Telford, R.J., 2009. Holocene climate variability in the Southern Ocean recorded in a deep-sea sediment core off South Australia. Quaternary Science Reviews 28 (19–20), 1932-1940.

Oke, P.R., England, M.H., 2004. Oceanic Response to Changes in the Latitude of the Southern Hemisphere Subpolar Westerly Winds. Journal of Climate 17 (5), 1040-1054.

Piola, A.R., Romero, S.I., Zajaczkovski, U., 2008. Space–time variability of the Plata plume inferred from ocean color. Continental Shelf Research 28 (13), 1556-1567.

Piola, A.R., Matano, R.P., Palma, E.D., Möller, O.O., Jr., Campos, E.J.D., 2005. The influence of the Plata River discharge on the western South Atlantic shelf. Geophys. Res. Lett. 32 (1), L01603.

Ribbe, J., 2001. Intermediate water mass production controlled by southern

hemisphere winds. Geophys. Res. Lett. 28 (3), 535-538.

Saenko, O.A., Weaver, A.J., 2001. Importance of wind-driven sea ice motion for the formation of Antarctic Intermediate Water in a global climate model. Geophys. Res. Lett. 28 (21), 4147-4150.

Santoso, A., England, M.H., 2004. Antarctic Intermediate Water Circulation and Variability in a Coupled Climate Model. Journal of Physical Oceanography 34 (10), 2160-2179.

Shevenell, A.E., Ingalls, A.E., Domack, E.W., Kelly, C., 2011. Holocene Southern Ocean surface temperature variability west of the Antarctic Peninsula. Nature 470 (7333), 250-254.

Appendix 1: Morphosedimentary and hydrographic features of the northern Argentine margin: the interplay between erosive, depositional and gravitational processes and its conceptual implications

Benedict M. Preu[1], Javier F. Hernández-Molina[2], Roberto Violante[3], Alberto R. Piola[3], Marcelo C. Paterlini[3], Tilmann Schwenk[1], Ines Voigt[1], Sebastian Krastel[4], Volkhard Spiess[1]

[1]MARUM –Center for Marine Environmental Sciences and Faculty of Geosciences, University of Bremen, D-28359 Bremen, Germany

[2]Facultad de Ciencias del Mar, Universidad de Vigo, Vigo, Spain

[3]Servicio de Hidrografia Naval (SHN), Buenos Aires, Argentina

[4]GEOMAR | Helmholtz Centre for Ocean Research Kiel, Germany

(*Accepted for Deep-Sea Research Part I*)

A1.1. Abstract

Bottom currents and their margin-shaping character became a central aspect in the research field of sediment dynamics and paleoceanography during the last decades due to their potential to form large contourite depositonal systems (CDS), consisting of both erosive and depositional features. A major CDS at the northern Argentine continental margin was studied off the Rio de la Plata River by means of seismo- and hydro-acoustic methods including conventional and high-resolution seismic, parametric echosounder and single and swath bathymetry. Additionally, hydrographic data were considered allowing jointly interpretation of morphosedimentary features and the oceanographic framework, which is dominated by the presence of the dynamic and highly variable Brazil-Malvinas Confluence. We focus on three regional contouritic terraces identified on the slope in the vicinity of the Mar del Plata Canyon. The shallowest one, the La Plata Terrace (~500 m), is located at the Brazil Current/Antarctic Intermediate Water interface

characterized by its deep and distinct thermocline. In ~1200 m water depth the Ewing Terrace correlates with the Antarctic Intermediate Water /Upper Circumpolar Deep Water interface. At the foot of the slope in ~3500 m the Necochea Terrace marks the transition between Lower Circumpolar Deep Water and Antarctic Bottom Water during glacial times. Based on these correlations, a comprehensive conceptual model is proposed, in which the onset and evolution of contourite terraces is controlled by short- and long-term variations of water mass interfaces. We suggest that the terrace genesis is strongly connected to the turbulent current pattern typical for water mass interfaces. Furthermore, the erosive processes necessary for terrace formation are probably enhanced due to internal waves, which are generated along strong density gradients typical for water mass interfaces. The terraces widen through time due to locally focused, partly helical currents along the steep landward slopes and more tabular conditions seaward along the terrace surface. Considering this scheme of contourite terrace development, lateral variations of the morphosedimentary features off northern Argentina can be used to derive the evolution of the Brazil- Malvinas Confluence on geological time scales. We propose that the Brazil-Malvinas Confluence in modern times is located close to its southernmost position in the Quaternary, while its center was shifted northward during cold periods.